THE
PHYSICAL REVIEW
A Journal of Experimental and Theoretical Physics
VOL. 44, NO. 12 DECEMBER 15, 1933 SECOND SERIES

The Relative Intensities of Certain *L*-Series X-Ray Satellites in Cathode-Ray and in Fluorescence Excitation

F. R. HIRSH, JR., AND F. K. RICHTMYER, *Department of Physics, Cornell University*
(Received October 30, 1933)

Using a specially designed x-ray tube, the authors have measured the relative intensity of satellites and their parent $L\alpha_1$ line, for both cathode-ray and fluorescence excitation for the elements Zr(40), Mo(42), Ru(44), Rh(45), Pd(46) and Ag(47). Cathode-ray excitation was by 20 kv electrons. Fluorescence excitation was caused by the radiation from a target of Ag(47) bombarded by 20 kv electrons. A photographic method is used; in which spectrograms, Moll microphotometric records and density plots are made, from which it is possible to obtain the relative intensity of the satellites and their parent $L\alpha_1$ line. The results for fluorescence excitation suggest that *LM* ionization is the most probable origin of the $L\alpha$ satellites. On the other hand, the rapid variation in relative intensity of the satellites with atomic number for cathode-ray excitation, seems to indicate that the peripheral electron structure of the atom plays a fundamental rôle in the production of satellites. The magnitude of the integrated intensity of the group of satellites accompanying $L\alpha$ varies from 10 percent to 70 percent of the intensity of the parent line, depending on the element and the method of excitation.

INTRODUCTION

D. COSTER,[1] in 1922, stated that if x-ray non-diagram (or satellite) lines are of true spark origin, they should not appear in fluorescence spectra; whereas they are present in spectra obtained by cathode-ray excitation. Agreeing with this conclusion is the statement of M. A. Dauvillier,[2] who also remarked that the "supplementary" *K* lines (*K* satellites) should not appear in fluorescence. Dauvillier's researches[3] apparently confirmed this opinion, for he failed to observe the satellite doublet $K\alpha_{3,4}$ in the fluorescent spectrum of Fe(26). D. Coster and M. J. Druyvesteyn[4] repeated Dauvillier's experiment, using a specially designed x-ray tube, and succeeded in exciting the so-called "spark lines" of the *K*-series of Fe(26). They noted that, relative to the parent line, the fluorescent non-diagram lines of Fe *K* were about 1/6 as intense in fluorescence as in cathode-ray excitation.

The study of x-ray satellites produced by fluorescence offers a suggestive line of approach to the puzzling question of the origin of these lines. There is need of additional quantitative data on the relative intensities of fluorescent, as compared with cathode-ray excited satellites. Further, in determining excitation potentials, there are certain advantages in the use of the definite quanta $h\nu$ of line spectra as exciting sources, as compared with the rather indefinite energies of the electrons in the cathode stream. The latter lose energy rapidly as they penetrate the target; whereas monochromatic radiation,

[1] D. Coster, Phil. Mag. **43**, 1106 (1922).
[2] M. A. Dauvillier, Comptes Rendus **174**, 445 (1922).
[3] M. A. Dauvillier, Comptes Rendus **177**, 167 (1923).
[4] D. Coster and M. J. Druyvesteyn, Zeits. f. Physik **40**, 765 (1927).

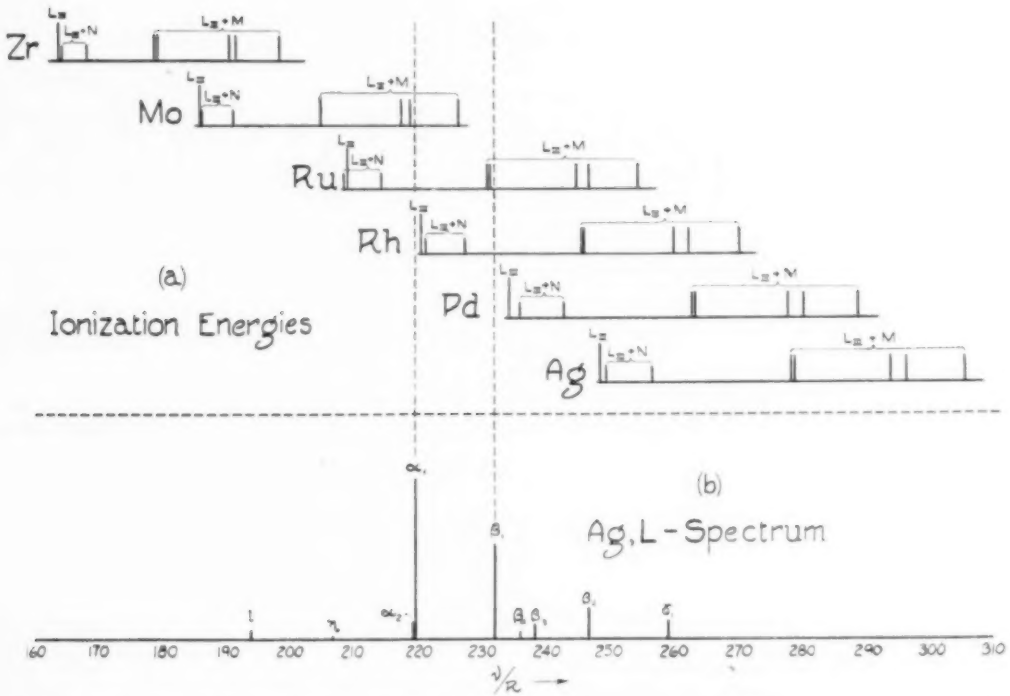

FIG. 1. (a) Plots of various single and double ionization energies. (b) The L-spectrum of Ag(47) showing approximate relative intensities.

as it penetrates the fluorescing substance, although suffering *reduction in intensity*, maintains the same $h\nu$ value, and therefore, when photoelectrically absorbed, gives to each atom exactly the same quantum of energy. Also, from the laws of absorption of x-rays, it is clear that the smaller the amount by which the frequency of the exciting radiation exceeds the absorption limit, the more intense is the fluorescence radiation; with cathode-ray excitation the reverse is the case.

In the present investigation the relative intensities of the satellites of the $L\alpha$ line of Zr (40), Mo(42), Ru(44), Rh(45), Pd(46) and Ag(47), produced by fluorescence excitation, have been obtained and compared with similar results for cathode-ray excitation. The fluorescence excitation was produced by the radiation from an Ag(47) target bombarded by 20 kv electrons. The cathode-ray excitation was by 20 kv electrons.

In Fig. 1b is shown the L-spectrum of Ag(47), plotted to a frequency (ν/R) scale. The heights of the lines represent approximate relative intensities. In Fig. 1a there are shown to the same frequency scale, the L_{III} absorption limits of Zr(40), Mo(42), Ru(44), Rh(45), Pd(46) and Ag(47). It is to be noticed from Fig. 1 that the quantum energy of Ag $L\alpha_1$, the most intense L-series line, is sufficient to ionize the L_{III} shells of Zr(40), Mo(42) and Ru(44) and *possibly* also their accompanying satellites. The L_{III} series of Rh(45), Pd(46) and Ag(47) will not be excited by Ag $L\alpha_1$. Similarly Ag $L\beta_1$, the other strong L-series line, will excite the L_{III} series of Zr(40), Mo(42), Ru(44) and Rh(45); but not the L_{III} series of Pd(46) and Ag(47).

It is generally agreed that satellites arise from some form of double ionization, which, for the satellites of $L\alpha_1$, should be $(L_{III}+M)$ or $(L_{III}+N)$ ionization. For an atom of atomic number Z the energy required for this double ionization will be[5] either $(L_{III})_Z+(M)_{Z+1}$ or $(L_{III})_Z+(N)_{Z+1}$. Plots of the energy, in ν/R units, for L_{III}, $(L_{III}+M)$ and $(L_{III}+N)$ ionization are shown in part (a) of Fig. 1 for the six elements used as fluorescers in this research. If the satellites of $L\alpha_1$ originate in $(L_{III}+N)$

[5] Approximately, since the screening effect of an L electron on the M or N shell is a little less than one.

ionization, their relative intensities in Ru(44) should presumably be similar to the intensities for Zr(40) and Mo(42), since both $L\alpha_1$ and $L\beta_1$ of Ag(47) can excite $(L_{III}+N)$ ionization in all three of these elements. If, however, the satellites originate in $(L_{III}+M)$ ionization, there should be an abrupt change in satellite intensity between Mo(42) and Ru(44), since, except for $M_{IV,\,V}$, $(L_{III}+M)$ ionization cannot be excited in Ru(44) by $L\alpha_1$ and $L\beta_1$ of Ag(47). For elements above Ru(44), such $(L_{III}+M)$ ionization as is produced arises mainly from the continuous spectrum of the Ag(47) target run at 20 kv. Since the mean v/R value of this continuous spectrum is around 1100, its effect in producing either single or double ionization should be nearly equal in all these elements.

Apparatus and Technique

Since at best, fluorescent x-ray spectra are very weak, it is necessary that the exciting radiation should be as intense as possible. This requires: (1) that the anticathode, which is the source of the exciting radiation, should be close to the fluorescing material and (2) that the physical properties of the anticathode material should be such as to make it possible to put a relatively large amount of power into the x-ray tube. Thus the K radiation from a Cu(29) target can be most effectively used to excite the K fluorescence radiation of Ni(28), Co(27), Fe(26) and Cr(24). Similarly the L radiation from a Ag(47) target may be used to excite the L_{III} series of lines in Rh(45), Ru(44), Mo(42) and Zr(40); or with a Au(79) target we may excite the M-series of Ir(77), Os(76), W(74) and Ta(73).

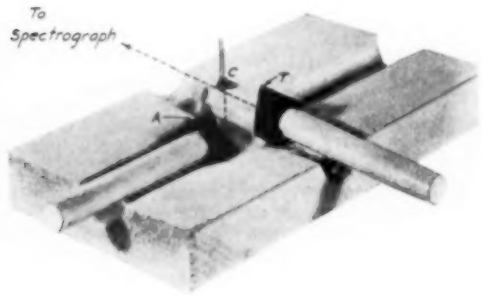

Fig. 2a. Schematic model of x-ray tube, showing relation of cathode, C, to x-ray anticathode, A, and fluorescent target, T.

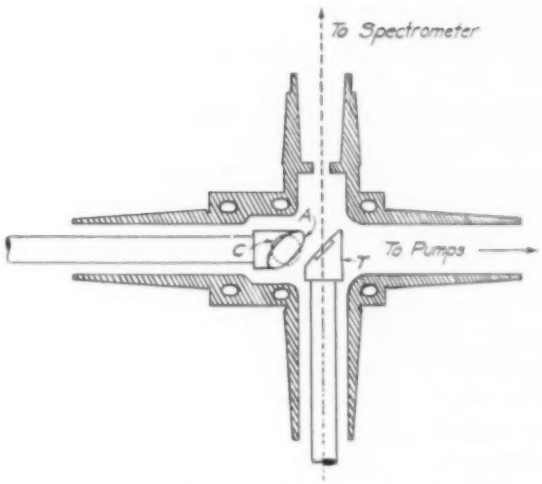

Fig. 2b. Central section of fluorescent x-ray tube.

A special x-ray tube, designed for use with a Siegbahn vacuum-spectrograph, is shown schematically in Fig. 2a and in cross section in Fig. 2b. The hot cathode, C, is centered over the primary x-ray anticathode, A. This anticathode and the fluorescent target, T, are centered in the x-ray tube by the usual glass insulating sleeves. The end of the cylindrical pure-silver head of the anticathode is bevelled off at 45°. The plane face thus formed is tilted (see Fig. 2a) in such a manner that none of the primary (exciting) x-rays from it may enter the spectrograph directly. The primary anticathode, A, is maintained at a high positive potential during operation of the tube; is adequately water-cooled; and faces the fluorescent target, T, which is also water-cooled. Both fluorescent target, T, and cathode, C, are grounded; so that no scattered electrons can reach the target with energy sufficient to excite x-rays. The x-ray tube was run at 20 kv d.c. and 30 m.a. The excitation potential for the L_{III} series of Ag(47) is 3.79 kv.

A preliminary investigation showed that it was essential to clean both the anticathode and the fluorescent target after every hour of operation. Without this precaution, the tungsten layer formed by evaporation from the hot tungsten cathode would actually prevent the emission of the easily absorbed secondary radiation from the fluorescent target, T, and would also prevent much of the silver L radiation from leaving the anticathode.

The most suitable thin window for use between the x-ray tube and spectrograph was found to be a thin film of collodion covered with aluminum leaf to exclude light. The collodion film when freshly made may be subjected to considerable abuse without breaking. Collodion carefully dropped on the surface of clean water immediately spreads into a transparent film. This, if carefully removed, dried and covered with very thin aluminum leaf, serves admirably as a thin window, transmitting about 80 percent of the energy of the Ru $L\alpha_1$ line, ($\lambda = 4.836$A).

The slit of the Siegbahn spectrograph was used at a width of 0.5 mm. This width was found necessary in order to secure sufficient intensity of the fluorescence radiation but was narrow enough to resolve the $L\alpha_{1,2}$ lines and satellites of the elements used as fluorescers (see Fig. 3).

Analysis of Spectrograms

Spectrograms of the $L\alpha$ doublet and satellites of Zr(40), Mo(42), Ru(44), Rh(45), Pd(46) and Ag(47) were obtained by both fluorescence and cathode-ray excitation. Microphotometric records of these spectrograms were made, by using a Moll microphotometer with a device for reducing grain effects as described by Richtmyer and Hirsh.[6] Fig. 3a and b show the microphotometric records of spectrograms of the $L\alpha$ lines of Zr(40) in cathode-ray and in fluorescence excitation, respectively. Similar records for Rh(45) are shown in Fig. 3, c and d.

It has been shown[7] that the density of a

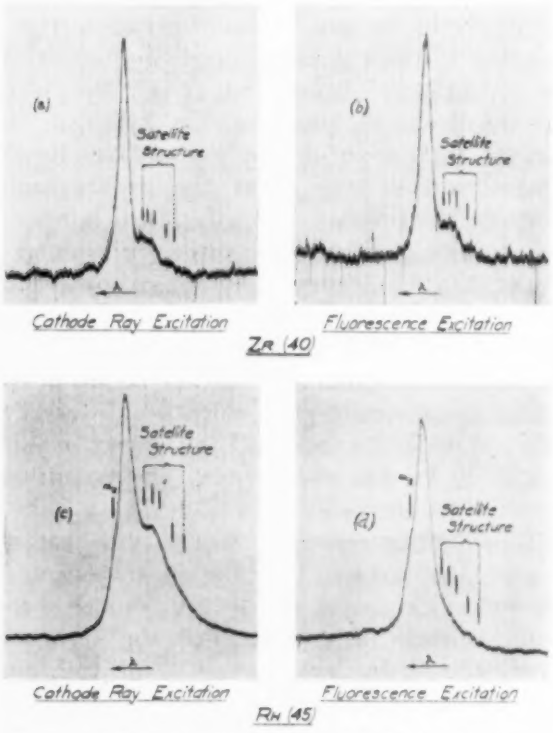

Fig. 3. Microphotometer records of the $L\alpha$ line of Zr(40), (a and b), and of Rh(45), (c and d), produced by cathode-ray and by fluorescence excitation, respectively. Short vertical lines designate positions of satellites and of $L\alpha_2$ as measured by comparator.

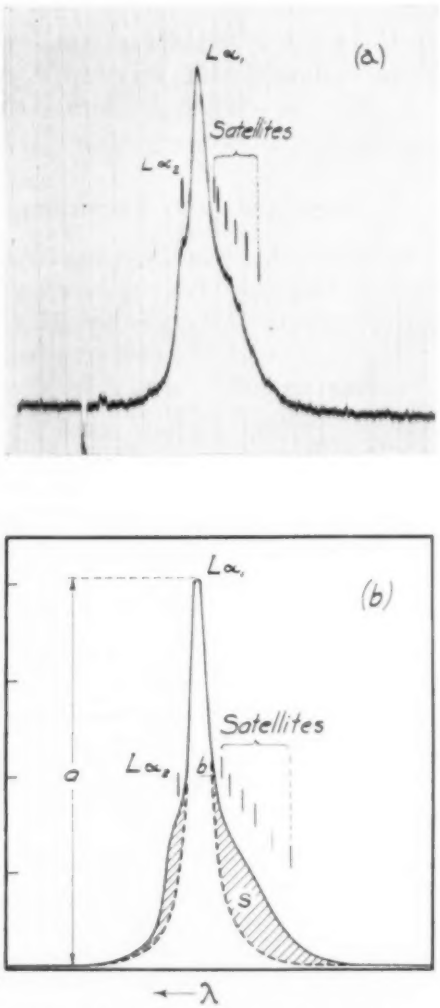

Fig. 4. (a) Microphotometer record of the $L\alpha$ doublet of Ag(47). (b) Density plot derived from microphotometer record. Dotted lines show the foot of $L\alpha_1$ as computed by the Hoyt equation.

[6] F. K. Richtmyer and F. R. Hirsh, Jr., R. S. I. **4**, 353 (1933).

[7] Unpublished work by Professor C. C. Murdock.

photographic plate resulting from exposure to x-rays, is very nearly proportional to exposure[8] for densities up to 0.5. Accordingly, density plots of the microphotometric records were made to show the true energy distribution through the line.[9] Fig. 4a shows the microphotometric record of Ag $L\alpha$ (excitation by 20 kv cathode rays); and Fig. 4b shows the corresponding density plot.

To separate the satellite structure from the parent line, these density plots were analyzed as follows: the location of the background of the parent line was carefully estimated, and its maximum ordinate, a, and half width at half maximum, b, were determined. By using the Hoyt equation[10] $y=a/(1+(x/b)^2)$ the shape of the lower part of the parent line was computed. (See dotted part of Fig. 4b.) The (shaded) area S representing the satellite structure, and the area P of the parent line were then determined. The ratio S/P is then a measure of the relative energy sought.

Results

The relative energies of the satellites and their parent lines, secured by the method described in the preceding section, are given in Table I.

Table I.

Element	Relative Energies	
	Cathode-ray excit.	Fluorescence excit.
Zr(40)	0.19	0.19
Mo(42)	0.30	0.20
Ru(44)	0.54	0.11
Rh(45)	0.72	0.07
Pd(46)	0.40	0.10
Ag(47)	0.33	0.08

The data of Table I are plotted as Fig. 5. The relative energies for cathode-ray and for fluorescence excitation, respectively, are seen to be equal (see also Fig. 3, a and b), for Zr(40). From there, towards increasing atomic numbers, the cathode ray curve (Fig. 5a) rises to a maximum at Rh(45) where the disparity between cathode-ray and fluorescence excitation is the greatest (see also Fig. 3, c and d). From there on, the relative intensity by cathode-ray excitation decreases to the last element studied.

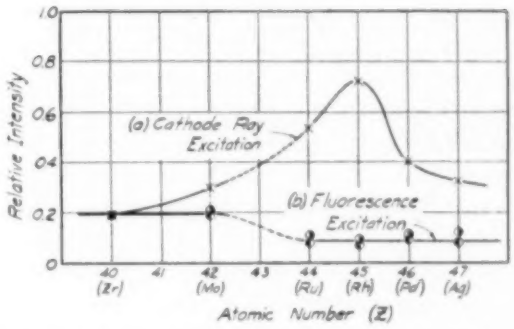

Fig. 5. Relative (integrated) intensities of satellites of $L\alpha_1$ for (a) cathode-ray excitation, and (b) fluorescence excitation

The relative intensities for fluorescence excitation[11] (see Fig. 5b) exhibit a different behavior. For Zr(40) and Mo(42) the satellites' relative intensities are nearly the same; however, at Ru(44) and on through Ag(47) *the relative intensity is about half of the value for Zr(40) and Mo(42).*

The Wentzel-Druyvesteyn hypothesis[12] of satellite origin suggests a reason for this decrease. According to this hypothesis, the $L\alpha$ satellites occur as a result of the simultaneous ionization of the L_{III} electron shell and some of the M-shells, with a single electron transition. H. C. Wolfe[13] has recently considered the possible merits of the Wentzel-Druyvesteyn hypothesis with encouraging results in the calculation of the frequency separations of the K-satellites and their parent $K\alpha_1$ line for K(19). Very recently, an article by Coster and Thijssen[14] reports that the excitation potential for the satellites $K\alpha_{3,4}$ of S(16) is 2700 ± 25 volts, whereas 2675 is the theoretical value for S(16) KL ionization.

The decrease in the relative intensity for the fluorescent satellites in passing from Mo(42) to Ru(44),[15] (Fig. 5, curve b), suggests $(L+M)$

[8] G. W. Brindley (Phil. Mag. **16**, 686 (1933)), finds that for the Mo $K\alpha$ doublet, ($\lambda\sim0.7$A), density is proportional to intensity for values of the density up to 1.4.

[9] The reciprocity law of photographic exposure is assumed to hold for x-rays. See F. C. Blake, Rev. Mod. Phys. **5**, 193 (1933).

[10] A. Hoyt, Phys. Rev. **40**, 477 (1932).

[11] In Fig. 5b independent data from two sets of plates are recorded.

[12] M. J. Druyvesteyn, *Dissertation*, Groningen (1928).

[13] H. C. Wolfe, Phys. Rev. **43**, 221 (1933).

[14] D. Coster and W. J. Thijssen, Zeits. f. Physik **84**, 689 (1933).

[15] It is to be regretted that Ma(43) is not available in sufficient quantity for study.

ionization as the origin of some, at least, of the satellites of $L\alpha_1$, as explained in the introduction.

However, curve *a* of Fig. 5 shows that the relative intensity of satellites for cathode-ray excitation varies rapidly as we pass through the atomic number range studied. Since, in this small range of atomic numbers, the only changes in electron configuration which take place are in N and O shells,[16] we must conclude that, in cathode-ray excitation at least, the electron population of N and O shells exerts a profound influence on the production of the satellites of $L\alpha$. It is not at all clear how this influence could be exerted if these satellites originate in $L+M$ ionization.

Attention should be called to the magnitude of the intensity of the satellites. Frequently, satellites are spoken of as weak lines; and, indeed, many of them are. But the present data show that the integrated intensity of the group of lines which make up the satellites of $L\alpha_1$ may be as high (in the case of Rh(45)) as 72 percent of the intensity of the parent line. No theory of double ionization yet advanced accounts for intensities as great as this.

[16] See, for example, the *Structure of Line Spectra* by Pauling and Goudsmit for a table of the electron configuration of the elements.

Acknowledgments

The senior author (F. K. R.) wishes to acknowledge his indebtedness to the Heckscher Research Council of Cornell University, for grants which made possible the purchase of certain apparatus used in this study.

The junior author wishes to express his sincere appreciation of the action of the Physics Department of Cornell University in placing research facilities at his disposal.

Measurement of the Ionization Per Centimeter of Path by Individual Secondary Cosmic Rays[1]

W. F. G. SWANN, *Bartol Research Foundation of The Franklin Institute*

(Received October 16, 1933)

The paper describes measurements of the ionization caused by individual secondary cosmic rays and groups of rays in a vertical cylinder 15 cm high and 7.5 cm in diameter. The experimental results are represented by plotting $F(n)$ against n, where $F(n)dn$ is the number of rays or groups passing through the cylinder in an assigned time and giving rise to spurts containing between n and $n+dn$ pairs of ions. If $f(l)dl$ is the number of rays of path length between l and $l+dl$, the theoretical curve for $f(l)$ for single rays shows a discontinuous increase at a value of l equal to the length of the cylinder, and this is followed by a sharp decrease. This phenomenon enables one to ascertain on the $F(n)$ curve the value of n which corresponds to the length of the cylinder, and so to deduce the ionization per centimeter of path in spite of the existence of multiple rays and of unavoidable amplifying tube background. The value for argon comes out as 89 ions per centimeter at atmospheric pressure. This value includes the contribution cited by G. L. Locher as caused by the Auger effect. The corresponding values for nitrogen and oxygen are 61 and 57, respectively. By a further analysis of the results, and particularly of those giving simultaneous spurts of ions with two cylinders in line, the existence of multiple rays is actually verified. These rays contribute two-thirds of the total ionization observed in the cylinder, and constitute one-third of the total number of ionizing entities, groups and singles. By a consideration of their effects it is possible to reconstruct the high values obtained for the *apparent* ionization per centimeter of path by former observers who have deduced their values from ionization measurements combined with counter data and from fluctuation measurements.

INTRODUCTION

THE fact that secondary cosmic rays contain electrons and positrons of energies higher than those observed in radioactive substances causes the investigation of their ionization per centimeter of path to be a matter of considerable interest, particularly as indirect investigations of this number have given values ranging all the way from 36 to 165 for the ions produced per centimeter of path at atmospheric pressure, in air, for example.[2] The experiments here described constitute a direct attack upon the problem in that the plan involves the actual measurement of the ionization of the individual rays. The accuracy at present is not high, but modifications of the method designed to secure a better approach to precision measurements have been made and the results of such measurements will be reported in due course. The accuracy of the present measurements is sufficient to bring to light certain interesting features, to establish the ionization per centimeter of path as around 90 ions per centimeter at atmospheric pressure in argon (which would correspond to about 60 for air rather than about 150), and to demonstrate the importance of double and triple rays in having contributed to the reason for the higher figure found by certain former observers.

[1] Presented in preliminary form before the American Physical Society, at the New York meeting, February 24, 1933, and in greater detail before The American Philosophical Society, at Philadelphia, April 22, 1933.

[2] By counting the individual drops in a cloud chamber, values of the order 40 ions/cm in air have been obtained by D. Skobelzin, by G. L. Locher and by C. D. Anderson. On the other hand, from counter data combined with the magnitude of the total ionization per second in a vessel, W. Kolhörster and L. Tuwin, working jointly, also W. Messerschmidt, and T. H. Johnson, have obtained values ranging from 110 to 165 ions/cm.

EXPERIMENTAL PROCEDURE

The essentials of the apparatus will be clear from Fig. 1. A vertical cylinder A was provided with a central insulated rod which was connected to an FP-54 Pliotron, which in turn was connected to a four stage amplifier operating a short period galvanometer which recorded upon mov-

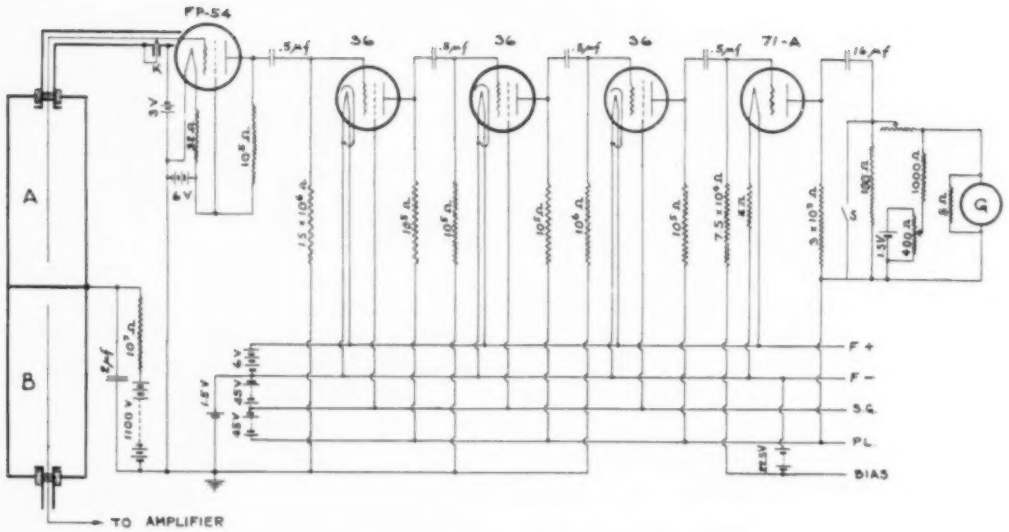

FIG. 1. Diagram of apparatus and electrical circuits.

ing photographic paper. The cylinder was filled with argon in the main experiments, to a pressure of 5 atmospheres in some cases and 10 atmospheres in others. A potential difference of 1100 volts was applied between the outer cylinder and the rod, so that the ions produced by an individual ray were swept across and caused to record upon the galvanometer. The more rapidly the ions are swept across, the sharper the kicks on the galvanometer and the greater the certainty in resolving them. The time taken to carry an ion from the central rod to the wall of the cylinder was of the order 0.05 second. The time for an electron is much less. The galvanometer used was of the Kipp and Zonen short period type modified to have a period comparable with 0.05 second.

For the purpose of securing additional information, two such systems as the above were employed, with the cylinders A and B arranged end to end, and with the galvanometers arranged to record upon the same photographic paper.

The main features of the electrical circuits will be clear from the data given in Fig. 1. The 1100 volt potential was applied through a resistance of 10^7 ohms to the outer cylinders which were connected to one terminal of a 2 microfarad condenser, whose other terminal was connected to the common point which served as the "earthed point" of the apparatus. In this way, battery fluctuations were ironed out. The insulated system was of course protected by a suitable guard ring system, and the FP-54 Pliotrons were incased in very thick copper cylinders with lids making electrical contacts with the cylinders all over their top surfaces through the agency of mercury. The reason for this was to secure very high conductivity in the shield for the purpose of eliminating electromagnetic disturbances of relatively low frequencies.

In spite of the fact that the apparatus was mounted in a ferro-concrete building of very rigid construction, the additional precaution of mounting the FP-54 tubes with their associated cylinders A and B on spring supports was found desirable and was adopted. The best test of the absence of spurious kicks produced by vibrations, electrical oscillations, etc., was that provided by taking a set of observations with the cylinders A and B at atmospheric pressure, in which case the ionization effects were reduced to relatively small amounts, and any spurious disturbances showed up. Since the kick obtained upon the galvanometer for a given number of ions collected depended upon the time of collection of the ions, and upon the time constants of the circuit to some extent, the calibration was carried out in such a manner as to minimize the error due to this cause. A known potential was applied to the external cylinder, A, for example, through a circuit

by which the time of application of the potential could be controlled to an amount comparable with the time of collection of the ions. A knowledge of the coefficient of induction between the cylinder and the insulated system then enabled the sensitivity of the apparatus to be calculated as nearly as possible under the conditions of the actual experiments. It may be of interest to remark that variation of the time of application of the potential from zero to 0.1 second caused a variation of about 20 percent in the kick obtained on the galvanometer.

In order to avoid trouble from electrons emitted from the walls of the cylinders *A* and *B* by gamma-rays from the atmosphere, the cylinders were shielded by about 8 cm of lead. By observing the modification produced in the records by the addition of the lead and by observations made with radium outside the lead, one could verify that the trouble due to natural gamma-radiation was negligible, at any rate in the shielded condition.

The Records Obtained

The complete records obtained involved many thousands of counts and it is naturally only possible to give typical illustrations. Such are shown in Fig. 2. Each kick of the galvanometer is accompanied by a back kick. This is not a phenomenon of inertia but is properly inherent in the action of the amplifier as a little consideration will show. The measurements were made on the basis of the primary kicks and were calibrated accordingly. In Fig. 2, the spot should be regarded as travelling from right to left.

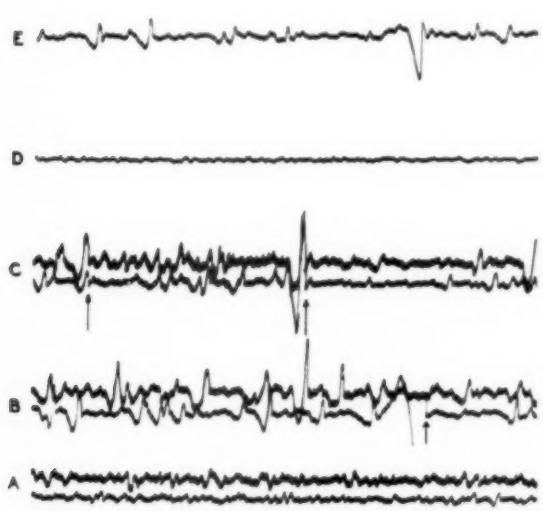

Fig. 2. Sample ionization records.

Fig. 2*E* represents a portion of a record taken with a cylinder 30 cm long and 4 cm in diameter filled with argon to 200 lb pressure. It is characterized by one very long kick which possibly represents an alpha-particle. The medium sized kicks are secondary cosmic-ray kicks. Fig. 2*D* is a trace for the same cylinder at atmospheric pressure and serves to show an upper limit for the magnitude of the background disturbances which are in part, at any rate, produced by the secondary cosmic rays. The sensitivity in the cases *D* and *E* is such that one millimeter kick on the original record corresponds to the instantaneous application of 4.0×10^{-5} volt to the central system. Fig. 2, *C* and *B*, represents simultaneous traces for two cylinders in line as in Fig. 1, each cylinder being 15 cm long and 7.5 cm in diameter filled with argon to 70 lb. pressure. The voltage sensitivity was about twice that for cases *E* and *D*. The arrow in case *C* indicates simultaneous kicks, and represents cases where a ray has passed through both cylinders. However, simultaneous kicks of this kind are unreliable of interpretation on account of the production of spurious coincidences by different rays which happen to coincide very nearly in time in the two cylinders. They are, however, reliable when used in the sense of *upper limits* to the number of real coincidences; and it is only in this sense that we shall use them. In Fig. 2*B*, the arrow indicates a portion of the trace of an alpha-particle for which the kick went completely off the photographic paper. Fig. 2*A* represents the same cases as *B* and *C* except that the pressure was one atmosphere.

Analysis of the Results

The full curve of Fig. 3*A*, shows, for a cylinder 15 cm long and 7.5 cm in diameter filled with argon at 5 atmospheres pressure, the values of $F(n)$ plotted against n where $F(n)$ is the coefficient of dn in the expression for the number of kicks in 2000 seconds which corresponds to a production of ions between n and $n+dn$ in number. The abscissae are the values of n. The curve

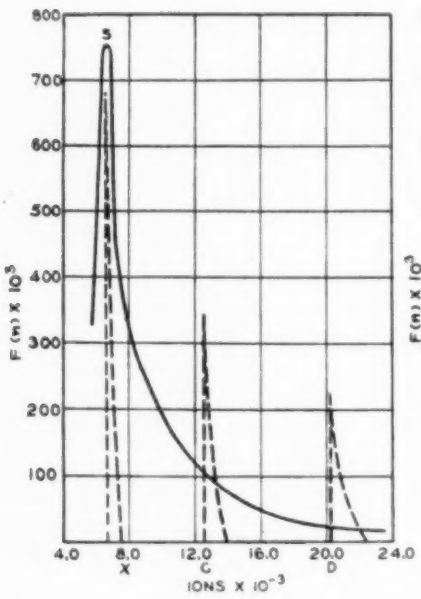

FIG. 3A.

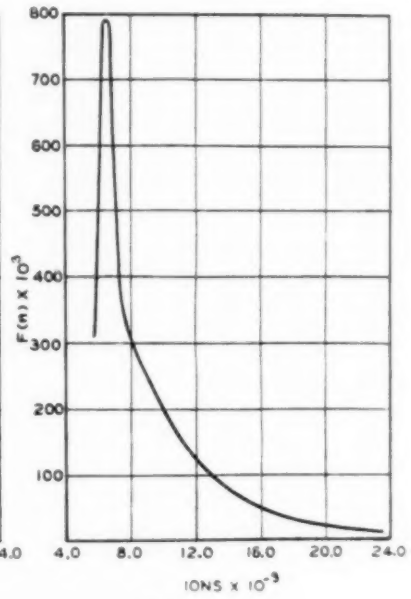

FIG. 3B.

represents the results of 2700 observations of kicks, about half of all the observations taken. Fig. 3*B* represents the results of the other half of the observations. The two are given merely to show the extent of reproducibility of the results. The curves are not continued back to $n=0$ because for the smaller values of n the observations become obscured by the background disturbances of the FP-54 tube. As far back as they are drawn they are definite and reproducible to the extent indicated. If all of the rays were single rays of the same kind, the curve should correspond in form to the curve representing $f(l)$, the coefficient of dl in the expression for the number of rays which travel lengths between l and $l+dl$ in the cylinder for which the observations represented in Fig. 3 were taken. In Fig. 4, the theoretical curve is shown. The complete derivation of the formulae upon which this curve is based is given by the writer in a paper, *The Distribution of Cosmic-Ray Paths in a Vertical Cylinder*.[3] The constant A incorporated with $f(l)$ in the ordinates is the number of rays falling per second per unit vertical solid angle per unit of area perpendicular to the vertical.[4] Small a is the

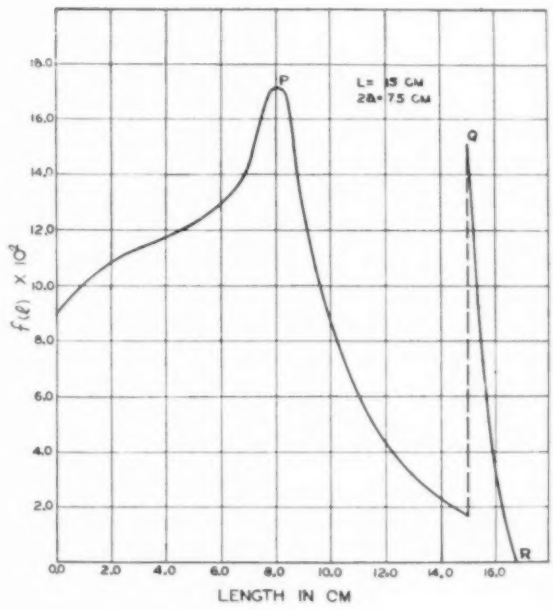

FIG. 4.

radius of the cylinder. The points P, Q and R correspond respectively to the diameter of the cylinder, the height of the cylinder and the longest line which can be drawn in the cylinder.

[3] W. F. G. Swann, J. Frank. Inst. **216**, 559 (1933).

[4] Its value in Fig. 4 is taken as 0.72×10^{-2}, which value was obtained by Dr. Gordon Locher by means of Geiger counters in an adjoining room on the same floor of the laboratory as that in which the experiments were conducted.

The point Q is preceded by an actual discontinuity in the curve. The theoretical curve is drawn under the assumption that the intensity of the rays is proportional to $\cos^2\theta$ where θ is the angle from the vertical, this law being an empirical expression of the facts of counter measurements. It must be remarked that the form of this law is representative of conditions in the open, while the observations here recorded were taken in a laboratory. However, the existence of peaks in the curve at P and Q and the positions of these peaks are phenomena depending upon the geometry of the cylinder rather than upon the law of distribution of the rays with θ. While a modification of the law of distribution would materially affect the relative heights of the ordinates of the curve for different values of l, it would not affect, except under very drastic conditions, the positions of the peaks. It will be mainly the positions of these peaks, and particularly that of the peak at Q which will be the basis of our comparison of the experimental and theoretical curves in what follows.

A casual inspection of Figs. 3 and 4 might suggest that the point S of Fig. 3 was to be associated with the point P of Fig. 4. However, a closer examination of the situation shows that such an association would be inconsistent with the facts. For if P of Fig. 4 corresponded to S of Fig. 3, then Q of Fig. 4 would correspond to C of Fig. 3. Now, for corresponding ranges dl and dn in the abscissae of the two curves $Tf(l)\,dl = F(n)\,dn$, where T represents the time interval (2000 seconds) to which the observations of Fig. 3 correspond. Moreover, if q is the number of ions per centimeter of path, $dn = qdl$. Hence $F(n) = (T/q)f(l)$. If we associate Q of Fig. 4 with C of Fig. 3, q becomes determined as n_c/L where n_c is the value of n at the point C. As a matter of fact, under these assumptions, q comes out as 850 and $F(n) = (2000/850)f(l)$. If we plot this quantity for the part of the graph to the right of C, we obtain the dotted curve shown near C in Fig. 3. This curve represents absolute magnitudes on the scale of the figure. The experimental curve shows no evidence of a discontinuity or peak to correspond to this condition. Experimental errors could not conceal such a peak if it really existed; for, such errors are all in the direction of giving spurious kicks, and so of increasing the apparent values of $F(n)$. We conclude that C cannot correspond to Q. If we choose such another point as D to correspond to Q, the theoretical contribution to $F(n)$ in the region of D would be given by the dotted curve there shown, and the absence of a peak would be still more difficult to explain. In fact, proceeding from the extreme right, the first and only place on the full curve of Fig. 3 which is capable of corresponding to Q is the point S. We must then conclude that Q and S correspond. The actual theoretical contribution to $F(n)$ resulting from this association is shown by the dotted curve in the vicinity of S. The absence of an absolute discontinuity in the experimental curve with accompanying broadening is only to be expected in view of the fact that $F(n)$ has to be determined by the utilization of finite ranges dn. The tube background plays an important part for values of n as small as those for the point S. On the other hand, the existence of an absolute and reasonably large discontinuity at Q, Fig. 4, combined with the sharp fall in the curve to the right of Q saves the situation as regards locating the abscissa of the peak in Fig. 3 in spite of the existence of the background. The peak should be able to show itself on the top of a background of ordinate much greater than its own, unless that background happened to have a sharp depression to cancel it, and this is highly improbable. The point which we wish to emphasize is that the abscissa of the peak at S has a significance which is unaffected by the background in spite of the fact that the actual experimental values of $F(n)$ there may be entirely unrepresentative of the ideal magnitudes freed from background.

The part of Fig. 3 which should correspond to P lies, of course, so far in the region of small kicks that it is entirely covered by the background; and, indeed, no attempt has been made to plot $F(n)$ in this region.

We must not expect to establish a close agreement between Fig. 3 to the right of S and Fig. 4 to the right of Q because, as will presently be seen, the right-hand portions of Fig. 3 are determined largely by doubles, triples, etc. These matters, like the existence of tube background have no effect upon the establishment of the correspondence between the abscissae of Q and S, and once that correspondence is established the

number of ions per centimeter of path becomes determined. Its value comes out as *89 ions per centimeter of path for argon at one atmosphere* on the basis of a linear relationship with pressure, which assumption is valid for the range of pressure concerned, and particularly so for argon.

Evidence of Existence of Doubles, Triples, etc.

It is now of interest to examine certain other features of the portion of the curves, Fig. 3, which lie well to the right of S. Theoretically, on the view that the rays are singles, there should be one kick length which is the greatest possible and which corresponds to the longest path length attainable in the cylinder. As a matter of fact, experiments show a more or less continuous distribution of kick lengths extending up to values which would correspond to several hundreds of ions per centimeter of path at atmospheric pressure, although the number of such kicks diminishes with the size of the kicks. Suppose we fix on any kick length, such for example as that corresponding to the point C, as representative of a path comparable with the whole length of the cylinder. Now it will be obvious from the geometry of the situation that, on the basis of single rays, the number of rays which pass through the top of the upper cylinder and the bottom of the lower cylinder is of the order of one-quarter the number passing through the top and bottom of the upper cylinder. Hence, if we should choose C as representative of the rays which have travelled the whole length of one cylinder, we should find that about one-quarter of the corresponding kicks for the upper cylinder should show coincidences of equal numbers of ions for the lower cylinder. The experimental data for the point C give only about 0.04 instead of a quarter where a relatively liberal range of about 20 percent is allowed in judging the equality of coincident kicks. Fig. 5 shows as a function of n the actual value of the ratio of the number of equal coincident kicks to the number of the same size in the upper cylinder. In no case from the kicks corresponding to S to those of the largest size measured did the ratio approach 0.25. At first sight one might suppose that the reason for the above fact was to be found in the supposition that some of the rays were

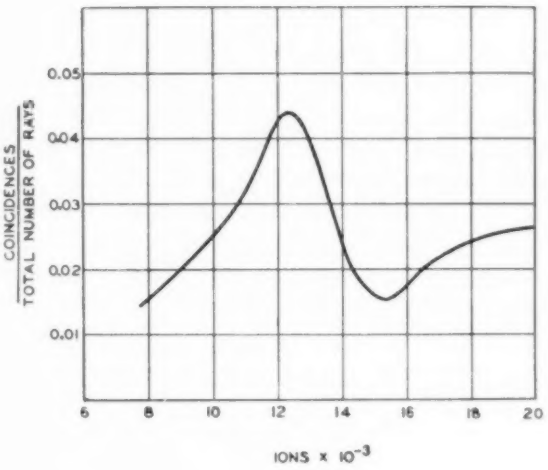

Fig. 5.

absorbed in the thin partition which separated the two cylinders. This partition, however, was only 2 millimeters thick, and we need only turn our attention to Fig. 6[5] which gives the theoretical variation of ionizing efficiency with the energy of the rays in the case of electron-like rays to see that absorption cannot be the cause. If we should assume that the rays corresponding to the point C were single electrons they would have to correspond to about 120 ions per centimeter of path for nitrogen. We know that β-particles of the order 3×10^6 volts velocity produce only

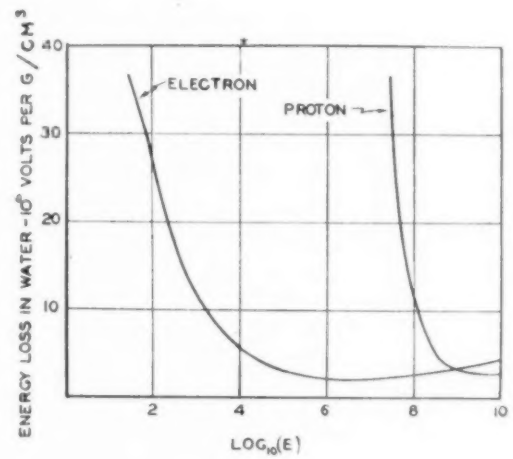

Fig. 6.

[5] This curve is copied with a change of units from a curve given in a paper entitled *Some Photographs of the Tracks of Penetrating Radiation*, by P. M. S. Blackett and G. P. S. Occhialini, Proc. Roy. Soc. **A139**, 699–726 (1933).

about 30 ions per centimeter of path in nitrogen so that in order to account for 120 ions per centimeter of path, it is necessary to assume that the electrons correspond to an ordinate of the curve Fig. 6 which is at least three times the minimum. As a result we should have to assume for the electron energies greater than 10^{10} volts or smaller than 10^{5} volts. With the former energy, the electrons would have no difficulty in getting through the two millimeters of brass partition, while, with the latter energy they would not be able to produce more than about three thousand ions, that is, less than corresponds to the measured kicks associated with the point C, which kicks correspond to about 12.6×10^{3} ions. We get an interpretation more consistent with the facts if we assume that these rays are doubles or triples with a finite angle between them, and with these conditions it is easily possible to see that the angle might be such that while two rays could frequently pass through the whole length of a single cylinder, they could never pass through the whole length of the double cylinder. In general, of course, the phenomenon under discussion would show itself not by a complete absence of equal coincidences between the upper and lower cylinders but by a paucity of such coincidences in comparison with what might be expected from the simple interpretation on the basis of single rays. Fig. 5 shows a peak at the value $n=12.2\times10^{+3}$. On the basis of the ionization per centimeter of path already established in the last section, this value 12.2×10^{3} is just the value corresponding to a *double* ray which has travelled the full length of a single cylinder.[6] It is probable that the same geometrical considerations which operate to cause the discontinuity in $f(l)$ at Q, Fig. 4, for a length of ray equal to the length of the cylinder operate here also. If we concentrate our interest on pairs of rays, the sum of whose path lengths in each cylinder is equal to l, it is probable that the number of such pairs per unit range of l will show a discontinuity for the value of l which is *just* great enough to insure that the rays enter through the top of the upper cylinder and pass through the bottom thereof, in which case, of course, they would also pass through the bottom of the lower cylinder. On such a view the existence of the peak in Fig. 5 and particularly the value of its abscissa are confirmatory evidence of the presence of doubles in these measurements.

Of course it is not intended to imply that all of the single branches of the rays are alike. Some may be positrons and some electrons; and the energies may vary widely. However, large variations of energy in the region of minimum ionization or in the region of higher energies give, theoretically, relatively small changes in ionization. It is probably for this reason that the peak in Fig. 3 is as sharp as it is.

Arguments against the larger kicks being caused by protons are to be found in the fact that, as may be seen from Fig. 6, there is such a narrow range of energies for which protons have ionizing efficiencies appreciably greater than the minimum and yet have enough energy to penetrate the partition between the cylinders.

Ionization in Other Gases

Experiments were made for argon, nitrogen and oxygen in a cylinder 30 cm long and 4 cm in diameter. Fig. 7 shows the curves for $F(n)$. Here, on account of the small numbers of rays which travel the whole length of the cylinder, the peak corresponding to S, Fig. 3, is not to be expected

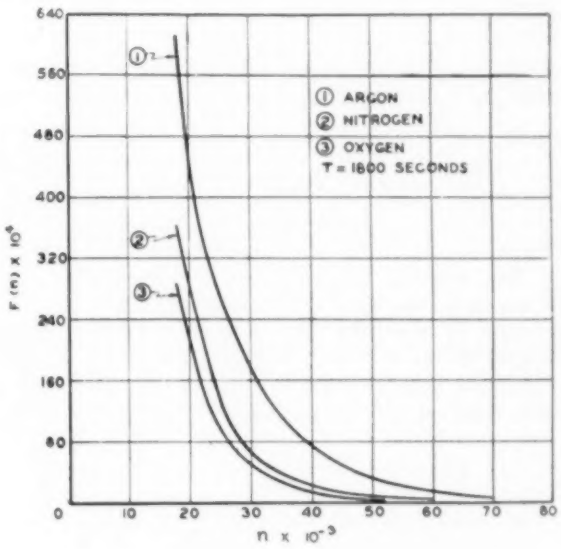

Fig. 7.

[6] The effect of tube background is such as to render impracticable the realization of the corresponding peak for single coincident rays.

to show itself. However, one may assume that the distribution of rays, singles, doubles, triples, etc., is the same for all gases. Hence, if we choose three points on the three curves which correspond in the sense that the total number of rays to the right of those points is the same for all, and if we add up the ionizations for all of these rays in each case, the ratio of the numbers so obtained should give the *ratio* of the ionization per centimeter of path for single rays for the three gases in spite of the fact that the measurements are actually based upon doubles and triples. By choosing several corresponding sets of three points in this manner, the ratio of the ionization was obtained and this combined with the absolute value cited above for argon gives the following values for the ionization per centimeter of path at one atmosphere in the three gases concerned. The values are: for argon, 89; for oxygen, 57; for nitrogen, 61.[7]

Correlation with Former Data

Referring again to the data obtained with the shorter vessel, and assuming, as we have done, that S, Fig. 3, corresponds to Q, Fig. 4, it is possible to mark on Fig. 3 a point X which corresponds to R of Fig. 4. It is certain that all rays to the right of X represent multiples. Regardless of what they represent, however, we can obtain their total number N_1; and, from the sizes of the kicks to which they correspond, we can obtain their total contribution I to the ions per cc per second in the vessel. We find $N_1=3500$ and $I=2.2$ ions/cc/second, the latter value being reduced to nitrogen at atmospheric pressure. The experimental curve to the left of X must involve mainly singles. Except as regards the position of the peak, it is unreliable in quantitative significance on account of tube background. However, the theoretical curve Fig. 4 which is based upon the experimental value 0.72×10^{-2} for the A occurring as a factor in $f(l)$ serves as a basis to calculate the number N_2 of single rays which occur to the left of X. We find $N_2=6150$. Incidentally, therefore, it is of interest to notice that the number of multiples is a little more than one-third of the total number. In terms of the ionization per centimeter of path already determined, but reduced to nitrogen, we find that the total ionization caused by the single rays corresponds to $I_2=1.1$ ions/cc/sec. Thus, the total ionization per cc per sec. in the vessel is $2.2+1.1=3.3$ which is not far from the recent value 2.48 given by Millikan. No precision accuracy is, however, claimed for the former figure. The total number of ions produced per second in the whole volume of the vessel is 2200. If we divide this by the average ion path in the vessel, as obtainable from Fig. 4, and by the total average number of kicks per second which in this case is $(N_1+N_2)/4000=9650/4000$, we obtain 126. This then is the value that we might expect to be found for the ionization per centimeter of path in an experiment which failed to take account of the fact that the rays were in part multiples and which sought the quantity by dividing the ionization per second by the average ion paths and by the total number of rays. It falls well within the range 110–165 ions per centimeter already quoted as cited by former investigators who have used such methods. It is perhaps of interest, however, to realize that in the present work the same set of observations which treated in this way yields the high values can also through proper interpretation of the significance of the multiple rays be made to yield the smaller value 61 ions per centimeter of path in nitrogen.

In conclusion, I wish to acknowledge the services of my research assistant, Mr. W. E. Ramsey, who has made the actual observations cited in this paper. I also wish to express my appreciation of the services of Mr. Oscar Steiner, the Chief Mechanician, and his assistants in the construction of portions of the apparatus.

[7] The ratio of ionization for argon to that for other gases is less than that found for the total ionization per cc as obtained by other observers. It is to be noted, however, that the ratio of the initial recombination loss in oxygen and nitrogen to that for argon is a function of the collecting time, which is particularly short in the present experiments.

X-Ray Diffraction in Long Chain Liquids

B. E. WARREN, *Eastman Laboratory of Physics, Massachusetts Institute of Technology*

(Received August 21, 1933)

The diffraction of x-rays in long chain liquids is calculated by the method of Zernicke and Prins. In the liquid, the long cylindrical molecules are arranged quite at random in space and orientation, except in so far as the condition for relatively dense packing necessitates that about any one long molecule, the nearest neighbors be roughly parallel. The main peak is due to a concentration of scattering matter at a distance about 8 percent larger than the lateral distance between chains. The inner peak, which is observed for the alcohols and the fatty acids, measures the distance from the heavy end group to the gap at the opposite end. For relatively long chains this distance becomes equal to the chain length.

INTRODUCTION

THE x-ray diffraction halos produced by liquids have been studied by a number of workers. For a summary of the work up to 1928, reference should be made to the paper by Drucker.[1] For liquids in which the molecules are essentially spherical, it has been shown[2, 3] that the position of the principal diffraction peak is satisfactorily given by the Ehrenfest-Keesom[4] relation

$$\lambda = 0.814 \times 2a \sin \theta. \qquad (1)$$

In this relation a is the mean distance between any one molecule and its nearest neighbors and under the assumption of a close packing of spheres is readily calculated from the molecular weight and the density.

$$a = 1.33(M/\rho)^{\frac{1}{3}}. \qquad (2)$$

As would be expected, for molecules which depart appreciably from spherical shape, the two relations above lose their simple meaning, and the values of a calculated by the two methods no longer correspond.

In this paper we shall consider the diffraction of x-rays in three series of long chain liquids; the fatty acids, normal alcohols and normal paraffins. These series of long chain liquids seem particularly attractive because of the distinctive shape of the molecule, and also because excellent experimental scattering curves are available in a series of papers from the laboratory of G. W. Stewart.[5, 6, 7]

The method which we shall use in treating the problem of x-ray diffraction in liquids is a modification of the method which has been used successfully by Zernicke and Prins.[8] The intensity of coherent scattering from an array of atoms which takes all possible orientations in space is given by the expression

$$I = \sum_m \sum_n f_m f_n \frac{\sin (sr_{mn})}{sr_{mn}}; \quad s = \frac{4\pi \sin \theta}{\lambda}, \qquad (3)$$

in which 2θ is the angle of scattering, f is the atomic scattering factor and the summation is taken with respect to any one atom over all the other atoms including the one singled out, and then the one singled out is in turn allowed to be each of the atoms in the array. For a liquid in which there is only one kind of atom present, and

[1] C. Drucker, Phys. Zeits. **29**, 273 (1928).

[2] W. Keesom and J. de Smedt, Proc. Amsterdam **25**, 118 (1922); **26**, 112 (1923); Physica **5**, 125 (1924).

[3] J. R. Katz, Zeits. f. Physik **45**, 97 (1927).

[4] Although the original derivation of this relation did not justify its application to liquid diffraction, its applicability to a liquid containing spherical molecules has since been fully established by the rigorous and elegant derivation of Zernicke and Prins.

[5] Stewart and Morrow, *Normal Alcohols*, Phys. Rev. **30**, 232 (1927).

[6] G. W. Stewart, *Normal Paraffins*, Phys. Rev. **31**, 174 (1928).

[7] G. W. Stewart, *Fatty Acids*, Proc. Nat. Acad. **13**, 787 (1927); R. Morrow, Phys. Rev. **31**, 10 (1928).

[8] Zernicke and Prins, Zeits. f. Physik **41**, 184 (1927).

if on the average each atom is surrounded in the same way as every other atom, then (3) reduces to

$$I = Nf^2 \sum_n \frac{\sin sr_n}{sr_n}, \qquad (4)$$

where N is the total number of atoms. The distribution of surrounding atoms can be represented by a radial density function $g'(r)$ in terms of which (4) becomes

$$I = Nf^2 \int_0^\infty g'(r) \frac{\sin sr}{sr} dr. \qquad (5)$$

To facilitate convergence, we imagine a uniform density of negative scattering matter spread throughout the liquid and just equal and opposite to the average positive density. So long as this negative density has an indefinite outer boundary and we do not consider angles of scattering which are less than several seconds, it will, of course, give rise to no diffraction effects and hence does not alter the problem.[9] By introducing a resultant density $q'(r)$, Eq. (5) becomes

$$I = Nf^2 \int_0^\infty q'(r) \frac{\sin sr}{sr} dr, \qquad (6)$$

where $q'(r) = g'(r) - 4\pi r^2 \rho$. At large distances the positive density just cancels the negative density, and $q'(r)$ becomes zero. Hence it is only necessary to carry out the integration in (6) over small values of r.

In a liquid made up of spherical molecules in approximately close packing, there will be a positive peak in the radial density curve at a distance equal to the inter-molecular separation $r = a$. The intensity, as given by (6), will show a maximum at a value of $(\sin\theta)/\lambda$ which gives the function $\sin s\alpha / s\alpha$ a positive maximum and this occurs first at a value $sa = 7.72$.

$$4\pi a \frac{\sin\theta}{\lambda} = 7.72; \quad \lambda = 0.814 \times 2a \sin\theta. \qquad (7)$$

This is the significance of the factor 0.814 in the Ehrenfest-Keesom relation.

[9] For any practical set-up the angle of scattering must be less than one second in order that the greatest path difference in the radiation scattered by different parts of the sample shall be less than one wave-length.

For small values of $(\sin\theta)/\lambda$ it should be noted that the function $\sin(sr)/sr$ approaches unity and (6) becomes

$$I = Nf^2 \int_0^\infty q'(r) dr.$$

But from the definition of $q'(r)$ this integral is equal to zero and hence at small angles of scattering the intensity approaches zero.[10] The statements to be found in the literature that small scattering at small angles necessarily indicates a crystalline scatterer are grossly incorrect. It merely indicates that the atoms are close together as in a solid or liquid, rather than widely separated as in a gas.

Liquid Paraffins

The scattering curves for the whole series of liquid paraffins[6] are essentially the same, regardless of the number of carbon atoms in the chain. There is a single strong peak occurring at roughly $(\sin\theta)/\lambda = 0.108$. This fact simplifies the problem enormously, because it shows that we can neglect end effects and hence treat a chain of indefinite length, along which all the carbon atoms are to be considered as equivalent. For a first approximation the effect of the hydrogens can be neglected. We will picture the chains as roughly cylindrical in shape and in a fairly dense packing in the liquid, such that about any one cylindrical chain, the six nearest neighbors are roughly parallel. (Fig. 1(a).)

The lateral inter-chain distance can be calculated from the effective cross-sectional area of the chain. From the molecular weight, density, and the known length of chain from measurements on crystalline paraffins, one obtains the area of 21.4A^2, which checks well enough the value 21.0A^2 obtained by Adam[11] from measurements on surface films of fatty acids. Using an

[10] At angles of scattering less than several seconds this statement is, of course, not true since the introduction of the continuous negative density is justifiable only for angles greater than several seconds. In directions differing from that of the main beam by angles of a second or less, the atoms re-enforce to produce the strong "zero order" diffraction beam.

[11] N. K. Adam, Proc. Roy. Soc. **A99**, 336 (1921); **A101**, 452 (1922); **A103**, 676, 687 (1923).

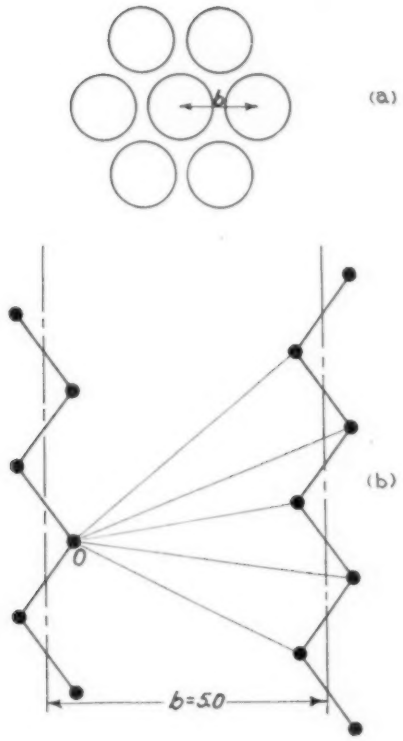

FIG. 1. Schematic representation of neighboring chains in a long chain liquid.

area of 21.2A² we obtain for the lateral separation

$$b = (2 \times 21.2 \times 3^{-1})^{\frac{1}{2}} = 5.0\text{A}.$$

We now fix our attention upon any one carbon atom, say at 0 (Fig. 1(b)) and proceed to tabulate the number of neighbors and their distances. In the same chain there will be 1 at distance zero, 2 at distance 1.54A, 2 at distance 2.50A and so on. On the six neighboring chains there will be 12 at distance 5.0±0.9, 12 at distance 5.3±0.9 and so on. The radial density function $g'(r)$ found in this way is represented graphically in Fig. 2(a), together with the radial negative density $\rho'(r)$ which is to be subtracted from it. There is no assumption involved as to spherical symmetry in the function $g'(r)$ since the fundamental diffraction equation (3) involves only the distances between atoms and not the relative orientations. It is seen at once that there is a marked positive peak in scattering matter at a distance of roughly 5.4A, and it will turn out that it is just this concentration of scattering

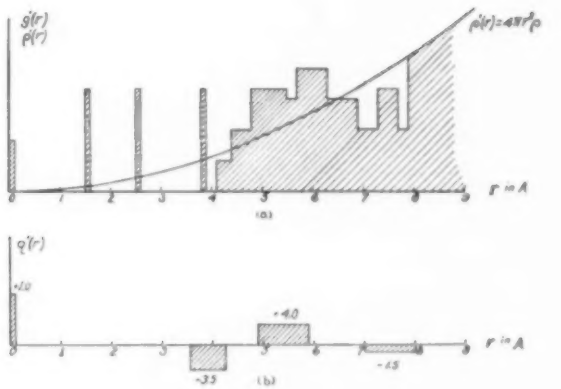

FIG. 2. Representation of radial density of scattering matter about any one carbon atom.

matter which gives rise to the main diffraction peak observed in the long chain liquids.

The resultant density function $q'(r)$ would then be obtained by subtracting $\rho'(r)$ from $g'(r)$. Actually, however, we have left out the random motion of the molecules, which of course tends to smooth out the irregularities in density. An attempt has been made to allow for this effect by retaining the essential features of Fig. 2(a) but making the concentrations considerably less pronounced. In choosing the final density function $q'(r)$ there is of course the condition to be fulfilled,

$$\int_0^\infty q'(r)dr = 0.$$

The extent of smoothing out has but little effect on the position of the main peak and is carried out only far enough to satisfy the self consistency condition which is implied in assuming every atom surrounded in the same way as every other atom. The resultant density function $q'(r)$ arrived at in this way is represented in Fig. 2(b). The integration of Eq. (6) is then carried out graphically[12] and, by taking the scattering factor for carbon from the table of James and Brindley,[13] the intensity is plotted out as a function of $(\sin\theta)/\lambda$. In Fig. 3 the resultant intensity curve is compared with the experimental curve of Stewart for pentadecane, which

[12] A most useful aid in this calculation is the new table of $(\sin x)/x$ by J. Sherman, Zeits. f. Krist. **85**, 404 (1933).

[13] James and Brindley, Zeits. f. Krist. **78**, 470 (1931).

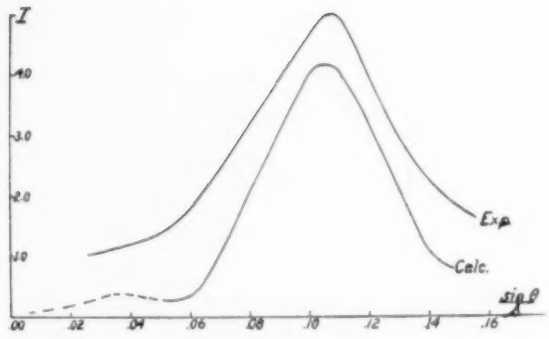

FIG. 3. Comparison of calculated and observed intensity curves for liquid paraffins.

is a typical curve for the whole series. The ordinates are, of course, in arbitrary units but the qualitative agreement is quite satisfactory. The exact shape of the curve at small angle is indefinite since it depends markedly upon the distribution at large distance.

The main peak, which occurs in the scattering curves for the normal alcohols and fatty acids at roughly the same position as in the paraffins, is, of course, to be explained in the same way. It should also be noted that the concentration of scattering matter at a distance 5.4A, which is responsible for the main peak, would have been obtained roughly by direct application of the Ehrenfest-Keesom relation

$$a=[0.814\times 2(\sin\theta)/\lambda]^{-1}=5.65\text{A}.$$

THE INNER PEAK

In the scattering curves from the normal alcohols[5] and fatty acids[7] there occurs a main peak at $(\sin\theta)/\lambda=0.108$ which we have already discussed and, in addition, a much weaker peak which occurs at smaller angle and which shifts continually to smaller and smaller angle as the number of carbons in the chain increases. This peak obviously has something to do with the length of the chain but direct application of the Ehrenfest-Keesom law gives a length which is roughly 5/3 the chain length as calculated by other methods.

To understand the origin of this peak two points should be noted. The peak occurs in the alcohols and fatty acids but not in the paraffins and hence is dependent upon the heavy end group OH or COOH which is present in the first two cases but not in the third. It occurs at very small scattering angle and hence arises from some variation in the density of scattering matter which exists at a considerable distance from the heavy end group. In the region surrounding any heavy end group there is only one distinctive point at a definite long distance and this point is the other end of the chain. As is well known, the intermolecular distances in organic compounds are large and hence there occurs a relatively empty gap at the end of the chain. We have then a deficit of scattering matter rather than an accumulation, and occurring at a distance from the heavy end group which is roughly equal to the chain length. Such a distribution will of course give rise to a negative peak in the $q'(r)$ density function. In carrying out the integration of (6), a positive peak in the intensity curve will be obtained at that value of $(\sin\theta)/\lambda$ which gives the function $(\sin sr)/sr$ a negative maximum, and this occurs at a value $sr=4.50$

$$4\pi r(\sin\theta)/\lambda=4.50,$$

$$(2\pi/4.50)2r\sin\theta=\lambda. \qquad (8)$$

Eq. (8) is, of course, the analogue of the Ehrenfest-Keesom relation applicable to density deficits. In Table I are tabulated the distances calculated by (8) from measurements on the normal alcohols.

The values of $(\sin\theta)/\lambda$ for the alcohols are taken from the paper by Stewart and Morrow,[5] and to avoid the slight errors in the individual measurements the values have been read off their straight line plot. The length which is calculated from the inner peak is, of course, the distance from the heavy end group to the center of the gap, and it is only for long chain molecules that this distance becomes roughly equal to the chain length. As seen in Table I for chains of 5 carbon atoms or more, the agreement is quite satisfactory. In view of the difficulty in measuring relatively weak peaks at such small angles of scattering, the agreement in Table I is a tribute to the skill and care of Professor Stewart and his co-workers.

TABLE I. *Comparison of chain lengths of alcohols calculated from the inner peak and from the molecular volume.*

Number of carbons	From inner peak $l=\frac{1}{2.79 \sin \theta/\lambda}$	From Mol. Vol. $l=\frac{M}{\rho \times 0.606 \times 21.2}$
1	4.3A	3.2A
2	5.7	4.5
3	6.9	5.9
4	7.9	7.2
5	9.0	8.5
6	10.2	9.8
7	11.3	11.2
8	12.3	12.3
9	13.4	13.7
10	14.6	14.9

GENERAL CONCLUSIONS

The agreement in Table I shows that, at least up to $n=10$, the chains remain essentially straight in the liquid. The picture of a long chain liquid, which we can draw from the above results, is one in which the positions and orientations of the molecules are quite at random, except insofar as the condition for a fairly dense packing of such irregularly shaped molecules necessitates that the immediate neighbors about any one molecule shall be roughly parallel to it.

With such a picture of the liquid, the x-ray scattering curve is given quite satisfactorily by the theory of Zernicke and Prins. The main peak does not measure directly the lateral distance between chains but rather the distance to a concentration of scattering matter. The latter is about 8 percent larger than the lateral chain separation. The inner peak measures the distance from the heavy end group to the hole at the opposite end and, for sufficiently long chains, this distance becomes equal to the chain length. While our picture of the diffraction of x-rays in a long chain liquid differs from that which has been used by Stewart, the general significance of the two peaks has turned out to be the same.

The Measurement of X-Ray Emission Wave-Lengths in the *M*-Series by Means of the Ruled Grating

E. G. Purdom and J. M. Cork, *Department of Physics, University of Michigan*

(Received October 20, 1933)

Measurements have been made by use of a plane ruled grating, of emission wave-lengths in the *M*-series for a number of elements having atomic numbers greater than (71). By making use of multiple positive orders, the correct determination of wave-lengths is secured even though uncertainties might exist in the position of the direct and reflected beams, or in the angle of incidence. The wave-lengths are found to be consistently greater than corresponding results obtained by means of the crystal method. The Moseley diagram for the results obtained are smooth curves.

Introduction

ABSOLUTE determinations of the wave-lengths of x-ray lines by the use of ruled gratings and the constants of the apparatus have been made by a number of investigators. In most cases the investigations have been carried out in the *K*- and *L*-series.[1,2,3] The results obtained for the wave-lengths of the x-ray lines have been consistently greater than the corresponding values found by the use of the usual crystal method. The magnitude of this difference as obtained in the more recent investigations seems to vary from 0.22 percent to 0.31 percent which is approximately ten times the probable error to be expected in the grating measurements.

In order to add to the existing data and thus possibly aid in the detection of the origin of this difference, it was considered desirable to carry out a series of measurements in the *M*-series by using a ruled grating. Prins and Takens,[4] using the grating method, have reported values of wave-lengths in this series for the elements Zr (40) to Sb (51). Prins[5] also secured values for two lines in the series for W (74). The present investigation was undertaken in order to obtain values of the wave-lengths in the *M*-series for the heavier elements, for which very little data now exist.

Apparatus

The experimental arrangement as well as the method of procedure has been described previously in this journal.[2,3] The elements studied, with the exception of osmium (76) were all obtainable as pure metals and could easily be attached to the face of the water-cooled target. In the case of osmium the oxide was employed. These stable targets allowed the application of considerable power to the x-ray tube so that on the spectrograms many measurable orders of the stronger lines were obtained. Reproductions of a few typical plates are shown in Fig. 1.

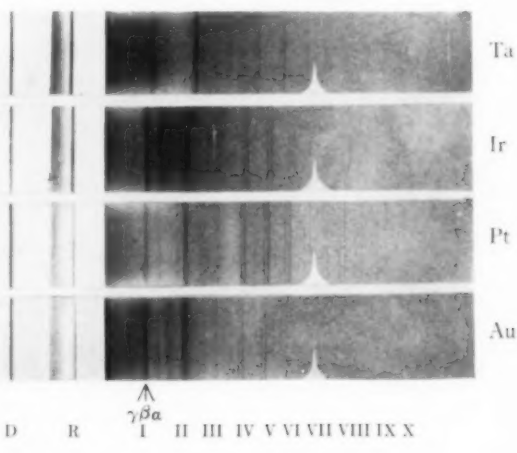

Fig. 1. Spectrograms of *M*-series.

[1] J. M. Cork, Phys. Rev. **35**, 1456 (1930).
[2] J. A. Bearden, Phys. Rev. **37**, 1210 (1931) *et seq.*
[3] R. B. Witmer and J. M. Cork, Phys. Rev. **42**, 743 (1932).
[4] J. A. Prins and A. J. Takens, Zeits. f. Physik **75**, 742 (1932).
[5] J. A. Prins, Physica **12**, 15 (1932).

In the *M*-series there are, for each element, two very strong lines of about the same intensity. These are denoted as the $\alpha_{1,2}$-line and the β-line and arise respectively from the electron transitions M_V to $N_{VI, VII}$ and M_{IV} to N_{VI}. As intimated, the former is a doublet consisting of the components α_1 and α_2 having an intensity ratio of about 20 to 1. In addition there are visible two weaker lines, one of shorter wave-length than the previously mentioned pair and one of longer wave-length. The former is usually denoted as $M\gamma$ and arises from the transition M_{III} to N_V. The line of longest wave-length is a rather broad doublet consisting of the components M_{IV} to N_{II} and M_V to N_{III}. Although these components could be observed separately the whole was so diffuse and weak except in the first order that it was not considered advisable to attempt to express their wave-lengths individually.

Calculations

Any attempt to determine the absolute wave-length of an emission line from measurements upon a single order, either outside or inside is unwarranted. Errors in expressing the grazing angle of incidence and the angle of diffraction must be expected of such magnitude as to place the final result outside the desired limits of accuracy. However, when several measurable orders of the same spectral line are available on the same photographic plate then, as has been previously shown, most of the uncertainties vanish. Errors of a general type such as those in determining the constant of the ruled grating and the distance between the grating and the photographic plate remain. The agreement that may be obtained for the results from the various orders is well illustrated by the figures in Table I which are averaged values from a set of five plates taken with platinum on the target.

Table I.

Order of spectral line		2	3	4	5	6
Wave-length (A)	$\alpha_{1,2}$	6.0601	6.0600	6.0601	6.0607	6.0591
	β	5.8415	5.8416	5.8417	5.8418	5.8417

Table II. *Collected values of wave-lengths of M-series lines in Angstroms. a, present investigation; b, crystal values, Lindberg.*

Element	Atomic number	Investi-gation	Line γ $M_{III}-N_V$	β $M_{IV}-N_{VI}$	α_1 M_V-N_{VII}	α_2 M_V-N_{VI}	$M_{IV}-N_{II}$	M_V-N_{III}
Hf	72	a		7.319	7.542			
		b		7.289	7.524			
Ta	73	a	6.330	7.040	7.271		9.347	
		b	6.299	7.008	7.237		9.297	9.311
W	74	a		6.774	7.004		9.001	
		b		6.743	6.969		8.943	8.977
Os	76	a		6.281	6.499		8.368	
		b		6.254	6.477		8.293	8.343
Ir	77	a	5.505	6.051	6.273		8.046	
		b	5.490	6.025	6.249	6.262	8.002	8.048
Pt	78	a	5.335	5.842	6.060		7.775	
		b	5.309	5.816	6.034	6.045	7.722	7.774
Au	79	a	5.150	5.642	5.859		7.529	
		b	5.135	5.612	5.828	5.842	7.451	7.507
Hg	80	a		5.441	5.655			
		b						
Tl	81	a	4.835	5.260	5.475		7.019	
		b	4.815	5.239	5.450	5.461	6.960	7.017
Pb	82	a	4.688	5.084	5.295		6.790	
		b	4.665	5.065	5.274	5.288	6.726	6.788
Bi	83	a	4.541	4.922	5.133		6.585	
		b	4.522	4.899	5.108	5.119	6.508	6.571
Th	90	a		3.941	4.148		5.323	
		b		3.934	4.130	4.143	5.229	5.329
U	92	a		3.723	3.911			
		b		3.708	3.902	3.916		

Results

The values obtained for the various wave-lengths are collected in Table II. Also noted here are the results for the same emission lines as reported by Lindberg[6] using the crystal method. With the spectrograph of this type it is possible to evaluate the wave-lengths of many of the fainter lines so that Lindberg reported as many as eighteen lines for several of the elements.

It may be observed that in every case the value obtained by the present grating method is greater than the corresponding value obtained by the use of crystals. The constancy of this difference which amounts to about 0.32 percent is shown in Fig. 2 which is a Moseley diagram representing the results for the two stronger lines in the *M*-series. The solid lines are drawn through the points as obtained with the crystal method, making the necessary interpolation between α_1 and α_2 when necessary. The lines appear to be smooth curves showing no discontinuities or irregularities for any element.

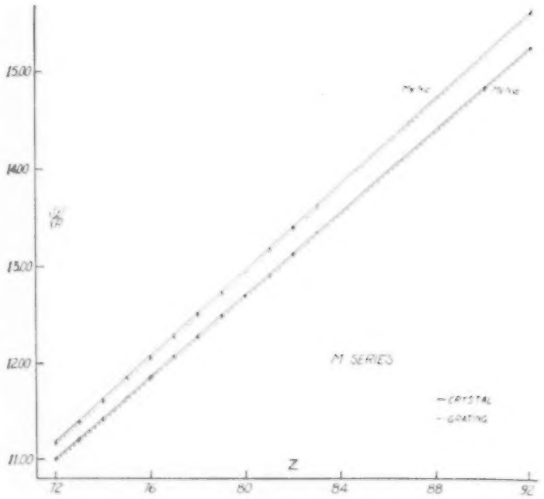

FIG. 2. Moseley diagram for *M*-series lines.

[6] E. Lindberg, *Dissertation*, Upsala, 1932.

The *K* Absorption Discontinuities of the Elements Zirconium to Iodine

P. A. Ross, *Stanford University*

(Received September 18, 1933)

A study of the *K* absorption limits in the elements Zr, Cb, Mo, Ru, Rh, Pd, Ag, Cd, Sn, Sb, Te, and I has been made with a double-crystal spectrometer. All of the elements studied except cadmium show faint fine structure on the high frequency side of the discontinuity, the structure appearing as narrow bands of slightly decreased absorption lying within a range of from 21 to 120 volts of the main discontinuity. The width of the main absorption step in volts has been measured and found to increase with atomic number. Defining the wave-length of the absorption discontinuity as that corresponding to the point of inflection of the main absorption curve values of the wave-length have been obtained to an estimated accuracy of ±0.02 x.u.

A COLLECTION of balanced filters[1] has been in preparation during the past two years. During the balancing in pairs certain peculiarities[2] were noticed that indicated the desirability of a more careful study of the structure and exact wave-length of the *K* absorption discontinuity in the elements to be used in the filter method of x-ray spectroscopy. This work is being done with the aid of a grant from the National Research Council.

Previous work[3] on the fine structure associated with absorption limits has been chiefly by photographic method and has been confined to the *L* limits and the *K* limits of the lighter elements. Recent work with the double-crystal spectrometer has been done by Richtmyer,[4] Barnes[5] and Hull.[6]

A double-crystal spectrometer described elsewhere[7] has recently been revised and improved. Crystal *A* (Fig. 1) was mounted on a carriage moving along milled ways midway between the x-ray tube and the axis of rotation of crystal *B*. A scale on the ways and divisions on the wheel *D* gave directly the tangent of the glancing angle on crystal *A*. Crystal *B* was mounted on a rebuilt Société Genevois optical spectrometer. The seconds wheel operated a micrometer screw bearing against a hardened steel ball. This screw was calibrated by attaching a 2 meter aluminum tube to the crystal table and observing the motion of a fine index scratch on a glass scale at the end of the long arm. Motion of the index was measured with a microscope mounted on a Hilger comparator. Various portions of the seconds wheel micrometer were checked against the same portion of the comparator screw. No error could be detected although a variation of 0.1″ should have been observable.

Calibration of the graduated circle was made both with the seconds wheel and with two microscopes at various intervals in the usual manner. The circle was less accurate than had been hoped. Four marks were in error by nearly one second and one was in error by 2.9″. No other errors greater than 0.4″ were found. By symmetrically bracketing each ruled division between two very fine and very closely spaced crosswires in the microscope eyepiece repeated settings could be made to ±0.1″. This method of setting is much more reliable than trying to set on the edge of a ruling or on the estimated center of a ruling on the circle. It is believed that the final correction curve enabled large angles to be measured to ±0.5″ and small angular differences to at least ±0.2″.

[1] Ross, J. Opt. Soc. Am. and Rev. Sci. Inst. **16**, 433 (1928).

[2] Burbank, Phys. Rev. **43**, 83 (1933).

[3] Linah, Zeits. f. Physik **31**, 2110 (1925). Davis and Purks, Phys. Rev. **36**, 336 (1928). Lindsay and Vorkees, Phil. Mag. **6**, 910 (1928). Hanawalt, Zeits. f. Physik **70**, 293 (1931). Coster and Veldkamp, Zeits. f. Physik **74**, 191 (1932). Bloch, Zeits. f. Physik **52**, 555 (1929). Kronig, Zeits. f. Physik **70**, 317 (1931).

[4] Richtmyer, Science **77**, 459 (1933).

[5] Barnes, Phys. Rev. **44**, 141 (1933).

[6] Hull, Phys. Rev. **40**, 676 (1932).

[7] Ross, Rev. Sci. Inst. **3**, 253 (1932).

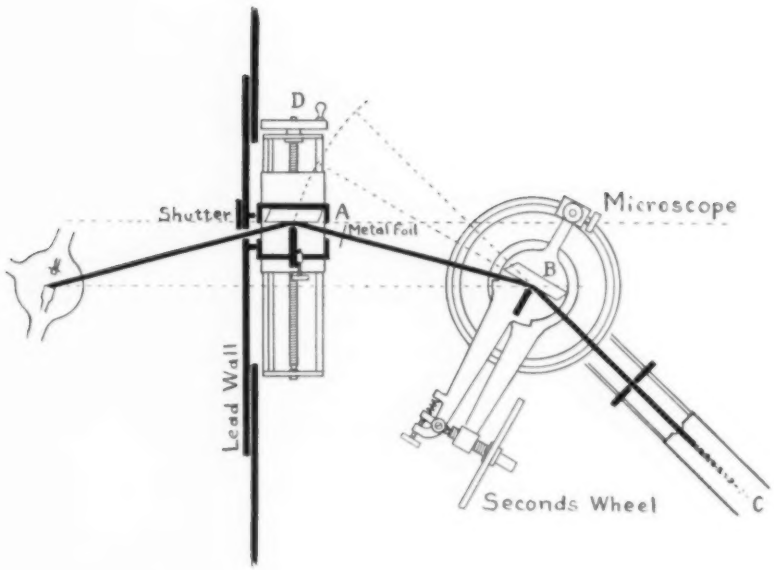

FIG. 1. Diagram of double-crystal spectrometer.

Since the zero position of crystal B is really determined by the reflecting planes of crystal A it is of the utmost importance that ways of the mounting of A should be accurately straight. The ways were tested by means of a good telescope with a Gauss-eyepiece and a mirror mounted on the carriage in place of the crystal. The ways were scraped and lapped until the image of the crosswires showed no displacement as the carriage was moved along the bed. As a second test rocking curves were run with the crystals in parallel position. Any angular displacement of A would be shown by a displacement of the maximum of the rocking curve as read on B when A was moved to larger angles. This test indicated that the ways were straight over the region used in this research to within $\pm 0.3''$.

The crystals were split from a large block of optical quality South African calcite. The half width of their rocking curve at half maximum in the first order was $3''$. The space lattice of calcite was assumed to be 3.02945A at 18°C and a temperature correction[8] made according to the formula $d\theta'' = 2.10(t-18°)\tan\theta$. Slit height corrections were made according to the formula given by Williams.[9]

Ionization currents were measured by the ballistic method[10] on a Compton type electrometer. Timing was done electrically by using a magnetic shutter between the x-ray tube and the spectrometer.

Power from a 550 cycle, 100 kilovolt outfit was rectified by kenotrons and filtered so that the ripple did not exceed 10 volts. The d.c. voltage was measured by a calibrated Kirkpatrick generating voltmeter[11] in parallel with the x-ray tube and was regulated by an assistant who held it to within ± 40 volts during the run. The tube current was also very carefully controlled by the assistant.

As a test of the accuracy of the spectrometer certain lines covering a range of wave-lengths that would more than include the K limits under consideration were carefully measured and compared with what seemed to be the best available measurements by other investigators. The zero setting as determined from parallel rocking curves was used. In Table I is presented the result of this test of accuracy.

In Figs. 2 to 13 typical transmission curves are shown. The ordinates are electrometer deflections (ballistic method) and the abscissae are

[8] Cooksey, Phys. Rev. **36**, 85 (1930).
[9] Williams, Phys. Rev. **40**, 636 (1932).
[10] Webster and Yeatman, J. Opt. Soc. Am. and Rev. Sci. Inst. **17**, 248 (1928).
[11] Kirkpatrick and Miyake, Rev. Sci. Inst. **3**, 1 (1932).

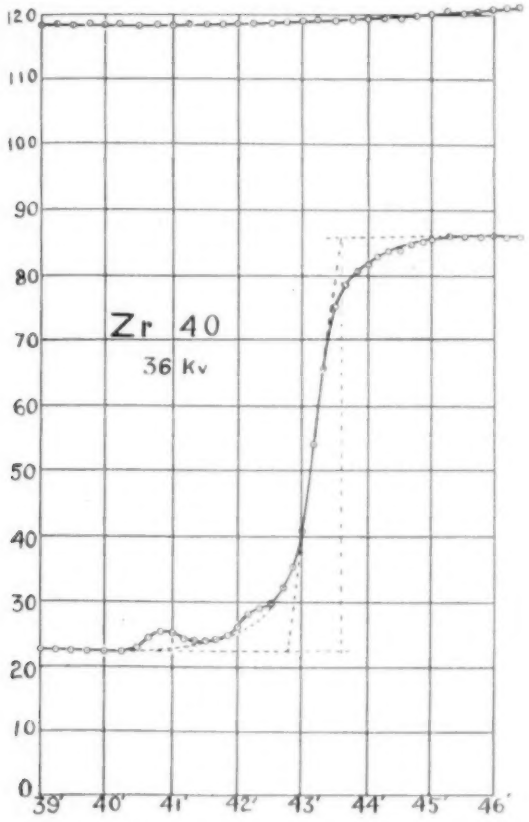

FIG. 2. Transmission curve through zirconium foil.

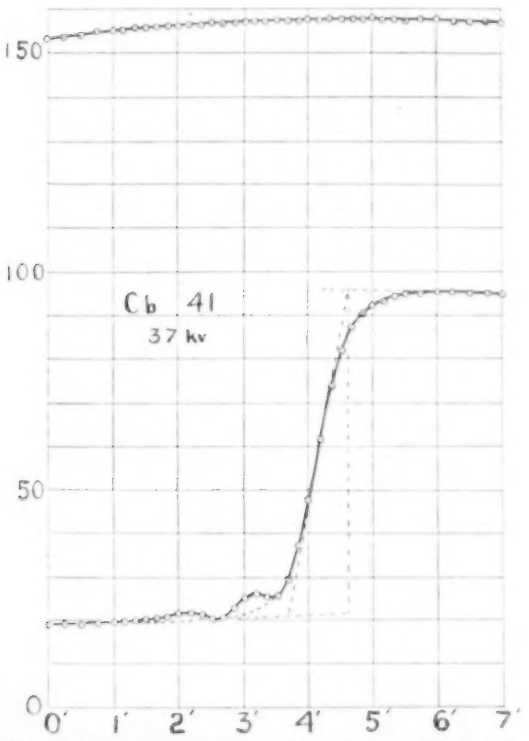

FIG. 3. Transmission curve through columbium foil.

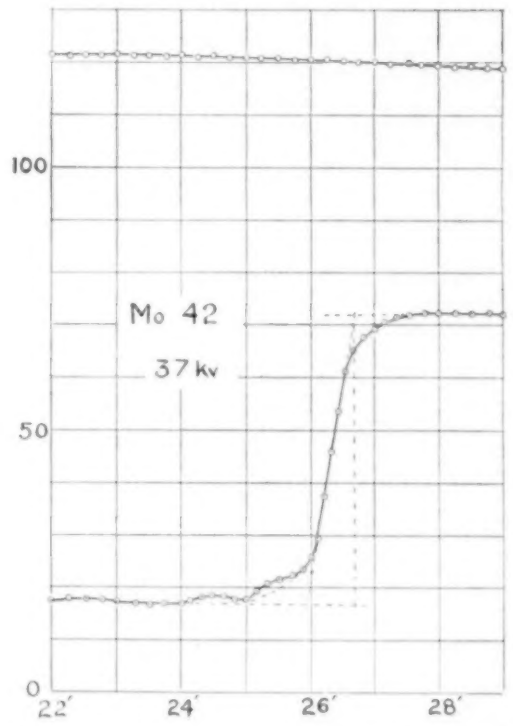

FIG. 4. Transmission curve through molybdenum foil.

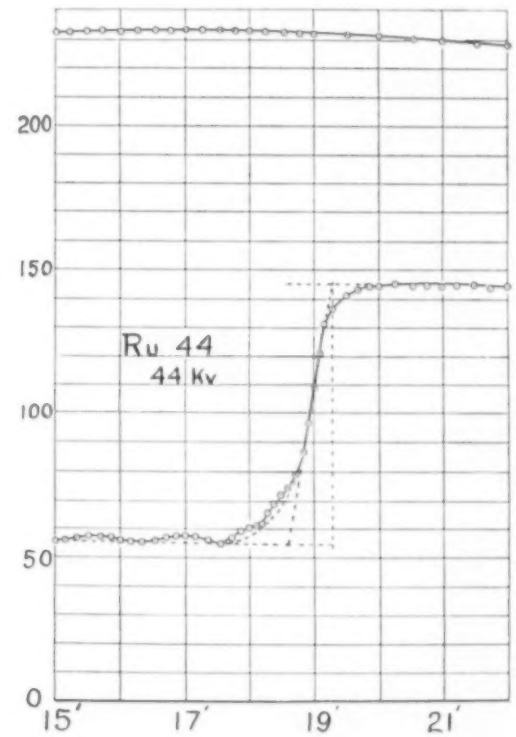

FIG. 5. Transmission curve through metallic ruthenium powder with beeswax binder.

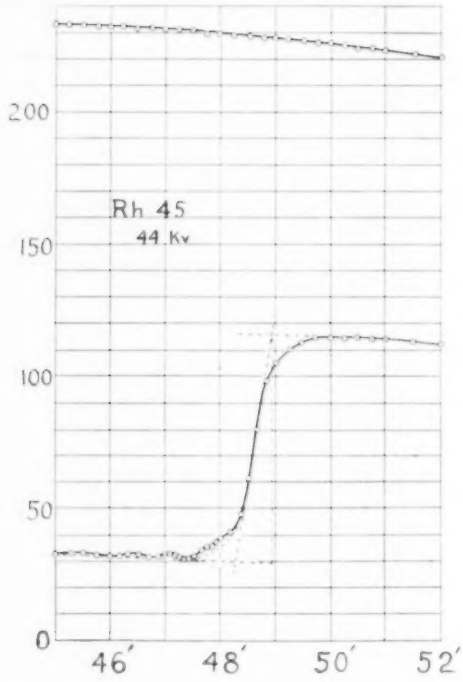

FIG. 6. Transmission curve through rhodium foil.

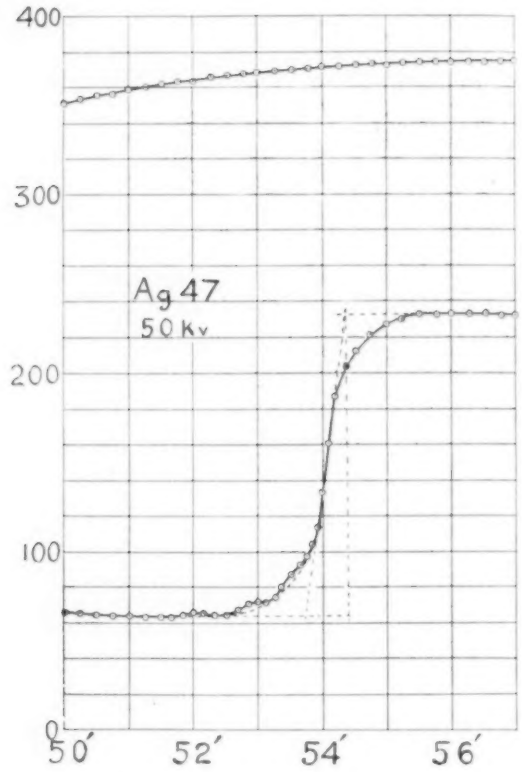

FIG. 8. Transmission curve through silver foil.

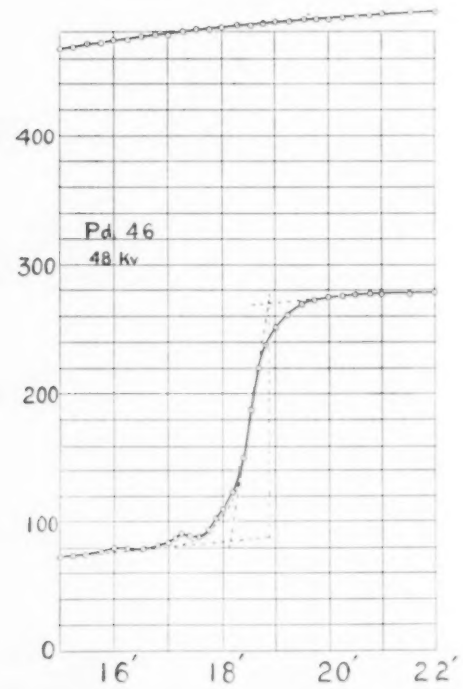

FIG. 7. Transmission curve through palladium foil.

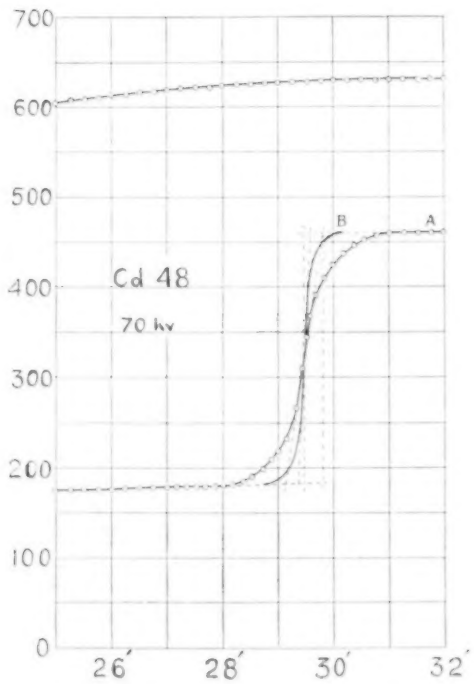

FIG. 9. Transmission curve through cadmium foil. Curve *B* is the integral of a Gaussian curve of the same width as the rocking curve of the crystals used.

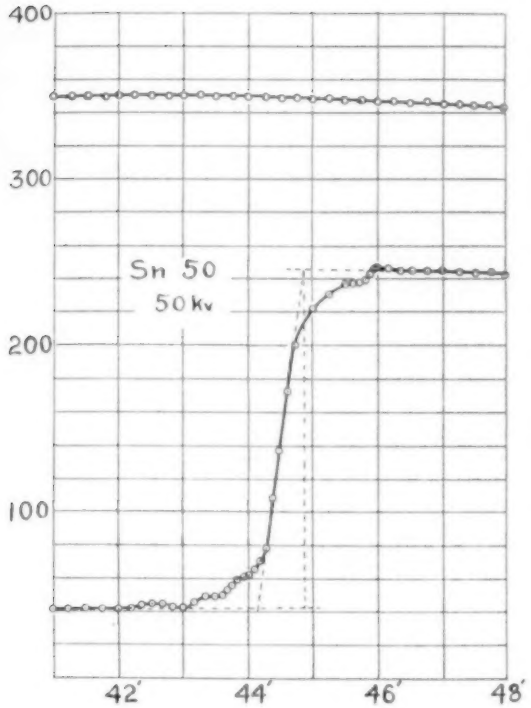

FIG. 10. Transmission curve through tin.

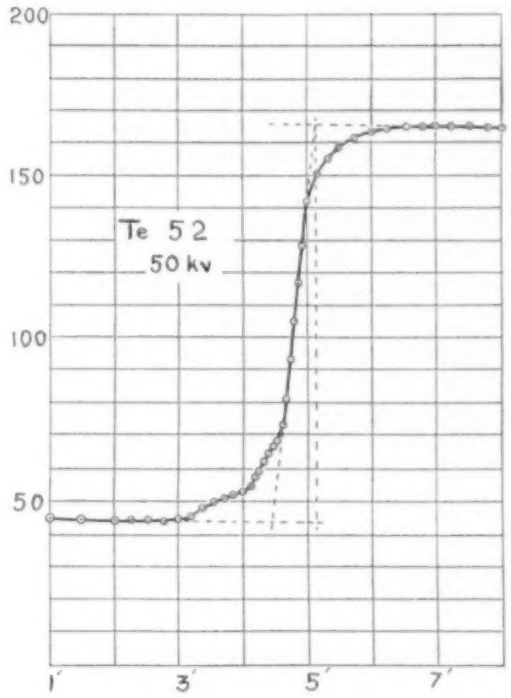

FIG. 12. Transmission curve through metallic tellurium powder with beeswax binder.

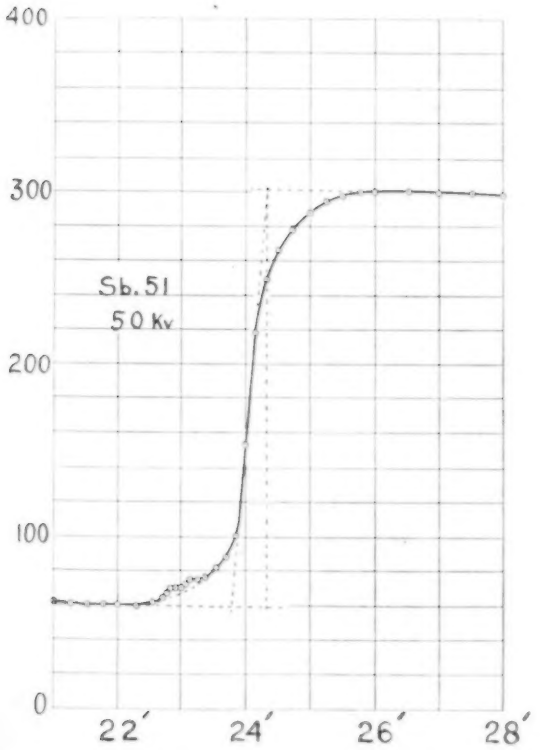

FIG. 11. Transmission curve through metallic antimony powder with beeswax binder.

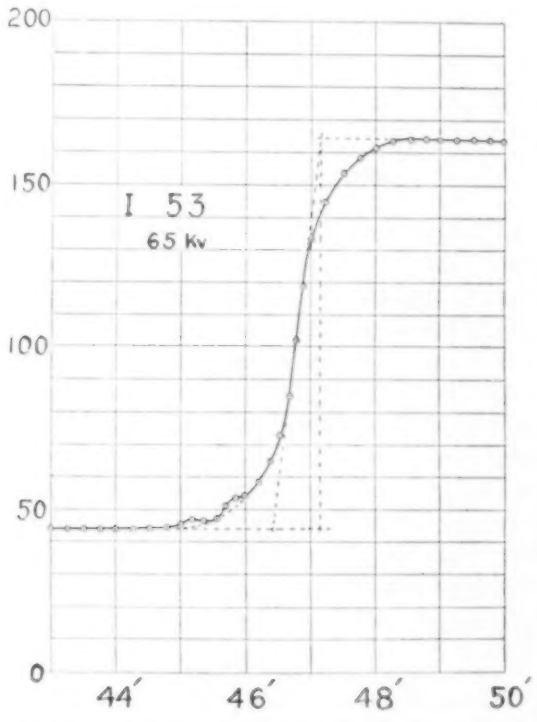

FIG. 13. Transmission curve through iodine powder with beeswax binder.

TABLE I. *Test of accuracy.*

	θ	λ	
Mo $K\alpha_1$	6° 42′ 35.4″	707.835	Bearden[12]
	6° 42′ 35.6″	707.838	Ross
Mo $K\beta_1$	5° 58′ 42.5″	630.978	Larsson[13]
	5° 58′ 43.2″	630.988	Ross
Ag $K\alpha_1$	5° 17′ 14.5″	558.257	Bearden
	5° 17′ 15.0″	558.264	Ross
W $K\alpha_1$		208.62	I. C. T.[14]
	3° 50′ 54.8″	208.602	Ross
	(2nd order)	208.60	Hudson and Vogt[15]

uncorrected angle readings. The primary radiation was from a water-cooled platinum target. In several cases a portion of the unfiltered radiation curve is presented at the top of the figure showing that the secondary fine structure cannot be ascribed to variations in intensity of the primary radiation.

TABLE II. *Widths of absorption edges.*

	$d\theta$	$d\theta'$	dv		Δv		
Zr	46	34	13		21	52	
Cb	54	42	18		29	52	
Mo	44	32	15		25.9	53.5	
Ru	45	33	19	19	28.9	61	120
Rh	43	31	20		25.5	58	
Rd	44	32	22		26	52	104
Ag	44	32	25		22.5	52	86
Cd	42	30	25				
Sn	42	30	30		36	66.5	120
Sb	40	28	30			68	
Te	41	29	35			74	99
I	41	29	38			77	120

In Table II column two gives the uncorrected width ($d\theta$) of the discontinuity expressed in seconds. This width has been defined in the usual way as the base of the dotted triangle shown in each curve. Column three gives the corrected width ($d\theta'$) in seconds obtained by subtracting four times the half rocking width at half maximum (i.e., 12″) from the $d\theta$ of column two. Column four gives this corrected width expressed in volts. Column five gives the separation in volts (Δv) of the transmission bands of the secondary fine structure from the center of the discontinuity. The position of the secondary fine structure is very constant with different foils but the relative intensity varies greatly with the foil thickness. Cadmium shows no fine structure with any thickness used between 0.01 and 0.05 mm. Tin alone shows any structure on the long wave-length side, this peculiar wiggle appearing on all of six curves run on allegedly pure tin from three different sources.

The curve of Fig. 14 presents the relation

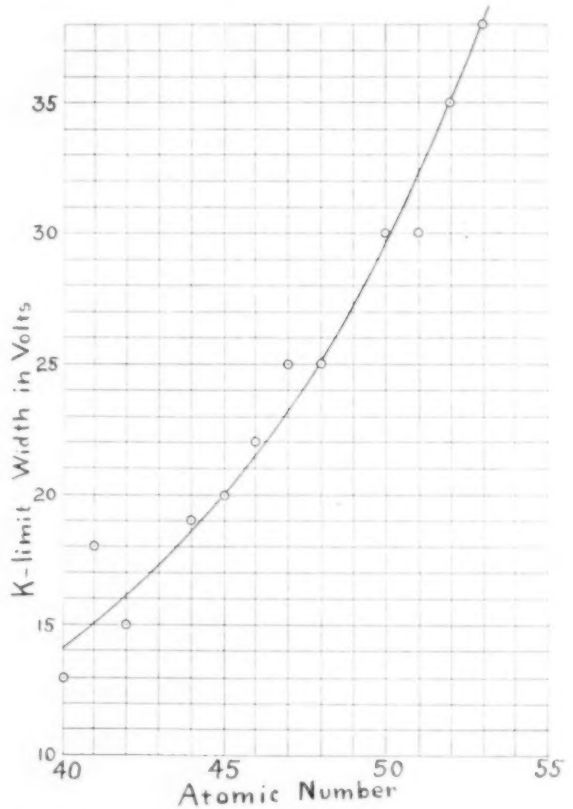

FIG. 14. Relation between width in volts of the K discontinuity and atomic number.

TABLE III. *Wave-lengths of absorption discontinuities.*

Element	θ (18°)(±0.5″)	(x.u.)(±0.02)	I. C. T. values
Zr	6° 30′ 56.5″	687.43	687.4
Cb	6° 10′ 32.6″	651.71	650.5
Mo	5° 51′ 35.7″	618.51	618.2
Ru	5° 17′ 51.8″	559.35	558.6
Rh	5° 2′ 44.7″	532.82	533.2
Pd	4° 48′ 38.7″	508.06	507.7
Ag	4° 35′ 26.7″	484.88	485.2
Cd	4° 23′ 6.3″	463.07	463.4
Sn	4° 0′ 40.2″	423.76	424.3
Sb	3° 50′ 27.2″	405.81	406.6
Te	3° 40′ 51.2″	388.93	389.7
I	3° 31′ 49.2″	373.04	383.7

[12] Bearden, Phys. Rev. **43**, 92 (1933).
[13] Larsson, Phil. Mag. **3**, 1136 (1927).
[14] International Critical Tables, weighted mean.
[15] Hudson and Vogt, Phys. Rev. **43**, 1049 (1933).

between the step width and atomic number. This curve extrapolated agrees fairly well with Richtmyer's values for the step width of tungsten and gold.

When the absorption discontinuity was plotted to a large scale the point of inflection, or midpoint of the nearly straight portion joining the foot and head of the curve, could be located to about 1″ on the double crystal curve. The position of the main step in no case deviated by more than 3″ on the double crystal curve from that corresponding to the mean value of θ recorded in Table III. From four to ten curves were run on each element. Column three of Table III gives the wave-length in x-units as found in this research. Column four gives the corresponding wave-length as given in the *International Critical Tables*.

The Infrared Bands and Molecular Constants of HBr

E. K. PLYLER, *University of North Carolina,*
and
E. F. BARKER, *University of Michigan*

(Received November 2, 1933)

The fundamental band of HBr has been remeasured, and the harmonic band examined for the first time under high resolution. From the equations representing line positions the values $\nu_0 = 2649.74$ cm^{-1}, $I_0 = 3.2634 \times 10^{-40}$ g cm^2, and $r_0 = 1.4096 \times 10^{-8}$ cm are obtained. Resolution of the isotopic components was just possible in the fundamental band, and the observed separations agree with those computed from the isotopic masses of Br.

THE fundamental band of HBr at about 4μ was first resolved by Randall and Imes[1] in one of the earliest studies of infrared absorption with high dispersion. It has not since been reexamined, though there have been great improvements in the sensitivity of the recording apparatus. The harmonic band was not observed at that time because of its low intensity, and until now it has not been studied in detail. For the following observations a standard prism-grating spectrometer was available, the grating having 7200 lines per inch. An absorption cell 25 cm long with windows of NaCl served admirably for the 4μ region, and at 2μ it was replaced by an iron tube 150 cm long with thin mica windows. HBr gas was generated by direct reaction of hydrogen and bromine in the presence of a catalyst, collected by freezing in liquid air and distilled into the evacuated cells to the desired pressure. In this way a high purity of gas was assured.

Curve *b* in Fig. 1 shows the fundamental band as observed with a slit 0.2 mm (0.4 cm^{-1}) in width and a pressure of 20 cm of HBr. The lines are well separated but show no signs of resolution into pairs. By reducing the slit width to 0.09 mm (0.18 cm^{-1}), deflections then being as small as permissible for trustworthy measurements, and advancing the grating by steps of only 10″ at a time, the separation indicated in curve *c* was obtained. Each of the four lines reproduced was defined by some fifteen or twenty points. The separations of the components are difficult to measure precisely due to overlapping of almost equally intense pairs, and it did not seem feasible to derive independent equations for the two isotopic bands. The expected displacements, as computed from the isotopic masses of Br, are indicated by pairs of vertical lines below the envelopes in curve *c* and it is clear that these agree very well with the experimental determinations.

The harmonic band, which is comparatively weak, appears in curve *a*, the gas pressure being atmospheric. The optical arrangement necessary for the accommodation of an absorption cell 150 cm long was not as advantageous as has since been devised,[2] and adequate deflections

TABLE I. *The fundamental band.*

m	Frequencies Observed	Frequencies Computed	Difference
+8	2675.36	2675.22	+0.14
+7	2662.60	2662.58	+0.02
+6	2649.38	2649.38	0.00
+5	2635.52	2635.64	−0.12
+4	2621.35	2621.37	−0.02
+3	2606.61	2606.58	+0.03
+2	2591.23	2591.29	−0.06
+1	2575.55	2575.52	+0.03
−1	2542.56	2542.54	+0.02
−2	2525.51	2525.37	+0.14
−3	2507.86	2507.76	+0.10
−4	2489.63	2489.73	−0.10
−5	2471.36	2471.28	+0.08
−6	2452.48	2452.44	+0.04
−7	2433.18	2433.22	−0.04
−8	2413.30	2413.62	−0.32

[1] E. S. Imes, Astrophys. J. **50**, 251 (1919).

[2] Hardy, Barker and Dennison, Phys. Rev. **42**, 279 (1932).

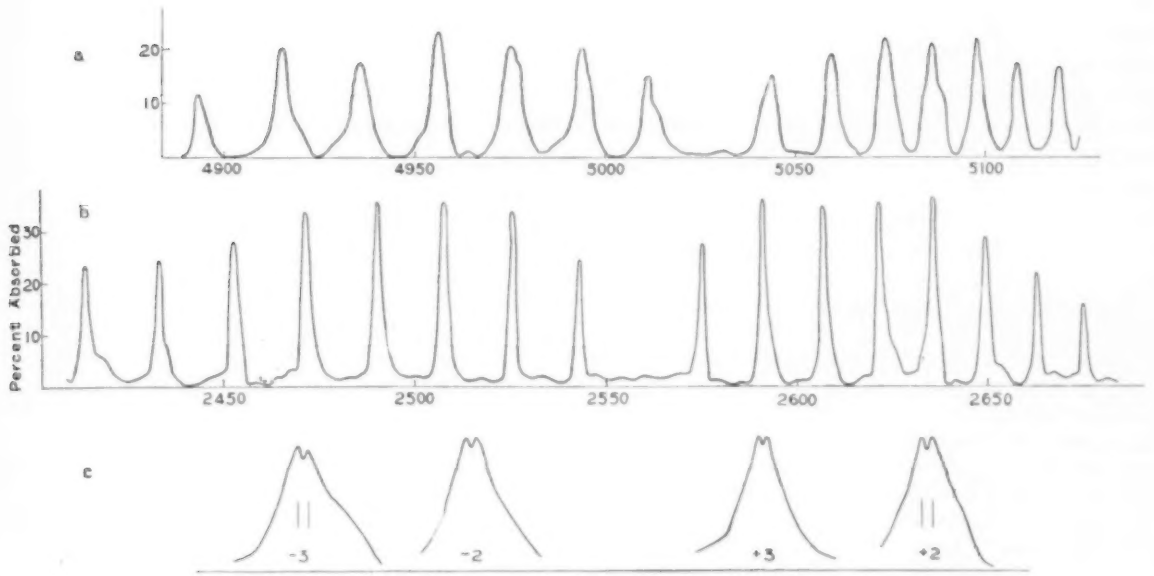

FIG. 1. Absorption bands of HBr. (*a*) First harmonic with slit width 1.2 cm^{-1}. (*b*) Fundamental slit width 0.4 cm^{-1}. (*c*) Four fundamental lines with higher resolution; slit width 0.18 cm^{-1}.

could be obtained only with relatively wider slits. Hence the definition is not as good and the isotopic separations, though greater than in the fundamental, were not observed. The positions of the rotation lines in the fundamental band are listed in Table I, together with corresponding values computed from the equation

$$\nu' = 2559.26 \pm 16.490m - 0.232m^2 \mp 0.0022m^3,$$

m being the ordinal number of any line counted outward from the center. Table II presents similar information regarding the harmonic band, for which the equation is

$$\nu'' = 5028.11 \pm 16.260m - 0.449m^2 \mp 0.0030m^3.$$

From these coefficients several of the molecular constants may be deduced, as indicated by Colby[3] in a study of HCl. (For definitions of B and C, and for comparison of the constants of HCl with those of HBr Colby's paper should be consulted.) The numerical values are as follows:

$\nu_0 = 2649.74\ cm^{-1}$, $B = 0.864 \times 10^{-8}$,

$I_0 = 3.2634 \times 10^{-40}\ g\ cm^2$, $C = 5.338$.

$r_0 = 1.4096 \times 10^{-8}\ cm$.

TABLE II. *The harmonic band.*

m	Frequencies Observed	Frequencies Computed	Difference
+7	5119.10	5118.88	+0.22
+6	5108.07	5108.85	−0.78
+5	5097.79	5097.81	−0.02
+4	5086.01	5085.78	+0.23
+3	5072.76	5072.77	−0.01
+2	5058.71	5058.81	−0.10
+1	5043.94	5043.92	+0.02
−1	5011.38	5011.40	−0.02
−2	4993.97	4993.81	+0.16
−3	4975.41	4975.37	+0.04
−4	4956.21	4956.08	+0.13
−5	4935.93	4935.95	−0.02
−6	4915.21	4915.03	+0.18
−7	4893.16	4893.30	−0.14

[3] W. F. Colby, Phys. Rev. **34**, 53 (1929).

Multiplet and Hyperfine Structure Analyses of Bi IV. Discussion of Perturbation Effects

A. B. McLay[1] and M. F. Crawford, *McLennan Laboratory, University of Toronto*

(Received August 23, 1933)

Three hundred and sixty lines of Bi IV, excited in an electrodeless discharge, have been classified. Twenty-seven terms of $6snx$ configurations, four terms of $6p^2$ and six terms of $5d^9\,6s^2\,6p$ have been identified. Evidence of perturbation of $6s5f$ and $6s7p$ by $5d^9\,6s^2\,6p$ and of $6s6d$ by $6p^2$ is presented. The perturbation of $6s6d$ by $6p^2$ in Bi IV and other members of the Hg I sequence is shown to agree qualitatively with Bacher's theory of $sd-p^2$ interactions. The hyperfine structure intervals of many of the terms of Bi IV have been evaluated. They are compared with the theoretical formulae for hyperfine structure separations and shown to be consistent with our multiplet analysis. Anomalous hyperfine structure has been observed in $6s7p_4$. This is interpreted as a coupling effect due to the approximate equality of the multiplet and hyperfine structure separations of $6s7p_4$. Goudsmit and Bacher's theory of hyperfine structure perturbations due to a change in coupling is applied to the four hyperfine levels of $6s7p_4$. Their theory accounts for the observed distribution of these levels and for the appearance of forbidden transitions.

I. Introduction

IN 1930 Arvidsson[2] reported the identification of 1317A as the resonance line $6s^2\,{}^1S_0 - 6s6p\,{}^3P_1^\circ$ of Bi IV, and of 1103A as a combination of $6s6p\,{}^3P_1^\circ$ with a higher level. Later Smith[3] tentatively classified 873A as the other resonance line $6s^2\,{}^1S_0 - 6s6p\,{}^1P_1^\circ$. Last year in a more complete paper Arvidsson[4] established the above levels ${}^1S_0$, ${}^3P_1^\circ$ and ${}^1P_1^\circ$ with greater certainty; identified $6s6p\,{}^3P_2^\circ$; and established, but did not name, a few higher even terms. He observed large hyperfine structure in some of the lines, and from the triplet splitting of a few of these evaluated the total interval of $6s6p\,{}^3P_1^\circ$ as about 12.5 cm^{-1}.

We report here the results of an extensive analysis of Bi IV wave-lengths. We have established many new terms and confirmed all of Arvidsson's terms except one, number "8" in his Table III. This term appears to be unreal, since the excitation of one of the three lines used by him to establish it is too high and the other two have been classified by us in Bi III.[5] We have assigned configurations to all the terms now known and evaluated the hyperfine structure intervals of many of them.

II. Experimental

The experimental data on Bi IV were obtained in the same investigation as that on Bi II and Bi III.[6] The spectra of bismuth were photographed by us in the region 1000A to 10,000A. For the extreme ultraviolet a vacuum grating spectrograph was used. Equipped with a two-meter N.P.L. grating, this spectrograph has an average dispersion of 8.75A per mm. A Hilger El spectrograph with interchangeable quartz and glass optical systems was employed to investigate the near ultraviolet and visible regions; and a Hilger constant deviation spectrograph for the infrared.

The spectra were excited by an electrodeless discharge in bismuth vapor. The source was a quartz tube, one inch in diameter and two feet long, containing metallic bismuth which was vaporized by heating the tube in an electric oven. When the source was used with the vacuum spectrograph one end of the tube was left open and attached directly by a taper to the slit of

[1] Assistant Professor of Physics, McMaster University, Hamilton, Canada.

[2] G. Arvidsson, Nature **126**, 565 (1930).

[3] S. Smith, Nature **127**, 855 (1931).

[4] G. Arvidsson, Ann. d. Physik **12**, 787 (1932).

[5] M. F. Crawford and A. B. McLay, Paper on Bi II and III, in press.

[6] J. C. McLennan, A. B. McLay and M. F. Crawford Proc. Roy. Soc. **A129**, 579 (1930). Also reference 5.

the instrument. The discharge was produced by passing a high frequency oscillating current through an exciting coil of fifty turns wound around the tube. The oscillating circuit consisted of the exciting coil, a capacity of 0.003 mf, and an adjustable spark gap, all in series; and was energized by a 2 kva, 60,000 volt transformer.

The advantages of this type of source are as follows: first, lines of Bi I, II, III, IV, and even Bi V, can be easily excited and differentiated by observing their behavior when the vapor pressure and the exciting circuit are varied; second, the individual components of complex lines are narrow enough to permit hyperfine structure measurements.

A number of plates were taken with the vacuum grating spectrograph, each with a different excitation. The exposures varied from one to six hours depending on the experimental conditions. Inspection of the intensities of a given line on the various plates usually showed very definitely in which ion of bismuth it originated. The same procedure was followed in the investigation of the region above 2000A. The exposures, however, were shorter ranging from fifteen minutes to two hours.

All lines between 1000A and 10,000A were measured. The wave-lengths of prominent carbon, nitrogen, oxygen and mercury lines, which appeared on the plates, served to check the accuracy of our measurements. In general, our wave numbers are reliable to within 1 or 2 cm^{-1}. This accuracy is adequate for the term analysis. The hyperfine separations, however, are much more accurate than the absolute values of the wave numbers.

In addition to our data Arvidsson's[4] wave-lengths from 1486A to 175A and his excitation and intensity estimates have been used and found very satisfactory.

III. Multiplet Structure

The term structure of Bi IV is presented in Table I. The hyperfine structure intervals of many terms are also given. A numerical designation of terms is used. The levels previously established by Arvidsson[4] are included, since most of them are interpreted here for the first time and all are needed for the identification of newly classified lines. The classified wave-lengths of Bi IV are listed in Table II. The wave numbers are as measured; the wave-lengths are given only to facilitate identification of the lines on a spectrogram. Since accurate intensity estimates could not be made because of the large wave-length range involved and the diversity of the line widths, the total intensity of each multiplet term combination is expressed qualitatively only. The relative intensities of the components of each hyperfine structure pattern, however, are more accurate. The values assigned apply within a given pattern only. Since the terms 8°, 9°, 10°, 11°, are hyperfine structure levels of $6s7p_1$ (see footnote, Table I), their combinations are grouped as a single hyperfine structure pattern.

There is considerable evidence to justify the configuration assignments as they are given in Table I. The mean energies of the configurations and their multiplet separations are consistent with the values predicted by extrapolation from energy levels of Hg I,[4a] Tl II[4b] and Pb III[4a] and of the spectra of the other ions of bismuth. The configuration assignments are also consistent with the hyperfine structure data (see Section V).

There is, however, evidence (see Section IV) of perturbation of a number of terms due to overlapping of configurations. The properties of a term when so perturbed cannot be completely described by a single configuration. However, as most of the perturbed terms show predominantly the characteristics of the configurations assigned to them, we consider the assignments sufficiently significant to warrant their use.

The only even term predicted in the energy range 0 to 270,000 cm^{-1} that has not been identified is $6p_{1\frac{1}{2}}6p_{1\frac{1}{2}}(J=0)$. It is predicted a little higher than 11_2. But its combinations with $2_1°$ and $4_1°$, which should be in the extreme ultraviolet, have not been identified among Arvids-

[4a] Bacher and Goudsmit, *Atomic Energy States*. Also unpublished data of authors.

[4b] J. C. McLennan, A. B. McLay and M. F. Crawford, Proc. Roy. Soc. **A125**, 570 (1929). S. Smith, Phys. Rev. **35**, 235 (1930). J. C. McLennan and M. F. Crawford, Proc. Roy. Soc. **A132**, 10 (1931).

son's wave-lengths.[4] Its combinations with other known terms are probably beyond 10,000A. The even term designation 12 is reserved for this unidentified term.

Ten odd terms besides those of $6s7p$ have been established in the range 224,000 to 238,000 cm^{-1}. They undoubtedly arise from the $6s5f$ and $5d^9\,6s^2\,6p$ configurations. An unambiguous differentiation of three of these terms, $17_3°$, $18_3°$, $21_3°$, two from $6s5f$ and one from $5d^9{}_{2\frac{1}{2}}\,6s^2\,6p_{1\frac{1}{2}}$, could not be made; hence both configurations are assigned to all three in Table I. The hyperfine structure intervals of $19_2°$ and $20_4°$ show that these two are $6s5f$ terms. That the remaining

TABLE I. *Terms of Bi IV.*

Configuration[1]	Term[2]	Value[3] cm^{-1}	Total hfs interval
$6s^2$	1_0	0 [4]	
$6s6p$	$1_0°$	70963	
	$2_1°$	75926	12.5±0.5
	$3_2°$	96423	13. ±3.
	$4_1°$	114602	
$6p_{\frac{1}{2}}6p_{\frac{1}{2}}$	2_0	166552	
$6s6d$	3_2	184160	2.5±0.5
$6p_{\frac{1}{2}}6p_{1\frac{1}{2}}$	4_1	185014	small
$6s6d$	5_1	197151	−6.2±0.2
$6s7s$	6_1	197446	16.0±0.2
$6s6d$	7_2	197829	7.0±0.5
	8_2	199769	13. ±1. .
$6s7s$	9_0	201581	
$6p_{\frac{1}{2}}6p_{1\frac{1}{2}}$	10_2	202434	−2.5±0.5
$6p_{1\frac{1}{2}}6p_{1\frac{1}{2}}$	11_2	217823	small
$5d^9{}_{1\frac{1}{2}}\,6s^2\,6p_{\frac{1}{2}}$	$7_2°$	224292	3.0±0.5
$6s7p_{\frac{1}{2}}$ [5]	8°	224584.6 ($F=4\frac{1}{2}$)	15.6±0.1
	9°	224600.2 ($F=3\frac{1}{2}$)	6.8±0.1
	10°	224607.0 ($F=4\frac{1}{2}$)	4.9±0.1
	11°	224611.9 ($F=5\frac{1}{2}$)	

Configuration	Term	Value cm^{-1}	Total hfs interval
$5d^9{}_{2\frac{1}{2}}\,6s^2\,6p_{1\frac{1}{2}}$	$12_4°$	225617	
$5d^9{}_{1\frac{1}{2}}\,6s^2\,6p_{\frac{1}{2}}$	$13_1°$	228127	1.5±0.4
$5d^9{}_{2\frac{1}{2}}\,6s^2\,6p_{1\frac{1}{2}}$	$14_2°$	230637	3. ±1.
$6s7p_{1\frac{1}{2}}$	$15_1°$	231913	−4.2±0.2
	$16_2°$	232627	11. ±1.
$5d^9{}_{2\frac{1}{2}}\,6s^2\,6p_{1\frac{1}{2}}$ and $6s5f$	$17_3°$	233238	small
	$18_3°$	233955	small
	$21_3°$	236518 [6]	small
$6s5f$	$19_2°$	235172	−7. ±1.
	$20_4°$	235657	13. ±4.[7]
$5d^9{}_{2\frac{1}{2}}\,6s^2\,6p_{1\frac{1}{2}}$	$22_1°$	237701	−1.5±0.5
$6s8s$	13_1	266674	14.2±0.2
$6s7d$	14_1	267576	−6.4±0.4
	15_2	267856	10. ±1.
$6s8s$	16_0	268191	
$6s7d$	17_3	268690	13. ±1.
	18_2	269758	−6.5±1.

[1] Evidence for the configuration assignments is discussed in the context.

[2] The numbers 5° and 6° have been reserved for the two terms of $5d^9{}_{2\frac{1}{2}}\,6s^2\,6p_{\frac{1}{2}}$, as yet unidentified; and 12 for the one unidentified term of the $6p^2$ group.

[3] The value assigned to each term whose hfs splitting has been determined is that of its middle ($F=4\frac{1}{2}$) hfs level. In regard to the values of the $6s7p_{\frac{1}{2}}$ terms see reference 5. Accuracy of term values is about ±2 cm^{-1}.

[4] The value of this term relative to $6s\ {}^2S$ of Bi V is about 365,500 cm^{-1}, obtained by applying a Rydberg formula to $6s6d\ 8_2$ and $6s7d\ 17_2$.

[5] 8°, 9°, 10°, 11°, are the four hfs levels of $6s7p_{\frac{1}{2}}$. Because of perturbation (see Section V) the J's lose their significance and only F values can be assigned to these levels. Their combinations are governed by the Laporte and F selection rules and are independent of the J rule.

[6] This term is not listed in the order of its term value; the usual order has been altered to facilitate grouping.

[7] The partially resolved line patterns involving this term indicate that it has a large total hfs interval.

TABLE II. *Classified wave-lengths.*

Order of Int.	λ I.A. (mean)	Classification	ν cm⁻¹	Relative int. and character of hfs components	Remarks
m	5347	$11_2 - 21_3°$	18696		
w	5029	$11_2 - 22_1°$	19877		
w	4509	$10_2 - 8°$	22150	1	
		$10_2 - 9°$	65.0	10	
		$10_2 - 10°$	73.0	7	
		$10_2 - 11°$	78.5	10	
m	4342	$9_0 - 8°$	23005.3	—	—strong O II line near this component
		$9_0 - 9°$	19.2	10	
		$9_0 - 10°$	26.0	6	
		$9_0 - 11°$	31	—	—red edge of strong Bi II line here
w	4077	$8_3 - 7_2°$	24523	B	
			29	—	—strong O II line at violet edge
w	4027	$8_2 - 8°$	24815	3b	
		$8_2 - 9°$	32	6b	
		$8_2 - 10°$	37	5b	
		$8_2 - 11°$	40	10b	
m	3891	$10_2 - 13_1°$	25693	b	
s	3868	$8_3 - 12_4°$	25848	B	
m	3778	$7_2 - 7_2°$	26464	B	—merged with O II line
m	3766	$9_0 - 13_1°$	26546		
s	3734	$7_2 - 8°$	26756	1b	
		$7_2 - 9°$	72	4b	
		$7_2 - 10°$	77	6b	
		$7_2 - 11°$	80	10b	
m	3724	$6_1 - 7_2°$	26839	10b	—also classified in Bi II
			46.5	6b	
			52.4	5b	
s	3682	$6_1 - 8°$	27130.4	5	
		$5_1 - 7_2°$	39	8b	
			41.5	3b	
			46	10	
		$6_1 - 9°$	53	8b	
		$6_1 - 10°$	57.4	6	
		$6_1 - 11°$	61.7	2	
			66.1	6	
			68.3	4	
s	3643	$5_1 - 8°$	27430.3	6	
			33.1	8	
			36.5	10	
		$5_1 - 9°$	45.9	2	
			48.6	3	
		$5_1 - 10°$	52.9	5	
			58.7	0?	
		$5_1 - 11°$	60.3	4	
			63.7	2	
w	3545	$10_2 - 14_2°$	28202	B	
m	3391	$10_2 - 15_1°$	29479	b	
w	3346	$22_1° - 14_1$	29874	B	
m?	3299	$7_2 - 13_1°$	30296.3	10	— classified in Bi II, the patterns of the Bi II and Bi IV lines probably nearly coincide
			98.3	8	
			301	8B	
m	3296	$9_0 - 15_1°$	30330	10	
			32	9	
			34	8	
w	3279	$22_1° - 16_0$	30491		
m	3259	$6_1 - 13_1°$	30672.0	10	
			80	8b	
			86.5	8	
m	3245	$10_2 - 17_3°$	30804	b	
s	3239	$8_2 - 14_2°$	30865	B	
m	3227	$5_1 - 13_1°$	30973	6b	
			76	7b	
			80	10b	
w	3190	$21_3° - 15_2$	31334.3	5	
			35.8	6	
			37.6	7	
			39.8	8	
			42.5	10	
m	3171	$10_2 - 18_4°$	31522	b	
m	3118	$22_1° - 18_2$	32059	B	
m	3085	$19_2° - 14_1$	32404	B	—merged with strong band component
w	3058	$19_2° - 15_2$	32678	10b	—merged with band component
			82	3b	
			85	2b	
			88	2b	
			94	8b	—merged with band component
m	3054	$10_2 - 19_2°$	32737	B	—also classified in Bi II
m	3047	$7_2 - 14_2°$	32808	B	
s	3042	$8_3 - 16_2°$	32860	B	
m	3026	$20_4° - 17_3$	33033	B	
s	3012	$6_1 - 14_2°$	33183.3	10b	
			90.5	9b	
			96.1	9b	
w	3007	$21_3° - 18_2$	33236.8	10	
			39.0	8	
			40.9	7	
			42.6	6	
			44.1	5	
m	2987	$8_3 - 17_3°$	33461.9	10	
			64.6	7	
			67.0	6	
			69.1	6	
			70.9	6	
			72.5	5	
			73.8	4	
m	2985	$5_1 - 14_2°$	33481.2	9b	
			85.0	9b	
			90.0	10b	
m	2949	$18_3° - 15_2$	33897.4	4	
			99.3	5	
			901.2	6	
			03.5	7	
			06.0	10	
s	2936	$16_2° - 13_1$	34042	—B	—also classified in Bi II
			48	10	
			52	4	
			55	5b	
s	2933	$7_2 - 15_1°$	34078	1	
		$10_2 - 21_3°$	85	10B	
			89	0b	
s	2924	$8_3 - 18_3°$	34179.7	10	
			82.4	7	
			84.8	6	
			86.9	6	
			88.8	6	
			90.4	5	
			91.7	4	
m	2901	$6_1 - 15_1°$	34455.7	10	
			58.0	9	
			64.5	8	
			68.7	8	
			74.0	8	
			75.9	7	
w	2888	$17_3° - 15_2$	34615	10B	
			19.4	5	
			22.0	8	
m	2875	$15_1° - 13_1$	34753	8b	—merged with a band component
			59	10b	
		$5_1 - 15_1°$	61	2	
			63	9b	
			65	8b	—merged with a band component
			68.9	3	
			71.2	4	
m	2873	$7_2 - 16_2°$	34800	B	
s	2842	$6_1 - 16_2°$	35172.4	2	
			75.3	5	
			79	10b	
			81.1	4	
			85	10b	
			88.3	3	
m	2838	$16_2° - 15_2$	35225	B	
m	2835	$10_2 - 22_1°$	35266	b	
m	2823	$7_2 - 17_3°$	35405.6	10	
			07.6	8	
			09.3	7	
			10.8	6	
			12.1	5	

TABLE II—(*Continued.*)

Order of Int.	λ I.A. (mean)	Classification	ν cm⁻¹	Relative int. and character of hfs components	Remarks
w	2792	$18_2°-18_2$	35799.0	9	
			801.3	6	
			65	10B	
s	2786	$8_2-20_2°$	35888	B	
			35934.4	6	—probably not a Bi line
			36.2	2	
			38.7	5	
m	2782	$15_1°-15_2$	41.2	6	
			43.9	7	
			46.4	4	
			49.4	10	—diffuse structure from this line to Bi I line=35954.5
			36033.4	9b	
m	2774	$14_2°-13_1$	38.4	9b	
			44.4	10b	
s	2772	$16_2°-17_3$	36061	B	
m	2768	$9_0-22_1°$	36118		
			36122.1	10	
			24.3	8	
s	2767	$7_2-18_2°$	26.2	7	
			27.9	6	
			29.4	5	
			36275.5	6	
m	2756	$15_1°-16_2$	77.4	8	
			79.7	10	
w	2737	$17_3°-18_2$	36520	B	—about five components resolved but too faint to measure
w	2720	$8_1-21_2°$	36751	B	—about seven components resolved but too faint to measure
			37122	10B	—also classified in Bi II
			28	2b	
w	2692	$16_2°-18_2$	32	3b	
			34	1	
			36	1b	
			37215	6b	
w	2686	$14_2°-15_2$	17	5b	
			19	6b	
			22	10b	
			37335.0	10	
			37.2	4	
s	2677	$7_2-19_2°$	39.9	3	
			41.4	8	
			44.9	8	
			48	9B	
			37714.0	10B	
m	2650	$6_1-19_2°$	25.6	9B	
			35.4	8B	
m	2642	$15_1°-18_2$	37845	B	—C II line at violet edge
s	2629	$5_1-19_2°$	38020	B	
			38049.6	6b	
			51.5	5	
			52.9	5	
m	2627	$14_2°-17_3$	54.3	6	
			55.9	7	
			58.0	10	
			59.0	2	
			38541	7	
w	2593	$13_1°-13_1$	46.8	4	
			48.3	4	
			55	10	
			38685.0	10	
			87.5	8	
m	2584	$7_2-21_2°$	89.1	7	
			90.9	6	
			92.5	5	
			39116	10b	
			18	2b	
w	2555	$14_2°-18_2$	21	6b	
			23	6b	
			25	5b	
w	2545	$4_1-7_2°$	39278	b	
			39444.0	10	
w	2534	$13_1°-14_1$	47.5	4	
			49.0	4	
			51.7	7	
			39571.5	10	
			86.8	2	
m	2525	$4_1-10°$	93	—	—strong unclassified Bi II line here
		$4_1-11°$	99	—	—strong Bi I line here
			39725.0	5	
			26.7	4	
m	2516	$13_1°-15_2$	28.6	5	
			30.7	6	
			33.0	10	
			39867.0	10	
			69.8	8	
w	2507	$7_2-22_1°$	72.4	6	
			74.0	5	
			75.7	5	
w	2495	$13_1°-16_0$	40066	—	—superimposed on faint classified Bi II line
w	2491	$3_2-7_2°$	40132		
			40245.5	10	
m	2483	$6_1-22_1°$	54.6	8b	
			62.0	8	
		$3_2-8°$	40425.7	2b	
m	2472	$3_2-9°$	42.3	10b	
		$3_2-10°$	47.9	7b	
		$3_2-11°$	51.8	9b	
			40546.1	8	
w	2465	$5_1-22_1°$	48.5	6b	
			51.5	10	
			41627.3	10	
			29.9	6	
			32.0	5	
m	2401	$13_1°-18_2$	33.9	4	
			36	4b	
			42060.8	3	
		11°	62.6	8	
		10° -13_1	67.6	5	
		9°	70.4	10	
s	2376		73.8	7	
			75.2	9	
			83.2	10	
		$8°-13_1$	89.6	9	
			97.5	8	
		$11°-14_1$	42960.2	6	—band component at red edge
			63.7	5	
		$10°-14_1$	68.2	3	—might be band line
			71.5	7	
		$9°-14_1$	75.2	5	
s	2326		78.2	3	
			87.3	10	—band component at red edge
		$8°-14_1$	90.8	8	
			93.7	6	—band at violet edge
m	2321	$12_1°-17_3$	43073	B	—structure confused by band components
w	2319	$4_1-13_1°$	43112		
			43246	6	
			48	6	
		11°	49.5	10	
		10° -15_2	51.1	7	
		9°	53	5	
s	2311		55	3	
			68.7	0	
		$8°-15_2$	70.7	1	
			73.0	2	
w	2295	$7_2°-15_2$	43565	B	—about five components, too faint to measure satisfactorily
		$11°-16_0$	43580.2	8	
		$10°-16_0$	85.0	7	
m	2293	$9°-16_0$	91.8	10	
		$8°-16_0$	608	1	
m	2274	$3_2-13_1°$	43966		
w	2251	$7_2°-17_3$	44399	B	—structure too faint to measure well; stronger line of unknown origin superimposed on red end
		$11°-18_2$	45145	—	—Hg III line here
—	2214	$10°-18_2$	53	—	—Bi II line here
		$9°-18_2$	62	—	—Bi III line here

TABLE II—(*Continued.*)

Order of Int.	λ I.A. (mean)	Classification	ν cm⁻¹	Relative int. and character of hfs components	Remarks
					This Bi IV pattern is either too faint to be observed or masked by the lines indicated
w	2199	$7_2°-18_2$	45465	b	
w	2151	$3_2-14_2°$	46476	—	observed only on grating plates; dispersion too small to detect structure
w	2099	$4_1-16_2°$	47615	b	
m	2093	$3_2-15_1°$	47748.3	10b	
			52.0	8b	
			54.8	6b	
	(mc.)				
w	1925.0	$4_1°-2_3$	51949		
m	1910.0	$3_2-21_2°$	52357		
w	1867.8	$3_2-22_1°$	53538		
w	1722.9	2_3- 9°, 10°, 11°	58042	b	also classified in Bi III
Arv.[1]					
w 2	1437.6	$4_1°-3_2$	69559		
2	1420.2	$4_1°-4_1$	70412		
s 60	1317.0	$1_3-2_1°$	75920	20	
			25.8	20	
			32.9	20	
3	1211.4	$4_1°-5_1$	82548		
1	1207.1	$4_1°-6_1$	82836.1	0	
			43.7	0	
			54.0	1	
0	1201.5	$4_1°-7_2$	83228	b	
w 7	1149.7	$4_1°-9_3$	86980		
m 6	1139.8	$3_2°-3_2$	87737	b	
6	1138.6	$4_1°-10_2$	87830		
w 7	1128.8	$3_2°-4_1$	88591	b	
s 24	1103.4	$2_1°-2_3$	90620.0	8	
			27.1	8	
			32.5	8	
			100718	1	
2	992.8	$3_2°-5_1$	100737	1	
8	989.8	$3_2°-6_1$	101027		
5	986.1	$3_2°-7_2$	101408		
8	968.8	$4_1°-11_2$	103222		
9	967.6	$3_2°-8_2$	103349		
15	943.3	$3_2°-10_2$	106002.9	5	number of components questioned by Arvidsson
			09.2	5	
			15.0	5	
12	923.9	$2_1°-3_2$	108231.2	4	
			36.8	4	
			41.4	4	
9	916.7	$2_1°-4_1$	109081.9	3	
			89.3	3	
			94.2	3	
8	876.8	$1_3°-4_1$	114051		
15	872.6	$1_3-4_1°$	114600		
12	824.9	$2_1°-5_1$	121217.2	6	
			30.4	6	
4	823.7	$3_2°-11_2$	121399	b	
9	822.9	$2_1°-6_1$	121512.5	3	number of components questioned by Arvidsson
			20.0	3	
			26.1	3	
10	820.3	$2_1°-7_2$	121899	b	
1	795.8	$2_1°-9_3$	125653		
8	792.5	$1_3°-5_1$	126188		
6	790.6	$1_3°-6_1$	126476.9	2	
			82.8	2	
			91.6	2	
6	790.5	$2_1°-10_2$	126500.4	2	
			07.8	2	
			14.2	2	
1	704.7	$2_1°-11_2$	141898		
1	651.1	$4_1°-16_3$	153591		
2	644.5	$4_1°-18_2$	155159		
3	587.4	$3_2°-13_1$	170253		
3	580.5	$3_2°-17_3$	172265		
2	524.2	$2_1°-13_1$	190752		
2	521.0	$2_1°-15_2$	191935		
2	508.6	$1_3°-14_1$	196607		
5	445.2	1_3- 9°, 10°, 11°	224607		
5	438.3	$1_3-13_1°$	228130		
6	431.2	$1_3-15_1°$	231911		
6	420.7	$1_3-22_1°$	237701		

b, Broad. s, strong. m, medium. w, weak.
B, Very broad; hfs partially resolved but difficult to measure.
[1] Data from G. Arvidsson's paper, Ann. d. Physik **12**, 787 (1932).

five and one of $17_3°$, $18_3°$, $21_3°$, are the six terms of the (*jj*) sub-groups $5d^9{}_{1\frac{1}{2}}\,6s^2\,6p_{\frac{1}{2}}$ and $5d^9{}_{2\frac{1}{2}}\,6s^2\,6p_{1\frac{1}{2}}$, is evident from their relative distribution and their J values. The differentiation of each sub-group is based on a comparison with the corresponding terms of the very similar $5d^9\,6p$ configurations of the Pt I sequence unambiguously interpreted by Mack[7] on the basis of near (*jj*) coupling.

We have not been able to identify the terms of the lowest and the highest (*jj*) sub-group of $5d^9\,6s^2\,6p$. The approximate positions of these are estimated at about 205,000 cm⁻¹ and 250,000 cm⁻¹, respectively. Thus most of the combinations of the two terms of the lowest sub-group with $6s6d$, $6s7s$, and $6p^2$ terms are probably in the red beyond the range of the available data, and their combinations with known higher even terms are probably weak. Combinations of the four terms of the highest sub-group with known even terms are probably weak. The numeral designations 5° and 6° are reserved for the two terms ($J=2$, 3) of the deepest sub-group since they are predicted among known terms. The terms of the highest sub-group are predicted above any known odd terms.

The multiplet structures of the various configurations are described and their special features indicated in the following.

[7] J. E. Mack, Phys. Rev. **34**, 17 (1929). Also a private communication.

(1) $6s6p$—The order of the J values is as predicted by simple theory; the energy distribution of the terms is consistent with Houston's equations[8] and characteristic of intermediate coupling.

(2) $6s6d$—The order of the J values is abnormal; one term 4_2 is below the other three which are in the order of their J values. This abnormality is also found in $6s6d$ and $6s7d$ of Hg I and Tl II and in $6s6d$ of Pb III and in many sd configurations of lighter elements; it is discussed more fully in Section IV.

(3) $6s7p$—The hyperfine structure intervals of the terms indicate near (jj) coupling, and their relative distribution except for two minor deviations is also consistent with this coupling. The $6s7p_{\frac{1}{2}}$ terms are almost coincident but it is doubtful if the coupling is as complete as the coincidence indicates. In all probability a small term perturbation effect is also involved (see Section IV). The $6s7p_{1\frac{1}{2}}$ terms are close together as expected; but are inverted, due undoubtedly to perturbation by adjacent terms (see Section IV).

(4) $6s7d$—The discussion in (1) applies to this configuration and also to $6s7d$ of Pb III. This is in contrast to $6s7d$ of Hg I and Tl II (see (2) above).

(5) $6s5f$—The distribution of terms is abnormal regardless of the ambiguity of its $J=3$ terms. If $21_3°$ is chosen as one of these and either $17_3°$ or $18_3°$ as the other, the distribution is very similar to that in $6s5f$ of Tl II and Pb III. The abnormal distribution is undoubtedly due to perturbation effects (see Section IV).

(6) $5d^9\,6s^2\,6p$—The distribution of the terms, which has already been discussed, shows that the coupling is near (jj).

(7) $6p^2$—The mean energies of the sub-groups indicate an approach to (jj) coupling, but the separation between the two terms 4_1 and 10_2 of $6p_{\frac{1}{2}}6p_{1\frac{1}{2}}$ is larger than expected for (jj) coupling. The large separation can be explained as a perturbation effect (see Section IV).

IV. Multiplet Perturbations

It is significant that $6s6p$ and $6s7d$ terms which are comparatively isolated show normal distributions, whereas $6s7p$, $6s5f$ and $6s6d$ terms, of which the first two overlap $5d^9\,6s^2\,6p$ and the third overlaps $6p^2$ and $6s7s$, show abnormal distributions. It is probable that the abnormalities are due to perturbations of the type suggested by Bacher.[9]

The interaction of $5d^9\,6s^2\,6p$ with $6s7p$ and $6s5f$ is sufficient to account qualitatively for the observed perturbations in these configurations. The unusually small separation between the $6s7p_{\frac{1}{2}}$ states can be explained as due to the perturbing effect of $13_1°$; the inversion of the $6s7p_{1\frac{1}{2}}$ terms as due to the mutual perturbation of $13_1°$, $15_1°$ and $22_1°$, and of $14_2°$ and $16_2°$; and the abnormal distribution of the $6s5f$ terms as due to mutual perturbation of $17_3°$, $18_3°$, and $21_3°$. The perturbation effects are less noticeable in the $5d^9\,6s^2\,6p$ terms than in the $6s7p$ and $6s5f$ terms, since the $5d^9$ and $6p$ doublet intervals are much larger than the $7p$ and $5f$ intervals.

Since the $5d^9\,6s^2\,6p$ terms of Hg I, Tl II, and Pb III are not as well known as those of Bi IV, we cannot trace their effect on the $6s7p$ and $6s5f$ terms as the relative separations of the groups change with ionization and nuclear charge.

The interaction of $6p^2$ with $6s6d$, which is expected to be large according to Bacher,[9] qualitatively explains the abnormal distribution of the $6s6d$ terms of Bi IV and the other members of the Hg I sequence. Sufficient data on the $6p^2$ and $6s6d$ terms of these spectra are available to compare their relative energies. They are tabulated in Table III. Only the $J=2$ terms of $6p^2$ are given, since they represent approximately the c.g. of the whole group and are mainly responsible for the perturbation of $6s6d$. Mutual perturbation of the $J=1$ terms of the two configurations is not immediately evident. One of the $6s6d$ terms with $J=2$ is for all the cases considered within the relatively narrow so-called triplet, and its displacement from the normal position is not large compared to the variation in the separation of the other $J=2$ term from the triplet. Accordingly, for this qualitative comparison the triplet is represented by its normal c.g. (calculated from the total triplet separation by the (LS) interval rule) which is

[8] W. V. Houston, Phys. Rev. **33**, 297 (1929).

[9] R. F. Bacher, Phys. Rev. **43**, 264 (1933).

TABLE III. *Relative energies of sd, p^2 configurations of Hg I sequence.*

Level		Hg I†	Tl II†	Pb III†	Bi IV
$6s7d$	normal c.g. of $J=1, 2, 3$	5718	21540	43436	69522
	$J=2$	5671	20337	44950*	71036
$6p_{\frac{1}{2}}6p_{1\frac{1}{2}}$ $J=2$		——	18774	20082*	19101
$6p_{\frac{1}{2}}6p_{\frac{1}{2}}$ $J=2$		23233*	12263	6468	3712
$6s6d$	normal c.g. of $J=1, 2, 3$	0	0	0	0
	$J=2$	−60	−1394	−6466	−14562

* Unpublished data of authors.

† Data from Bacher and Goudsmit *Atomic Energy States.*

taken as the datum level in Table III. The $6s7d$ configurations are also included for comparison.

With increasing ionization $6p^2$ drops from above $6s7d$ in Hg I to just above $6s6d$ in Bi IV. As the $6p^2$ configuration approaches $6s6d$, the $J=2$ term of the latter diverges much more rapidly from the c.g. of the other three than normally expected for increasing ionization. The unusually rapid divergence is undoubtedly due to the interaction of the $6s6d$ and $6p^2$ configurations. The order of magnitude and the direction of the effect are as predicted by Bacher's treatment of $sd-p^2$ interactions,[9] thus qualitatively confirming his theory. The presence of this effect accounts for the fact that the $6s6d$ intervals are not consistent with Houston's[8] equations.

In Pb III and Bi IV $6p^2$ is relatively remote from $6s7d$, and as expected the $6s7d$ terms in both spectra are in normal order and agree with Houston's equations. In Hg I and Tl II there is probably some interaction of $6p^2$ and $6s7d$, since the order of the latter terms is abnormal. Houston has shown that the $6s7d$ terms of Hg I deviate somewhat from his predictions. The corresponding terms of Tl II according to our calculations fit fairly well with a negative value of X; but their hyperfine structures[10] indicate some perturbation of the $J=2$ terms. It is, however, difficult to draw any definite conclusions about the significance of the observed distribution of the $6s7d$ terms of Hg I and Tl II, since there is a possibility of perturbation by other configurations in addition to $6p^2$.

In Bi IV there is a possibility of interchanging the term assignments of 3_2 and 10_2. The change would give a normal order for the $6s6d$ terms, agreeing fairly well with Houston's equations, but an unsatisfactory distribution of the $6p^2$ terms. The hyperfine structure intervals of the individual terms with $J=2$ are consistent with this alternative assignment but for overlapping configurations only sum relations and not the equations for the individual levels are applicable. The sum relations taken over all $J=2$ terms of $6s6d$ and $6p^2$ are consistent with either assignment. The given assignment, however, can be adequately correlated with the unambiguously identified $6s6d$ and $6p^2$ terms of Hg I, Tl II, and Pb III, whereas the alternative cannot. This evidence, together with the fact that the distribution as given can be accounted for by Bacher's theory, is the basis for our unique configuration assignments $6s6d\ 3_2$ and $6p_{\frac{1}{2}}6p_{1\frac{1}{2}}\ 10_2$. However, on account of the sharing of some characteristics these terms are only approximately described by the configurations assigned.

There is evidence of a slight mutual perturbation of the adjacent terms $6s6d\ 5_1$ and $6s7s\ 6_1$. The prominence of the combination line $6s7s\ 6_1 - 6s5f\ 19_2°$, which, although permitted by the Laporte rule, involves a single electron transition with $\Delta l=3$, indicates that 5_1 and 6_1 share some of their combining characteristics. The absence of the similar transition $6s5f\ 19_2° - 6s8s\ 13_1$ shows that the $\Delta l=3$ type of transition is normally not prominent when the terms are unperturbed. The mutual perturbation of 5_1 and 6_1 is not noticeable in their hyperfine structure intervals.

V. HYPERFINE STRUCTURE

Although all the hyperfine structure intervals have a limit of error of 0.1 cm^{-1} or greater, most of them are so large that they can be compared somewhat critically with theory. The comparison, presented in this section, shows: (1) that the hyperfine structure levels 8°, 9°, 10°, 11°, arising from $6s7p_{\frac{1}{2}}$ exhibit perturbation of the

[10] J. C. McLennan, A. B. McLay and M. F. Crawford, Proc. Roy. Soc. **A133**, 652 (1931).

type (violation of interval rule and intensity relations) found in Hg I by Schüler and Jones[11] and explained by Goudsmit and Bacher;[12] (2) that for our configuration assignments the observed interval factors are consistent with the theory of hyperfine structure separations;[13] and (3) that the mutual perturbation of overlapping configurations of the same parity affect the interval factors of the states with the same J values.

$6s7p_1$—Normally one expects first the two electrons of $6s7p_1$ to couple giving two multiplet states with J values 0 and 1, and then each of these J's to couple with the nuclear moment, $J=0$ giving one hyperfine structure level with $F=4\frac{1}{2}$ and $J=1$ giving three levels with $F=3\frac{1}{2}$, $4\frac{1}{2}$, $5\frac{1}{2}$. For this coupling the three levels arising from $J=1$ should obey the interval rule, and all four levels should combine according to the J and F selection rules and the normal intensity formulae.[14] In Bi IV, however, the interaction between the two electrons, $6s$ and $7p_1$, is small and of the same order of magnitude as their resultant interaction with the magnetic nucleus. For this case the J's lose their significance as quantum numbers and only F values can be assigned to the levels. Accordingly the four levels of $6s7p_1$ are not expected to exhibit the characteristics predicted for normal coupling. A theoretical treatment of hyperfine structure perturbation due to a change in coupling has been published by Goudsmit and Bacher.[12] Their theory is applied in the following.

Expressions for the hyperfine structure interactions can be readily derived for the two extreme cases where the hyperfine structure is much smaller and where it is much larger than the separation between the two J states. The relative energies of the four hyperfine structure levels of $6s7p_1$ for the extreme cases are given in Table IV. Here X represents the distance between the two J states in the absence of hyperfine structure, and a_{6s} is the interaction constant that governs the magnitude of the interaction of the $6s$ electron with the magnetic nucleus. In these equations the interaction of the $7p_1$ electron with the nuclear moment ($a_{7p}(\frac{1}{2})=0.1$)[15] is neglected, since it is about 1/25 of that of the $6s$ electron and only introduces a correction of the order of the error in the observed intervals.

TABLE IV. *hfs levels of $6s7p_1$ for (jj) coupling.*

Level	$a_{6s} \ll X$	$X=0$
$F=5\frac{1}{2}$	$E=0$	$E=0$
$=4\frac{1}{2}$	$E=-11/4\cdot a_{6s}$	$E=0$
$=3\frac{1}{2}$	$E=-5a_{6s}$	$E=-5a_{6s}$
$=4\frac{1}{2}$	$E=-X-9/4\cdot a_{6s}$	$E=-5a_{6s}$

The information in Table IV is sufficient to determine[16] the coefficients of the set of equations the roots of which give the relative energies of the levels for any intermediate values of a_{6s} and X. These equations are:

$$F=5\tfrac{1}{2};\quad E=0 \tag{1}$$

$$=4\tfrac{1}{2};\quad E^2+E(X+5a_{6s})+11/4\cdot X\cdot a_{6s}=0 \tag{2}$$

$$=3\tfrac{1}{2};\quad E+5a_{6s}=0. \tag{3}$$

The values of X and a_{6s} can be determined from the two levels with $F=5\frac{1}{2}$ and $3\frac{1}{2}$ and either of the levels with $F=4\frac{1}{2}$. The values of X and a_{6s} obtained from the relative energies of 11°, 9° and 8° are $X=20.4$ cm^{-1}, $a_{6s}=2.34$ cm^{-1}. These values when substituted in Eq. (2) give the position of 10° as 4.81 cm^{-1} below 11°. The good agreement of this predicted value with the observed position of 10°, 4.9 ± 0.1 cm^{-1} below 11°, shows that the hyperfine structure perturbation in $6s7p_1$ is a coupling effect due to the approximate equality of the multiplet and hyperfine structure separations of $6s7p_1$. The magnitude of the perturbation is such that 10° is displaced from its normal position, 6.43 cm^{-1} below 11° as calculated by the interval rule, to its observed position, 4.9 cm^{-1} below 11°.

A value of a_{6s} determined from the hyperfine splitting of a term of another configuration could be used in the equations but as the value

[11] H. Schüler and E. G. Jones, Zeits. f. Physik **77**, 701 (1932).

[12] S. Goudsmit and R. F. Bacher, Phys. Rev. **43**, 894 (1933). See also H. Casimir, Zeits. f. Physik **77**, 811 (1932).

[13] S. Goudsmit and R. F. Bacher, Phys. Rev. **34**, 1501 (1929) and S. Goudsmit, Phys. Rev. **37**, 663 (1931).

[14] E. L. Hill, Proc. Nat. Acad. Sci. **15**, 779 (1929).

[15] R. A. Fisher and S. Goudsmit, Phys. Rev. **37**, 1057 (1931).

[16] S. Goudsmit, Phys. Rev. **35**, 1325 (1930).

of a_{6s} obtained from other terms is not overly accurate this alternative method has not been used. Although the value $a_{6s}=2.34$ derived from $6s7p_1$ might not be very reliable, since in its derivation the coupling was assumed strictly (jj) and the interaction constant of $7p_1$ neglected, it is probably the best obtainable from the present data; and is consistent within the limits of the experimental errors with the interval factors of the terms of the other configurations (see Table V). This value of a_{6s} in Bi IV also compares favorably with the values of a_{6s} in other spectra of bismuth,[15] namely: Bi II, 1.60; Bi III, 1.80; Bi IV, 2.34; Bi V, 2.6.

Anomalies in the combinations of 8°, 9°, 10°, 11°, have been observed, as expected for perturbations of this type. The relative intensities of the hyperfine components of the combinations of 8° and 10° with $J=1$ terms, which are permitted by the J rule, indicate that 8° and 10° share their characteristics as expected. Forbidden combinations of 8°, which normally would be characterized by $J=0$, with $J=0$ and $J=2$ terms have been observed; the ratio of the sum of the intensities of the hyperfine structure components involving 8° to the sum of the intensities of the components involving 9°, 10°, 11° (normally characterized by $J=1$) is of the order of the ratio 1/14 predicted by Eq. (4) of Goudsmit and Bacher's paper.[12] Combinations of 8°, 9°, 10°, 11°, with the term 8_3, all of which are normally forbidden, have also been observed as weak lines.

In all respects the hyperfine structure of $6s7p_1$ confirms Goudsmit and Bacher's theory.

The hyperfine structure of other terms of Bi IV are discussed in the following. The value $a_{6s}=2.34$ deduced from $6s7p_1$ is used in the appropriate separation formulae[13] to predict the interval factors (A) of the terms. The predicted

TABLE V. *hfs interval factors.*

	Formula	A(calc.)	A(obs.)	Remarks
$6s7p_{1\frac{1}{2}}$	$A(15_1°)=-\frac{1}{4}a_{6s}$	−0.585	−0.42*	Coupling (jj). Since $a_{7p}(1\frac{1}{2})=0.01$, it is neglected[15]
	$A(16_2°)=\frac{1}{4}a_{6s}$	0.585	0.55	
$6s7d$	$A(14_1)=-\frac{1}{4}a_{6s}$	−0.585	−0.64	Coupling intermediate, a_{7d} is neglected
	$A(15_2)+A(18_2)=1/12\cdot a_{6s}$	0.195	0.18	
	$A(17_2)=1/6\cdot a_{6s}$	0.390	0.43	
$6s5f$	$A(19_2°)=-1/6\cdot a_{6s}$	−0.390	−0.35	Coupling intermediate, a_{5f} is neglected
	$A(20_4°)=1/8\cdot a_{6s}$	0.292	0.3	
$6s6p$	$A(2_1°)=\frac{1}{2}a_{6s}+\frac{1}{2}a_{6p}(\frac{1}{2})$	1.5	1.3†	Coupling intermediate, $a_{6p}(\frac{1}{2})=0.7$, $a_{6p}(1\frac{1}{2})=0.01$ [15]
	$A(3_2°)=\frac{1}{4}a_{6s}+3/4\cdot a_{6p}(1\frac{1}{2})$	0.59	0.65	
$6s6d$	$A(5_1)=-\frac{1}{4}a_{6s}$	−0.585	−0.62	a_{6d} is neglected; independent of coupling
	$A(8_2)=1/6\cdot a_{6s}$	0.390	0.43	
$6s6d$ and $6p^2$	$A(3_2)+A(7_2)+A(10_2)+A(11_2)=1/12\cdot a_{6s}+\frac{1}{4}a_{6p}(\frac{1}{2})$	0.37	0.35	Mutual perturbation of the two configurations. a_{6d} & $a_{6p}(1\frac{1}{2})$ neglected

* Although the agreement for this term is not as good as for the other terms, the observed interval has the right sense and order of magnitude. Strictly this term should not be treated alone but should be summed with $13_1°$ and $22_1°$ since they mutually perturb. Although the intervals of $13_1°$ and $22_1°$ are known, the predicted sum of the interval factors of the three terms cannot be computed for comparison since sufficient data are not available to determine the interaction constant of $5d^9$.

† The observed interval factor of this term is smaller than the value calculated by means of the (jj) formula. This is as expected since the coupling is intermediate tending to (jj). The interval of $4_1°$ is needed for a more critical discussion of the hyperfine structure of $6s6p$.

values are compared in Table V with the observed values.

The interaction constants a_{7s} and a_{8s} can be determined from the intervals of $6s7s\ 6_1$ and $6s8s\ 13_1$ and the value $a_{6s}=2.34$ as follows:

$$A(6_1)=\tfrac{1}{2}a_{6s}+\tfrac{1}{2}a_{7s}=1.60, \text{ hence } a_{7s}=0.86;$$

$$A(13_1)=\tfrac{1}{2}a_{6s}+\tfrac{1}{2}a_{8s}=1.42, \qquad a_{8s}=0.50.$$

The value of $a_{7s}=0.86$ determined from Bi IV is larger than $a_{7s}=0.47$ obtained from Bi III[15] by an amount of the order expected when the decrease in screening is considered. The value of $a_{8s}=0.50$ relative to the value of a_{7s} is of the order expected. These values, however, are not very accurate.

The data presented above show that the hyperfine structure of Bi IV is consistent with our configuration assignments. The intervals, however, are hardly accurate enough for a rigorous determination of the interaction constants of the various electrons. Hence we are preparing to investigate the hyperfine structure with a new twenty-one foot grating.

In conclusion the authors wish to thank Professor E. F. Burton, Director of the laboratory, for his interest in this investigation.

Hyperfine Structure Absorption in Optically Excited Mercury Vapor

M. L. Pool and S. J. Simmons, *Department of Physics, Ohio State University*

(Received July 18, 1933)

The radiation 4047, 2967 and 2752, all terminating on the $2\,^3P_0$ state of mercury, was passed through optically excited mercury vapor and the absorption of each wavelength for various lengths of excited vapor and for various pressures of admixed nitrogen was measured photometrically. With low dispersion the intensity of 2752 decreased nearly exponentially with increase in length of excited vapor giving a constant linear absorption coefficient. But the lines 4047 and 2967 were found not to obey the exponential law, the fractional decrease in intensity per unit length of path decreased rapidly as the total length of the absorbing vapor increased. With high dispersion the absorption of the five components of 4047 was strong and increased with increase of admixed nitrogen. The strongest component showed the strongest absorption and the amount of absorption decreased with decrease in intensity of components. The intensity of each component decreased nearly exponentially with increase in length of excited mercury vapor. Both components of 2967 showed strong absorption. None of the components of 4358 or 5461 showed measurable absorption.

Introduction

ONE of the most direct methods of determining the presence of the $2\,^3P_0$ metastable state of the mercury atom in excited mercury vapor is by measuring the absorption of the 4047 line. If this line has a constant absorption coefficient, then the relative number of metastable atoms under various experimental conditions may be readily ascertained. Since the 2967 and 2752 lines of mercury also terminate on the $2\,^3P_0$ level, the absorption of these lines could also be used to determine the variation in the concentration of the metastable state.

Numerous experiments,[1] however, have shown that the 2537 line of mercury has a variable absorption coefficient, the smaller the concentration of atoms in the ground state the larger the atomic absorption coefficient. At present no data or values for the absorption coefficients for either 4047, 2967 or 2752 can be found in the literature. The purpose of the experiment reported here is to determine the character of the absorption of these mercury lines and the linear absorption coefficients for them in optically excited mercury vapor.[2]

[1] A. L. Hughes and A. R. Thomas, Phys. Rev. **30**, 466 (1927).

[2] M. L. Pool and S. J. Simmons, Phys. Rev. **42**, 909 (1932); **43**, 1045 (1933).

Apparatus and Procedure

A schematic diagram of the quartz resonance tube 30 inches by 1 inch is shown in Fig. 1. The outside walls were painted black, save for a two millimeter hole on each of the end windows and three lengths of 6.4 cm each on the sides of the tube. The lengths could be diminished by

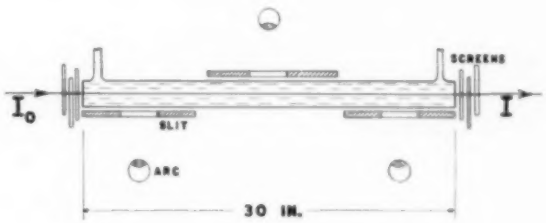

Fig. 1. Absorbing mercury resonance tube.

replaceable shields of different widths. The three exciting Uviarcs were water-cooled and magnetically deflected. The source arc, emitting the lines 4047, 2967 and 2752 used for absorption, was of the same type and similarly operated. Agitated calibrated neutral screens were placed between the resonance tube and the spectrograph for calibrating the photographic plates. Eastman No. 33 plates were used and developed with a unit contrast developer recommended by L. A. Jones of the Eastman Kodak Company. The nitrogen was moved continuously over P_2O_5,

hot copper and copper oxide by means of a circulating system.

For low dispersion a small Steinheil spectrograph was used with a wide slit. The exposure time was about twenty seconds. On each plate there were about forty exposures of which nearly half were density markings. For high dispersion a 30,000 line 21 ft. grating was used in the second order for 4047 and third for 2967. The exposure time was about thirty minutes for 4047 and several hours for 2967. A Moll self-recording microphotometer and also a photoelectric densitometer were used to determine the plate transmissions.

Results

(A) Low dispersion

For the 4047 and 2967 lines a plot of log I/I_0 against the increase in length of optically excited mercury vapor gave a curve that markedly departed from a straight line. The slope of the curve decreased as the length of excited vapor increased. This behavior may be interpreted by assuming that the linear absorption coefficient μ, defined by $\mu x = \log I_0/I$, is not constant but decreases as the above lines pass through more and more excited vapor. The maximum coefficient for both lines was about the same, 0.25. The minimum was approximately 0.027 for 4047 and 0.045 for 2967 and occurred when the length of excited vapor was about 20 cm. The 2752 line is very weakly absorbed compared with the 2967 line and within experimental error has a constant linear absorption coefficient of about 0.007.

The characteristic absorption of the 4047 line was tested for various kinds of arcs. It was found that if capillary arcs were avoided and if the larger diameter arcs were run somewhat below their normal current rating, the absorption curves varied very little. Water cooling was always necessary.

(B) High dispersion

Since the 2967 and 4047 absorption could be described within experimental error as though there were two constant linear absorption coefficients,[2] it was thought desirable to investigate the absorption of the hyperfine structure of these lines. Fig. 2 shows a fifteen times enlargement of the hyperfine structure of 4047 when passed through 0 cm and when passed through 22.1 cm of excited mercury vapor. The central component was over exposed in order to bring out clearly the faint $+0.668$ cm^{-1} component. Fig. 3 shows the microphotometer record of 4047 when passed through 0, 3.7, 7.4, 14.6 and 21.1 cm of optically excited vapor. It is interesting to note how rapidly the central component decreases in intensity with increase in length of excited

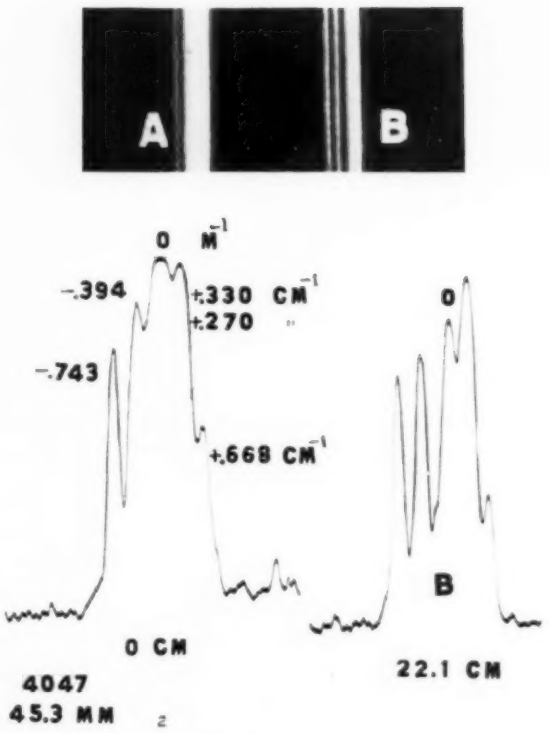

Fig. 2. Above: *A*, components of 4047 when no absorption; *B*, when absorbed by 22.1 cm of excited mercury vapor with 45.3 mm of admixed nitrogen. Below: The microphotometer record.

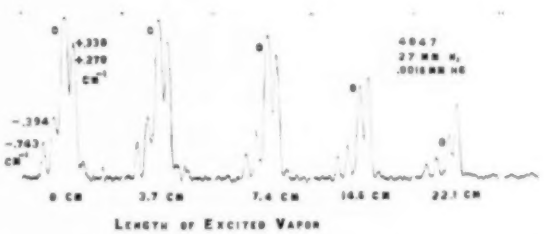

Fig. 3. Microphotometer record of 4047 when absorbed by various lengths of excited mercury vapor.

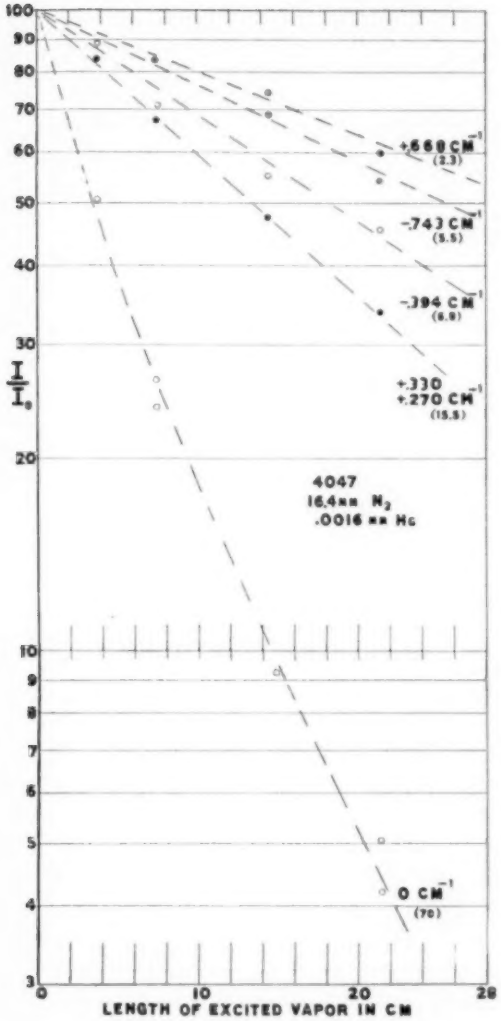

FIG. 4. Semi-logarithmic plot of the intensity of the components of 4047 against thickness of absorbing vapor at 16.4 mm N_2.

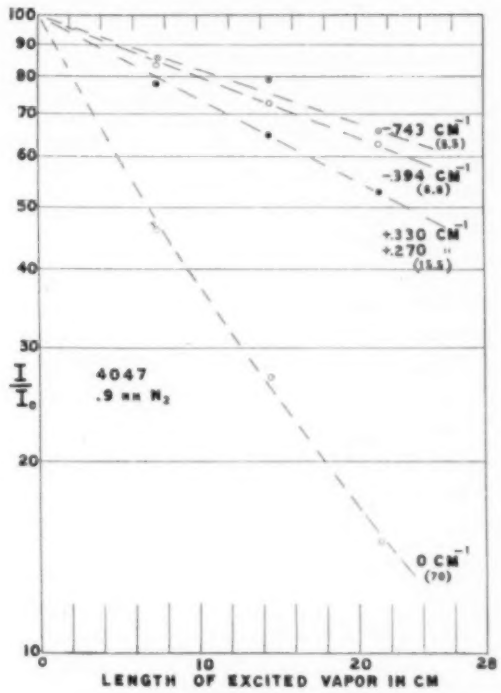

FIG. 5. Semi-logarithmic plot of the intensity of the components of 4047 against thickness of absorbing vapor at 0.9 mm N_2.

vapor. After passing through 14.6 cm of vapor the central component is weaker than the +0.330 and +0.270 cm^{-1} component. In Fig. 4, showing a semi-logarithmic plot of I/I_0 against the length of excited vapor for all the five components of 4047, it is noticed that all the components except the central one have constant linear absorption coefficients and that the coefficients decrease with decrease in intensity of the components. The relative intensities are represented by the numbers in parentheses.[3] Fig. 5 shows a similar plot on the same scale for a low pressure, 0.9 mm, of admixed nitrogen. For one set of observations at one pressure it would be doubtful, as is evident in Figs. 4 and 5, whether drawing a straight line for all components except the zero component is justified. However, for many sets of observations and pressures the central component was always concave upward while the other components were concave downward about as often as concave upward. The fact that the absorption coefficient of the central component is thus not strictly constant is probably due to the fact that the central component itself consists of four components.[4] In Fig. 6 are plotted the linear absorption coefficients for the various components against the pressure of nitrogen. An average slope was taken in determining the absorption coefficient for the central component. In Table I are listed some coefficients which are more accurate than could easily be read from Fig. 6.

None of the components of 4358 or 5461 showed measurable absorption.

[3] H. Schüler and J. E. Keyston, Zeits. f. Physik **72**, 423 (1931).

[4] K. Murakawa, Sc. Pap. I. P. C. R. **18**, 177 (1932).

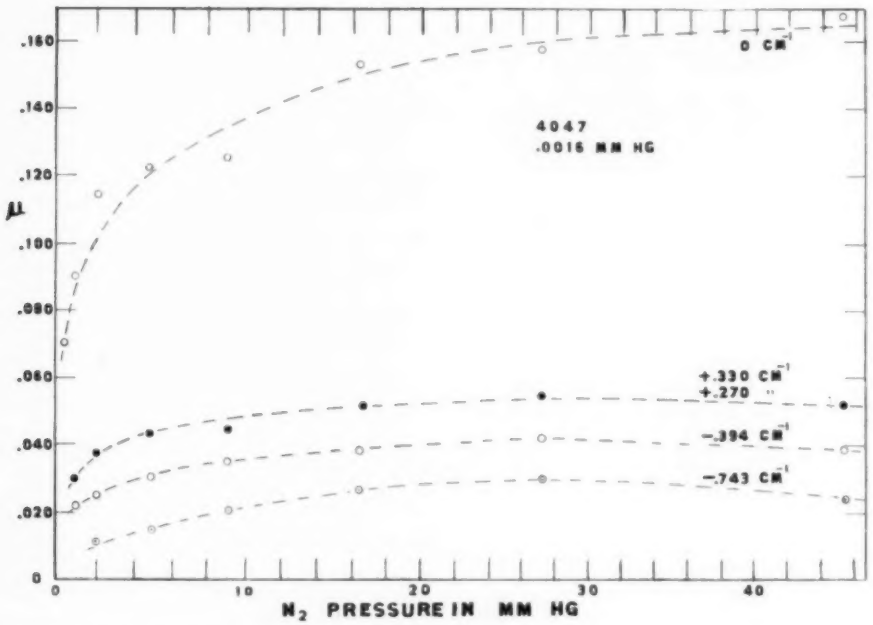

FIG. 6. Linear absorption coefficients of the different components of 4047 plotted against the nitrogen pressure.

The 2967 line in third order showed the two strongest components well separated.[5] Both of these components were strongly absorbed and the more intense one the more strongly. Since the exposure time was several hours, a series of runs to determine the absorption coefficients of these two components as well as the other weaker ones was not feasible.

TABLE I. *Linear absorption coefficients for the components of 4047.*

N_2 pressure	0 cm^{-1}	+0.330, +0.270 cm^{-1}	−0.394 cm^{-1}	−0.743 cm^{-1}
2 mm	0.101	0.036	0.024	0.010
5	.121	.044	.032	.016
10	.138	.049	.036	.022
20	.155	.053	.040	.029
40	.164	.054	.040	.028

DISCUSSION

The above results may be interpreted with respect to the hyperfine energy levels involved. In Fig. 7 are shown the six components of the 2537 line.[3] Each of these components is absorbed by one or more of the isotopes of mercury; for example, the $-0.333\ cm^{-1}$ component is absorbed by three isotopes, 199, 201 and 204. The decrease in intensity of a given component as it passes through a certain distance of mercury vapor will depend upon the number of absorbing isotopes, the statistical weights of the hyperfine levels involved and the atomic absorption coefficient. Since the diameter of the resonance tube in this experiment was 2.5 cm, each component of 2537 had to travel 1.25 cm of mercury vapor before reaching the region where the absorption of 4047 takes place. The total number of mercury atoms in this distance per sq. cm cross section is 67.5×10^{12}. The atomic absorption coefficient for each isotope or for each component of 2537 has not been determined directly. The absorption of the 2537 line as a whole has been made by many observers, who then by certain assumptions concerning the contour and intensity of each component arrive at an expression for the atomic absorption coefficient. Using Zemansky's[6] coefficient of 1.41×10^{-13}, which is assumed the same for all isotopes, one finds that the intensity of the various components decreases differently and rapidly in the distance of 1.25 cm and that the comparatively weak component, +0.161

[5] W. H. McCurdy, Phil. Mag. **5**, 386 (1928).

[6] M. W. Zemansky, Phys. Rev. **36**, 219 (1930).

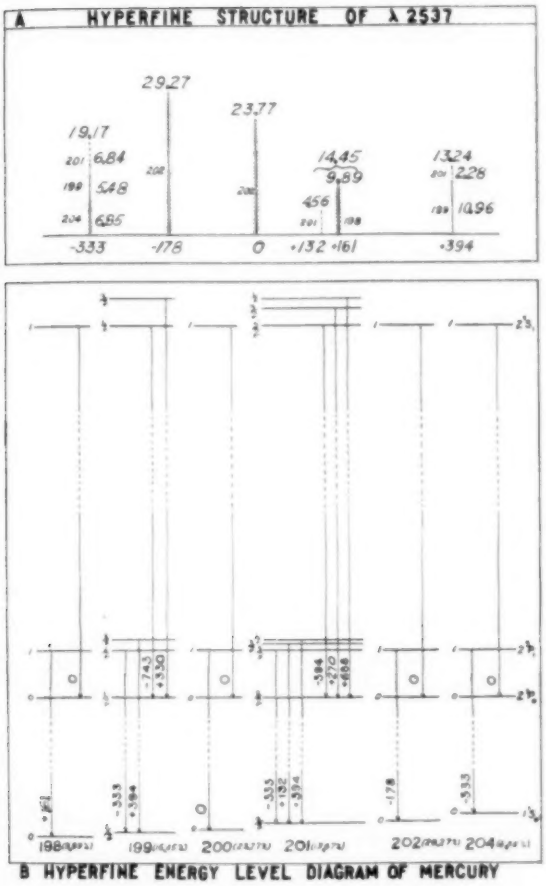

FIG. 7. Hyperfine structure of 2537 and energy level diagram for mercury.

cm^{-1}, is, at 1.25 cm within the resonance tube, the strongest component of the 2537 line. The intensity of the various components at this point in the resonance tube will determine the number of the various isotopes at this point that are put into the excited $2\,^3P_1$ state. For example, the number of 201 isotopes excited to the middle $2\,^3P_1$ hyperfine level divided by the number of 200 isotopes excited is 1/3.86, while at the wall of the tube where 2537 first enters this ratio is 1/21.8.

It is now assumed that all the excited isotopes have an equal chance of suffering a collision of the second kind with the nitrogen in the resonance chamber, whereby each isotope is left in the metastable $2\,^3P_0$ state. The absorption of the components of 4047 from this state will likewise depend upon the number of the various isotopes excited to this state, the statistical weights of the hyperfine levels involved and the atomic absorption coefficient, again assumed the same for all isotopes. Since the central component of 4047 is due solely to even isotopes, it is desirable to add together the number of even isotopes excited to the $2\,^3P_0$ state, this sum in arbitrary units is 385. The number of the excited 199 isotopes is 138 and that of the 201 isotopes is 100. These numbers together with the statistical weights give the ratio of the linear absorption coefficient of the central component of 4047 to that of the -0.743 cm^{-1} component, due to the 199 isotope, equal to 8.4. A similar ratio for the -0.394 cm^{-1} component due to the 201 isotope is 7.6.

Referring to Table I it may be seen that the observed ratio for the first case varies from 10 to 5.3 as the nitrogen pressure is varied from 2 to 40 mm. For the second case the observed ratio is 4.0 and nearly constant. Since the observed ratios are not in very good agreement with the predicted ones, it is interesting to see if there is some value of the atomic absorption coefficient of 2537 that would give a much better agreement. The value $k=2.37\times10^{-13}$ gave the best set of ratios, namely 6.4 and 4.6. Since this value of k is much greater than the Zemansky value and since this experiment cannot be used to evaluate k, because of the numerous assumptions involved, it is quite desirable to have a direct determination of the atomic absorption coefficient for the components of 2537.

The Production of Secondary Electrons by Argon Positive Ions and by Argon Atoms

CHARLES J. BRASEFIELD, *Sloane Physics Laboratory, Yale University*

(Received October 24, 1933)

Argon positive ions with energies up to 150 equivalent volts were found to be very inefficient in producing secondary electrons (from a lamp-blacked nickel collector) as compared with argon atoms of equal kinetic energy. The efficiency of production by these atoms, which were probably in metastable states, was approximately 3.5 percent. It is concluded that positive ions, as such, play little or no part in the production of electrons necessary for the maintenance of a cold cathode discharge in gases.

DURING the course of some experiments on the ionization of argon under impact of argon atoms,[1] it was noticed that the production of secondary electrons by a beam of argon atoms and positive ions was only slightly reduced when the positive ions were eliminated from the beam. Measurements were taken to establish this fact, the results of which turn out to be more interesting than the results obtained from the primary experiment.

APPARATUS

The experimental tube is shown in Fig. 1 and the wiring diagram in Fig. 2.[2] Spectroscopically pure argon was admitted to the tube through a variable artificial leak. The pressure in the discharge chamber was 0.0095 mm. A discharge was maintained between the oxide-coated filament F and the anode A. The potential difference across the discharge, V_d, was kept at 35 volts and the current at 75 milliamperes. Those positive ions from the discharge which pass through the 1 mm hole in the plate P_1 are accelerated between P_1 and P_2 by an applied potential of V_a volts. Beyond P_2, these ions enter the field free region inside the hollow cylinder H (1 cm long) where some are neutralized by exchange of charge with "resting" gas atoms. The beam now passes between the plates of a condenser K which can be used to remove the remaining positive ions. A potential difference of 50 volts across K was found sufficient to eliminate from the beam even the fastest positive ions. The beam continues through a canal 6 mm long and 1 mm in diameter and emerges into a region which is kept at a low pressure by means of mercury diffusion pumps.

The collector C, placed in the path of the beam, was a strip of sheet nickel 5 mm wide completely surrounded by a shield of sheet nickel except for a 5 mm by 5 mm opening which was covered by a coarse meshed grid of fine nickel wires. To prevent reflection of positive ions, the collector C (and its shield) were coated with lamp black.[3] The collector C was given no especial heat treatment before secondary electrons were measured except that it was bombarded by the beam of high velocity ions and atoms until a steady state was reached. The broken lines in Fig. 1 represent metallic shielding of the glass.

PROCEDURE AND RESULTS

First, the velocity distribution of the positive ions in the beam, and the variation in the total

[1] The ionization potential of argon under impact of argon atoms was studied as a function of the angle between the direction of the impinging atoms and the direction of the positive ions resulting from the collisions. The results obtained were somewhat ambiguous due to complications arising from secondary electrons. It appears, however, that the ionization potential varies little, if any, from 75 or 80 volts for angles up to 30°.

[2] The current to the collector C was normally measured by means of a Bell Telephone Laboratories Type 7567-A electrometer tube. For the particular experiments described here, however, the electrometer tube was replaced by a galvanometer of sensitivity 3×10^{-11} amp. per mm.

[3] It has been shown by C. Ramsauer and R. Kollath, Ann. d. Physik **16**, 567 (1933), that less than one percent of 175 volt protons are reflected from a lamp-blacked surface and we might expect that even a smaller fraction of argon ions of the same energy would be reflected.

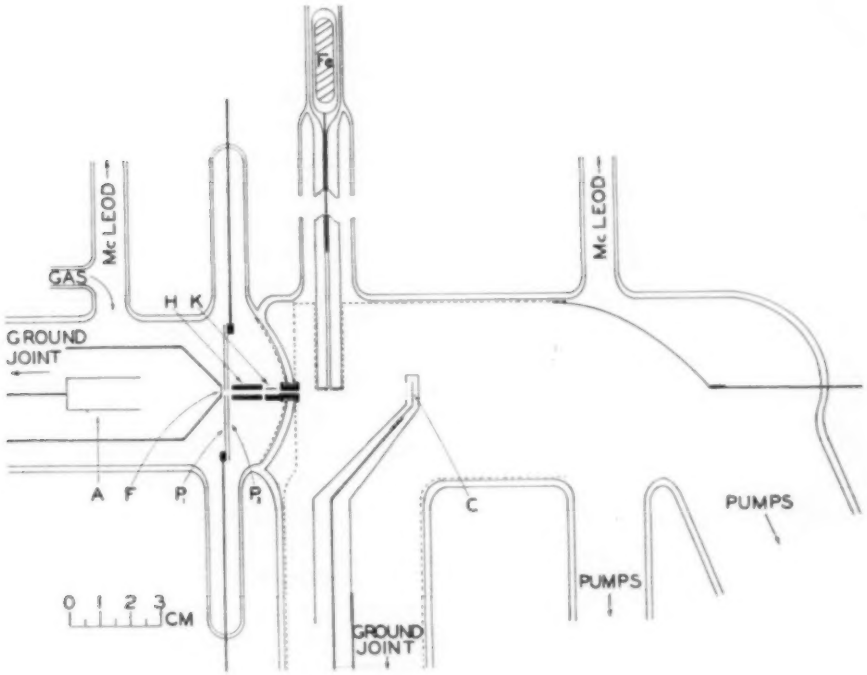

FIG. 1. The experimental tube.

number of positive ions with the accelerating voltage, V_a, were investigated. With both plates of the condenser K grounded and for various values of V_a (0, 25, 50, 75, 100 volts), readings were taken of the current I_c to the collector C, as the potential of the collector above ground, V_c, was increased. Curves similar to the one

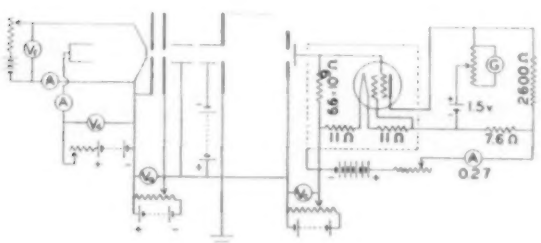

FIG. 2. The circuit diagram.

shown in Fig. 3 for $V_a = 100$ volts were obtained. By plotting ΔI_c (the change in I_c for equal steps of 5 volts in V_c) against the mean value of V_c, the velocity distribution of the positive ions was found. In all cases the peak of the velocity distribution curve was at a value of V_c approximately 30 volts greater than V_a, showing that

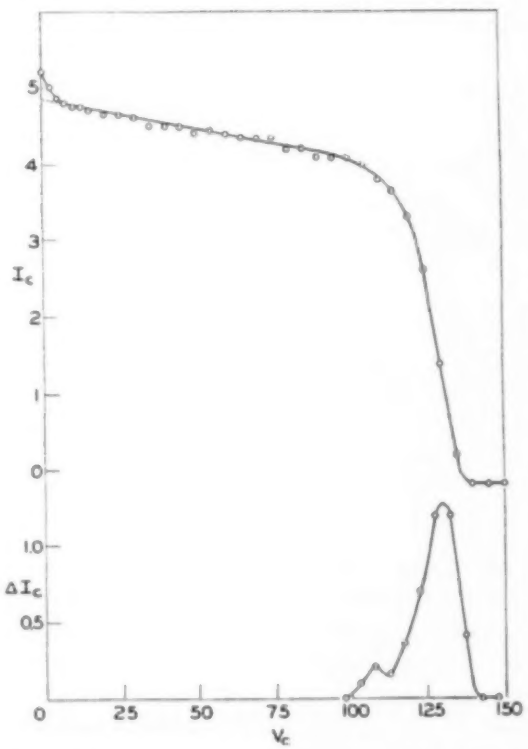

FIG. 3. The variation of the current to the collector with the retarding potential when $V_a = 100$ volts. Also the velocity distribution of the positive ions.

the positive ions had a mean initial velocity of 30 volts, i.e., 5 volts less than V_d.

The variation with V_a in the total number of positive ions under the peak is shown in Fig. 4*A*. Moreover, from the known absorption by neutralization of argon ions of various energies in argon,[4] we can calculate the number of atoms

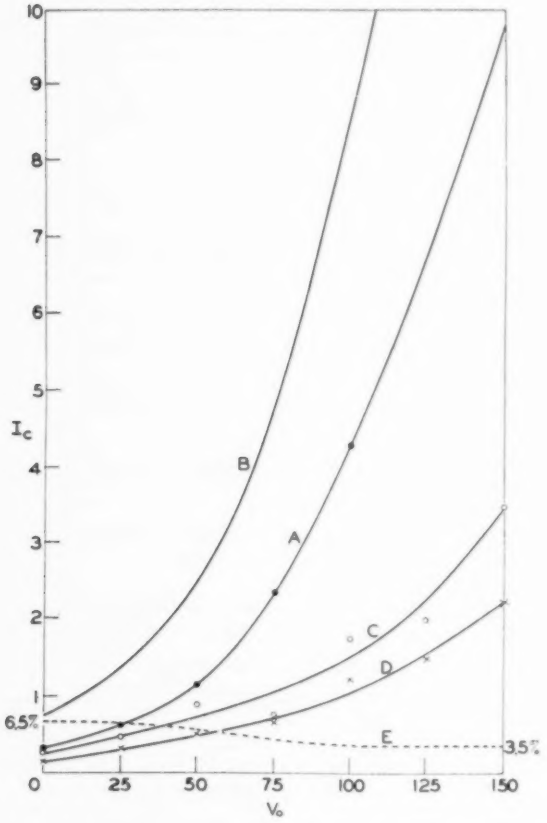

FIG. 4. The variation in the number of positive ions (*A*) and neutral atoms (*B*) with the accelerating voltage; (*C*) secondary electrons due to a beam of argon atoms and ions in the ratio 2 : 1 (magnified 5 times); (*D*) the same after the positive ions were eliminated and the atoms reduced to 2/3 the original number (magnified 5 times); (*E*) the efficiency of emission of secondary electrons by neutral (metastable?) argon atoms. *Note:* In the ordinate axis V_0 should be V_a.

in the beam. The variation with V_a in the number of atoms is shown in Fig. 4*B*. It is assumed that little or no kinetic energy is lost when a positive ion is neutralized, and consequently that the atoms in the beam have the same velocity distribution as the corresponding positive ions.

[4] F. Wolf, Zeits. f. Physik **74**, 585 (1932).

From Fig. 3 and similar curves, it was found that $V_c = +5$ volts eliminated almost all the secondary electrons. Consequently the decrease in I_c produced by increasing V_c from 0 to +5 volts was taken as a measure of the total number of secondary electrons due to a beam of argon atoms and ions in the ratio 2 : 1. The variation with V_a in the total number of secondary electrons, so obtained, is shown in Fig. 4*C* (ordinates multiplied by 5).

The positive ions were now eliminated from the beam by applying a potential of 50 volts across the condenser K. The decrease in I_c produced by increasing V_c from 0 to +5 volts was again found for various values of V_a. The results are shown in Fig. 4*D* (same scale as 4*C*). When the positive ions are eliminated, the path over which neutralization can take place is reduced from 2 cm to 1 cm and hence the number of neutral atoms is reduced to approximately 2/3 the original value. In other words, curve *D* represents the number of secondary electrons emitted when the positive ions have been eliminated and the neutral atoms reduced to 2/3 their previous number.[5] If, now, the ordinates of curve *D* are increased 50 percent, curve *C* is approximately reproduced. Hence, the decrease which occurs in the number of secondary electrons when positive ions are eliminated from the beam, can be wholly accounted for by the simultaneous decrease in the number of neutral atoms. From which we conclude that the efficiency of ejection of secondary electrons by argon positive ions is negligible compared to the efficiency of emission of secondary electrons by neutral argon atoms of the same kinetic energy, at least up to energies of 150 equivalent volts.

DISCUSSION

It is customary to assume that if a secondary electron is produced from a metal surface by impact of a neutral atom, this atom must have been in an excited state. As far as these experiments go, this opinion may still be held, for it is quite probable that when an argon positive ion is

[5] Both curves *C* and *D* may include some photoelectrons resulting from the discharge, but since these must be less than the values for $V_a = 0$, they are negligible.

neutralized, the resulting atom will remain in a metastable state.

By dividing the number of secondary electrons (Fig. 4*C*) by the corresponding number of neutral atoms (Fig. 4*B*) we get the efficiency of emission of secondary electrons by neutral (metastable?) argon atoms under the conditions of this experiment. The variation in this efficiency with V_a is shown in curve *E*, which indicates that the efficiency increases from 3.5 percent for 180 volt atoms to 6.5 percent for 30 volt atoms. This apparent increase in efficiency at lower energies is not believed to be real. Rather it is thought that the neutralization of A^+ in argon increases even more rapidly in the range 180 to 30 equivalent volts than is indicated by Wolf's curve[4] (this would raise curve *B* and lower curve *E* for smaller values of V_a). The comparatively low value here found for the efficiency of emission of secondary electrons by neutral (metastable?) argon atoms is due to the fact that a lamp-blacked surface is a very poor emitter of secondary electrons. Ramsauer and Kollath have shown[3] that covering a metal surface with lamp black reduces the emission of secondary electrons under proton bombardment by approximately 50 percent.

Similar experiments have been described by Oliphant.[6] He found that the secondary emission produced by a beam of helium positive ions and (metastable?) atoms "persisted almost unchanged" when the ions were eliminated from the beam. He used ions (and hence atoms) of energies between 120 and 2100 equivalent volts and gives no estimate of the relative number of atoms and ions in the beam. Consequently his work is perhaps not so directly applicable to the theory of the gaseous discharge as that presented here.

At the pressures customarily used in gaseous discharges, the mean free path before neutralization of positive ions is extremely small and consequently the number of high speed neutral (metastable?) atoms is many times the number of positive ions. This, combined with the fact that the efficiency of emission of secondary electrons by neutral (metastable?) atoms is so much larger, indicates that the electrons produced at a cold cathode in a gaseous discharge must be due almost exclusively to bombardment by neutral (metastable) atoms and photons. Moreover, it has been shown[7] that a positive ion must have very high energy in order to ionize a similar atom. The conclusion is, therefore, that positive ions, as such, play little or no part in the production of electrons necessary for the maintenance of a cold cathode discharge.

[6] M. L. E. Oliphant, Proc. Roy. Soc. **124**, 228 (1929).

[7] F. Wolf, Zeits. f. Physik **74**, 575 (1932). C. J. Brasefield, Phys. Rev. **42**, 11 (1932).

Electron Orbits in Crossed Electric and Magnetic Fields

A. E. SHAW, *Ryerson Physical Laboratory, University of Chicago*

(Received September 8, 1933)

The focussing properties of crossed electric and magnetic fields for electrons have been investigated for the case of circular orbits, and it has been found that this combination of fields provides extremely sharp focussing, which is in very good agreement with the theoretical predictions. Measurements of the electric field intensity have revealed the presence of polarization layers which form on the plates of the electric field. These layers reduce the effective potential which is used to deflect the electron beam. The absolute magnitude of these layers has been measured for gold and bronze, and it has been found to depend upon; (a) material of the plates, (b) gas pressure, and (c) electron intensity. These layers are found to be constant under a fixed set of conditions and to vary in a reversible manner as conditions are altered. In addition, permanent insulating layers may be formed if electrons bombard a metal surface. Errors in e/m determinations may be traced to these layers and tests are developed for their elimination.

I. INTRODUCTION

IT has been shown by Bartky and Dempster[1] that both velocity and direction focussing of a beam of charged particles can be obtained with crossed electric and magnetic fields. Recently Bondy and Popper[2] have investigated the characteristics of this type of combination of fields for the case of positive ions of sodium and potassium. The present paper is an account of the behavior of electrons in crossed fields.

In Fig. 1 is shown a schematic representation of a cylindrical condenser in which a beam of charged particles is free to move under the action of a radial electric field and a magnetic field which is normal to the plane of the orbit.

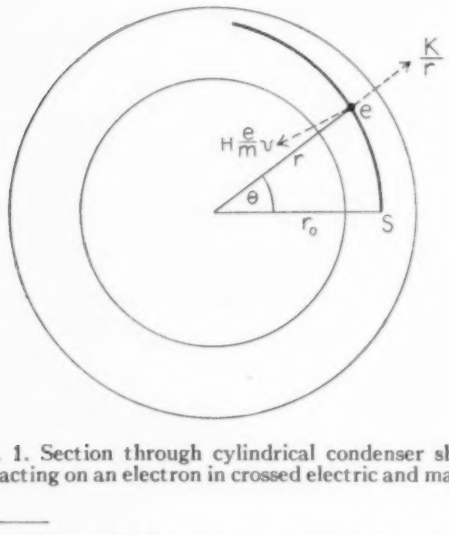

FIG. 1. Section through cylindrical condenser showing forces acting on an electron in crossed electric and magnetic fields.

A charged particle entering the field at S describes an orbit under the influence of a radial acceleration K/r, due to the electric field, and of an acceleration Hev/m, due to the magnetic field which acts at right angles to its direction of motion at every point of the orbit. The solution[1] of the differential equations of motion gives a general equation for the radius vector of the path at the point of focus, *viz.*, $\theta=\pi/2^{\frac{1}{2}}=127°\,17'$, as follows,

$$r=\rho\left(1-c_0+\frac{c_0^2}{3}+\frac{c_1^2}{3}+\delta^2+\frac{\pi}{2^{\frac{1}{2}}}c_1\delta\right). \qquad (1)$$

This equation contains the initial conditions associated with the entering slit, that is where $\theta=0$, we have for the point of entry, $r_0=\rho(1+c_0)$, and for the angle of entry, $(dr/\rho d\theta)_{\theta=0}=c_1$, and for the angular velocity at entry, $(d\theta/dt)_{\theta=0}=\frac{1}{2}H(1+\delta)e/m$, where c_0, c_1 and δ are small. For a first approximation, that is when c_1 and δ are very small and $c_0=0$, $r_{\theta=\pi/2^{\frac{1}{2}}}=r_0=\rho$, where $\rho^2=4K/(He/m)^2$. If K be evaluated in terms of the applied potential V and the radii of curvature of the condenser plates r_1 and r_2, we find,

$$\frac{e}{m}=\frac{4V}{\rho^2H^2\log_e(r_2/r_1)}, \qquad (2)$$

[1] W. Bartky and A. J. Dempster, Phys. Rev. **33**, 1019 (1929).

[2] H. Bondy and K. Popper, Ann. d. Physik **17**, 425 (1933).

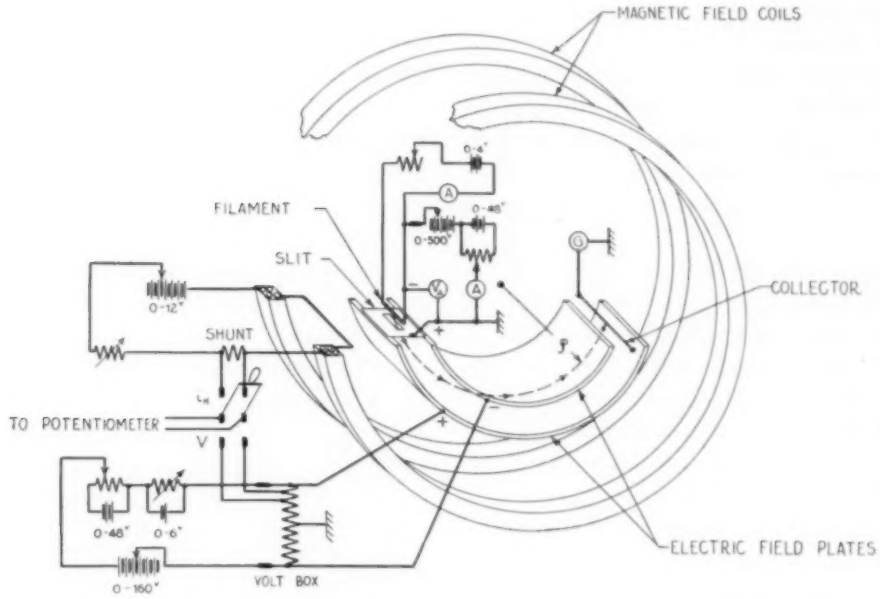

FIG. 2. Schematic diagram of the electric and magnetic fields and associated circuits.

where H is the intensity of the magnetic field. The significance of this equation lies in its being independent of the velocity and hence uncertainties in the accelerating potential do not enter.

II. General Experimental Arrangement

The schematic diagram of the entire apparatus is shown in Fig. 2, where the electric and magnetic fields are represented in oblique projection.

The source of electrons is a coated cylindrical filament, 0.025 mm in diameter which is mounted like a monochord string under the slight tension of a spring, in order that its expansion when heated will not throw it out of the line of the slit. The filament is operated with currents of 0.04 to 0.06 ampere to minimize its magnetic field. The slit shown serves to collimate the electron beam. Directly beneath this slit, a distance of 2.5 mm, is a pair of fine molybdenum wires, not shown in Fig. 2. These wires, which determine the width of the beam used, are supported on two fine pitch radial screws in such a manner as to be parallel to each other and to have their common plane radial. The effective slit width of these wires was varied from 0.025 mm to 0.060 mm. These two wires serve as the initial slit, the inverted image of which is focussed onto the collector, located 127° 17′ away. The use of these two wires for the slit reduces the distortion of the radial electric field. The filament was placed in such a position that the electrons, under the influence of the accelerating field and the magnetic field, entered the slit normally.

The electron beam is picked up at the collector which is joined to a galvanometer. It was found that the collector acquired a net positive charge under the electron impact. This is due to the fact that the ratio of secondary electrons to primary electrons is greater than unity. When operating at pressures of the order of 10^{-7} mm Hg and exceedingly small beam intensities, the deflections are very constant.

(a) Electric field

The electric field is formed between two concentric cylindrical surfaces, which are held concentric by means of an accurately turned glass cylinder and upon the front face of which is engraved the center of curvature. The effective axial length of the field is about 30.0 mm, whereas the axial width of the beam is only 2.0 mm. The field plates were made of bronze with a low magnetic susceptibility with provision for mounting upon their adjacent surfaces thin metallic layers for the study of the polarization phenomena which are described later. The complete cylin-

drical condenser is mounted inside a glass tube which can be exhausted. The glass tube is supported on six points, four of which are rigid and the other two flexible. This provides two degrees of freedom in angle, which, together with an additional degree in translation, allows the electric field to be located symmetrically inside the magnetic field.

The grounded wire slit and the wire collector are located midway between the two plates of the condenser. One plate was charged positively and the other negatively to such potentials that the slit and collector were located on a circular equipotential surface at zero potential.

(b) Magnetic field

The magnetic field is furnished by two coils, each of which has 119 turns. The entire physical structure of the apparatus was cast from a low magnetic susceptibility bronze whose susceptibility is less than 10^{-5}. The common median plane of the two coils is coincident with the median plane of the electron beam.

The magnetic field coils are shown schematically in Fig. 2. The absolute value of the field of these coils is obtained, not by computation, but by null comparison with two accurate, concentric, single-layer coils not shown in the figure. These two single-layer coils consist of seven turns each and are wound in an 80° helical groove on the surface of a bronze cylinder inside the larger coils. The field of the accurate pair is arranged to oppose the field of the large pair and a small oil-damped magnetometer, placed at the radius of curvature of the trajectory, namely $\rho = 31.00$ mm, and in the median plane of the beam, indicates when they are equal. The magnetometer is so arranged that it can be placed in different parts of the field in order thus to explore the field over the entire volume of the electron ribbon.

The field of the single pair was determined, (1) by series computation, (2) by a new method[3] for the approximation of the values of elliptic integrals, and (3) by comparison with a standard, single coil having a single layer of 24 turns. This coil is arranged on a double eccentric so that its axis can be made coincident with the trajectory. When this occurs, all terms of the series vanish except the first, thus providing an additional check on the rapidity of the convergence of the series. It is of interest to note that the results of these different methods are self-consistent to one part in 10,000.

As is evident from Fig. 2, the absolute value of the applied potential and the magnetic field current can be read directly on the same potentiometer.

III. Experimental Results

(a) Focussing curves

In Fig. 3 are two curves which show the changes in the current to the collector, for variations in either the applied potential or the magnetic field. Fig. 3a illustrates the case when the beam is moved past the collector by a variation of the applied potential, with a constant magnetic field, whereas 3b shows the case for a variation of the magnetic field, with a constant applied potential. The points were plotted from the experimental data, whereas the curves represent

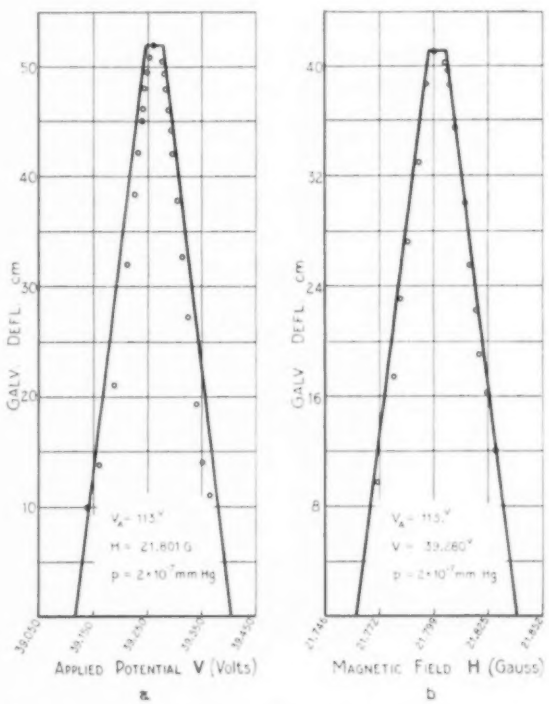

FIG. 3. Typical curves illustrating the great sharpness of focus of electrons obtained with crossed electric and magnetic fields. The theoretical curve in either case is represented by the solid lines and the experimental values are shown as points.

[3] This new method is due to Professor W. Bartky and will be published shortly.

the theoretical values computed from the geometrical fraction of the beam intercepted by the collector.

The two experimental curves show exceedingly sharp focussing. In fact, the relative changes in either the electric or the magnetic field are found to be slightly less than would be anticipated from the widths of the slit and the collecting wire used. The flat top of these curves is due to the use of a slit which is slightly wider than the collector.

(b) Surface polarization phenomena

The value of e/m was calculated from the peak values of the experimental curves in Fig. 3. It was found that instead of being a constant, the value of e/m varied with the intensity of the electric field. For low intensities of the applied electric field, e/m was greater than for higher field values. This apparent difference was finally ascribed to the formation of surface charges upon the plates of the electric field which changed the force acting on the electrons from that computed in terms of the applied potentials.

The equation from which the absolute magnitude of these surface charges can be determined is developed as follows. If there be added to the actual deflecting potential E, an extraneous potential ϵ, such that the applied potential is given by $V=E+\epsilon$, it is found from Eq. (2) that,

$$\frac{e}{m}=\frac{e}{m_0}\left(\frac{V}{V-\epsilon}\right)=\frac{e}{m_0}\left(1+\frac{\epsilon}{V}\right), \text{ for } \epsilon \ll V; \quad (3)$$

where e/m_0 is the true value, and e/m the apparent value, as computed from the applied potentials. Eq. (3) represents the slope-intercept form of the equation of a straight line, where $\epsilon e/m_0$ is the slope and e/m_0 is the intercept.

In order to examine the validity of Eq. (3), preliminary experiments were carried out by using aluminum, gold and platinum. At pressures of the order of 2×10^{-4} mm Hg, and collector current $i=10^{-8}$ ampere, aluminum showed surface potentials of 11.8 volts. Gold under identical conditions developed a surface layer of only 0.446 volt. At pressures of 6×10^{-5} mm Hg, the layer on aluminum fell to 6.0 volts. Platinum was so awfully erratic in its behavior—there was no provision made for outgassing—that no reliable data could be secured.

Provision was made to secure gas pressures and electron intensities as low as possible. In order to detect small electron currents in the collector, an FP-54 Pliotron,[4] operated at current sensitivities of 10^{-14} ampere, was joined into the collector circuit between the galvanometer and the collector. Fig. 4 shows the experimental results for

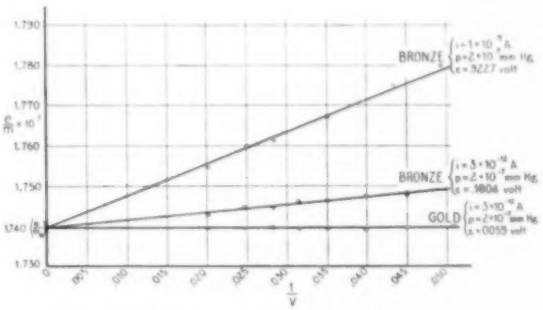

FIG. 4. Curves showing the magnitude of surface polarization for bronze surfaces and gold surfaces, under the conditions indicated.

bronze and gold. The data for each of these curves were taken under the same pressure conditions, namely 2×10^{-7} mm Hg, as read on an ionization gauge. The first curve for bronze was taken at $i=10^{-9}$ ampere. Under these conditions a surface layer of 0.9227 volt developed, whereas when the current i was reduced to 3×10^{-12} ampere, the same bronze showed a surface layer of only 0.1804 volt. Gold was tried under these conditions of low current and low pressure. A thin layer of pure gold foil, 0.025 mm thick, was stretched over each of the bronze plates of the electric field, correction being made for the change in the effective radius of curvature of the plates of the field. Under the conditions indicated, gold developed a surface layer of 0.0059 volt, as shown by the last curve of Fig. 4. That these layers are transient is shown by the fact that when focussing is resumed under some particular set of conditions, after having focussed under different conditions of pressure or of intensity, the original value of the surface layer is obtained.

Thus far we have made no suggestion as to the possible nature of these polarization layers. They behave somewhat like a space charge, which in this case may be due to the ions formed by the

[4] L. A. DuBridge, Phys. Rev. **37**, 392 (1931).

electron beam. That these layers depend upon the gas pressure and the electron intensity lends some support to this hypothesis.[5]

(c) Surface changes under electron impact

In addition to the surface layers discussed in the preceding paragraph, it was found that permanent insulating layers are formed under direct electron bombardment. The polarization layers that were considered under (b) are formed without electron impact, the beam merely passing between the plates of the field.

It has previously been observed[6, 7, 8] that when a beam of electrons bombards a metal surface an alteration of the surface takes place. Electrons of 100 equivalent volts and beam intensities of 10^{-9} ampere, striking the surface of a metal such as platinum, gold, aluminum, tantalum or molybdenum, cause a noticeable change in the surface in about 10 minutes, at pressures of the order of 10^{-5} mm Hg in air. One characteristic of this type of layer is its high resistivity. Even the layers which develop in 10 minutes are definitely insulating, as shown by the progressive decrease of the deflection of the galvanometer joined to the collector wire. If the bombardment be continued for several hours, an optically visible layer is formed, and the deflection may vanish entirely. These heavier layers are dark toward the center of the deposit and out near the edges they show bright interference colors.

The changes that take place on a metal surface under electron impact represent a permanent alteration of the surface. The layer which developed on Pt after several hours of bombardment, was found to be insoluble after 30 minutes in concentrated HNO_3 at 21°C, or in a mixture of concentrated HCl and concentrated HNO_3 of equal proportions, at the same temperature. The layer which formed on Pt vanished very slowly in air at 320°C, and almost instantly at 1000°C, the surface being restored to its original, bright luster. Under extremely good vacuum conditions and a low intensity beam, the collector used showed no indication of a surface alteration after a period of 4 or 5 hours.

Webster, Hansen and Duveneck[9] have called attention to the carbon deposits which formed on the targets of their x-ray tubes. They suggest that these carbon deposits are due to the breakdown, under electron bombardment, of the organic molecules which collect on the targets due to the presence of the vapors of stopcock grease, *n*-butyl phthalate, etc. They find that when the x-ray tubes are baked out and good vacuum conditions prevail no visible deposit is formed.

(d) Dependence of path upon velocity

Although Eq. (2) does not contain the velocity explicitly, electrons of a certain preassigned voltage equivalent must be used with given values of the electric and magnetic fields. Let us consider the case of the dependence of the path upon the velocity only, and suppose the beam to have no divergence, that is $c_1=0$ in Eq. (1). Suppose further that the slit and collector are adjusted to the same distance from the center ($c_0=0$). Then at the collector, $r=\rho(1+\delta^2)$, where the velocity of the rays is defined in terms of δ by, $v=\rho\theta_0'=\frac{1}{2}H\rho(1+\delta)e/m$. Thus the beam reaches the collector at the minimum distance ρ when $\delta=0$, or $v=\frac{1}{2}H\rho e/m$. Introducing the accelerating potential V_A in place of the velocity v, and substituting for $H\rho$ in (2) we find,

$$V=2V_A \log_e (r_2/r_1). \qquad (4)$$

This value of V_A gives a minimum value to r, so that a slight variation in V_A moves the beam outward a very small amount. It may be calculated that a change in V_A of 2 percent gives a change in r of 10^{-4}. However, with the sharpness of focus, as exemplified by the curves in Fig. 3, a variation of this amount could nevertheless be detected.

It was found that the values of V_A, which were required to give this adjustment for minimum distance, did not agree with the values computed from Eq. (4). To illustrate the differences noted in the values of V_A, it was found experimentally, for example, that for a given value of V and H, the measured value of V_A was 115 volts, whereas

[5] Analogous effects are observed in cathode-ray tubes. See P. P. Eckersley, J. Inst. E. E. (London) **66**, 513 (1928); J. T. MacGregor-Morris and H. Wright, J. Inst. E. E. (London) **71**, 57 (1932).

[6] E. Gehrcke and R. Seeliger, Vehr. der Deutschen Phys. Gesell. **15**, 438 (1913).

[7] J. E. Henderson, Phys. Rev. **29**, 360 (1927).

[8] R. Suhrmann, Phys. Zeits. **30**, 939 (1929).

[9] Webster, Hansen and Duveneck, Rev. Sci. Inst. **3**, 736 (1932).

from Eq. (4), V_A should have been 99.5 volts. Likewise for the next higher value, V_A was 129 volts experimentally and only 113 volts theoretically. Throughout the entire range of values, there is practically a constant difference between successive values of V_A obtained experimentally and theoretically. A possible explanation of this difference is that surface charges had formed on the two wires of the initial slit which had been subjected to considerable bombardment. These charges give rise to a retarding field which is followed by an accelerating field just beyond. This results in the path immediately beyond the slit having a large radius of curvature.

(e) e/m values

From Eq. (3), the intercept e/m_0 in Fig. 4 should be the true value of the specific charge. This is given as 1.740×10^7, a value which is low compared with the values generally accepted at present. This disagreement may be due to the presence of the retarding field mentioned in the last paragraph, which, with its subsequent acceleration, gives a ρ which is initially too large to intersect the collector. Hence, to secure a maximum, a larger H or a smaller V is used. This results in a relatively low value of e/m. A test for the absence of this experimental difficulty is the agreement of the accelerating potential, as calculated from Eq. (4), with the applied potential, as measured externally.

The great sharpness of the focussing obtained with this combination of crossed fields should allow a very accurate determination to be made of the specific charge for electrons, and as soon as this one point concerning the possibility of surface charges on the wire slit is cleared up completely, we hope to proceed with the determination.

It is a great pleasure to express my appreciation to Professor A. J. Dempster, under whose general direction this research was carried out, for considerable help and encouragement throughout the course of the work; and to Professor W. Bartky, for his kind interest. I am very grateful to Mr. Joe Getzholtz, instrument maker, who contributed his great skill to the construction of the electric and magnetic fields.

Electron Diffraction and the Imperfection of Crystal Surfaces

L. H. GERMER, *Bell Telephone Laboratories*

(Received October 25, 1933)

Bragg reflections are obtained by scattering fast electrons (0.05A) from the etched surfaces of metallic single crystals. The surfaces studied are a (100) face of an iron crystal, (111) face of a nickel crystal and (110) face of a tungsten crystal. In each case the reflections occur accurately at the calculated Bragg positions with no displacement due to refraction. A given reflection is found, however, even when the glancing angle of the primary beam differs considerably from the calculated Bragg value —by over 1° in some cases—so that several Bragg orders occur simultaneously. The accuracy with which this glancing angle must be adjusted is a measure of the degree of imperfection of the crystal. From the electron experiments, estimates are made of the widths at half maximum of electron rocking curves. These widths are 0.8° for the iron crystal, 1.5° for the nickel crystal and somewhat over 1° for the tungsten crystal. X-ray rocking curves for these same crystals are much narrower, although the observed widths vary considerably with the treatment of the surfaces. It is concluded that the values obtained from the electron measurements apply to projecting surface metal only, and that *the degree of misalignment is much greater at the surface than deep down within the crystal.* Furthermore, even the x-rays [Mo $K\alpha$ radiation -0.71A] are not sufficiently penetrating to yield values certainly characteristic of these metal crystals.

X-RAY reflection experiments lead to the well-known conclusion that many physical crystals are not perfect. With parallel and monochromatic radiation the reflection from a crystallographic plane of such a single crystal is of appreciable intensity only for incident angles very close to one of the Bragg angles. As the crystal is turned slightly from such a critical position the intensity of the reflection decreases rapidly, but its location remains unchanged. The apparently non-regular reflection of x-rays, when the crystal is slightly turned from a Bragg position, is attributed to crystal imperfection. Reflections of this sort are produced by regular and selective reflection from constituent parts of the crystal which are not in perfect alignment with the mean orientation. The maximum amount of the angular misalignment is measured by the angle through which the crystal can be turned without entirely destroying the reflection.

I have observed similar evidence of crystal imperfection in the reflection of electrons from metallic single crystals. Experiments have been carried out upon crystals of iron, nickel and tungsten. The imperfection which these experiments indicate are much larger than are found by x-ray methods. The electron experiments yield information concerning only the crystal surfaces, whereas, because of greater penetrating power, x-rays show the imperfection at considerable distances beneath the surfaces. *The present experiments then are interpreted to mean that the misalignment of the constituent parts of these metal crystals is much greater at the surfaces than deep down in the metal.*

* * * * * * * * * * * * * * *

The crystals are prepared first by cutting to expose a surface parallel to an etch plane, and then by careful etching. A sharply defined beam of electrons, of wave-length of the order of 0.05A, is incident upon such a prepared surface at small glancing angle. This glancing angle can be varied by rotating the crystal about a vertical axis lying in its face. The electrons scattered from the crystal register upon a photographic plate located normal to the primary beam at a distance of 365 mm from the axis of rotation.

Fig. 1 is the photographic record obtained with an iron crystal.[1] The four photographs are taken at four different glancing angles. After each exposure a second very short exposure is made with

[1] A figure similar to Fig. 1 was presented in July, 1932, in a paper by Dr. C. J. Davisson at the International Electrical Congress, Paris, France. This paper is reprinted, in translation, in the Bell System Technical Journal for October, 1932.

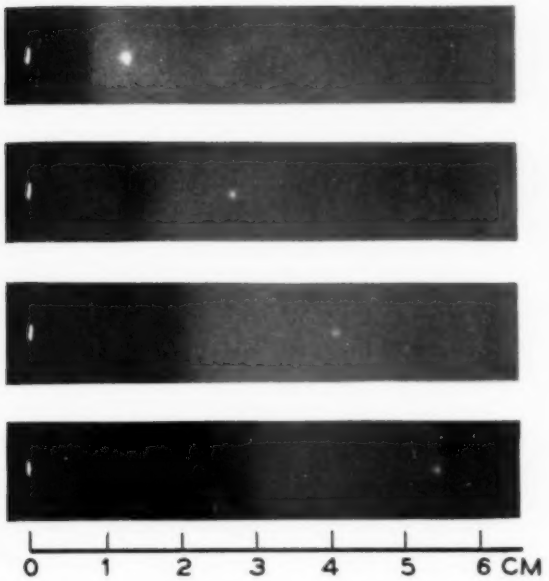

FIG. 1. Bragg reflections of 0.054A electrons from the (100) face of an iron crystal. Photographic plate located at 365 mm from the crystal.

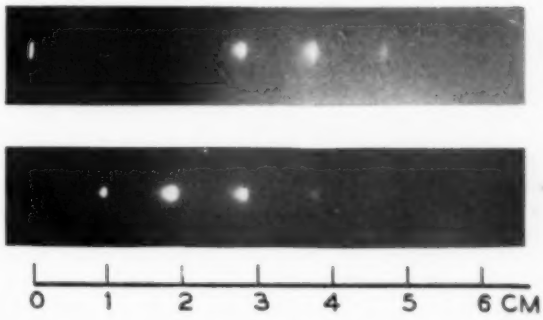

FIG. 2. Bragg reflections of 0.054A electrons from the (111) face of a stationary nickel crystal. The spots occur accurately at the calculated Bragg positions.

the crystal removed, to record the position of the primary electron beam—shown as a spot at the left of each figure. These four figures show the first four orders of Bragg reflection from planes parallel to the (100) surface plane. The reflections occur at just the positions calculated from the known spacing of (100) planes in iron and the independently determined electron wave-length, respectively 1.43A and 0.054A.

On each of these photographs the glancing angle is indicated by the edge of the darkening produced by general scattering. This edge is the intersection of the plane of the surface with the photographic plate. The glancing angle has the Bragg value when the distance from the central spot to this edge is just half the distance from the central spot to the reflection. One notes in each of the photographs that the reflection is produced when the crystal is set at just about the correct glancing angle. Thus no considerable crystal imperfection is indicated by these photographs. When, however, the crystal is set at glancing angle midway between the first and second Bragg angles, both the first and the second reflections can be seen weakly. This indicates that a small part of the surface of the crystal has an orientation differing from its mean orientation by 0.5°. If a curve were obtained similar to an x-ray rocking curve, it would have a total angular width of over 1.0°. The intensities of these first and second order spots appear to be somewhat less than half the intensities at the correct glancing angles. Thus the width of the rocking curve at half maximum is less than 1.0°. I estimate the total width at half maximum to be about 0.8°.

The two photographs of Fig. 2 were obtained from a nickel crystal at slightly different glancing angles.[2] Each of these photographs shows simultaneously four different orders of Bragg reflection from planes parallel to the (111) surface plane. This simultaneous occurrence of different orders indicates that the crystal is very imperfect. Portions of it are rotated with respect to its mean orientation by at least as much as 1.1°. If a rocking curve were obtained its total angular width would be at least 2.2°. Its width at half maximum I estimate to be about $1\frac{1}{2}$°.

The scattering of 0.059A electrons from a tungsten crystal is recorded in Fig. 3. The first three Bragg reflections from the (110) surface plane are indicated by the arrows 1, 2 and 3. By rotating the crystal to a slightly larger glancing angle, the third order becomes stronger and the

[2] In the lower photograph of Fig. 2 the position of the primary beam was not registered. In both photographs the edge of the darkening due to general scattering is not sharply defined. This poor definition appears to be due to rounding of the crystal surface which has resulted from repeated etchings without repolishing. One is unable to determine glancing angles from observations of the edge, but one does observe that the glancing angles of these two photographs differ by about 1.4°, corresponding to 9 mm in the figure.

fourth order is found. From the general darkening edge one sees that the glancing angle is about midway between the correct angle for the first Bragg reflection and that for the second. As the third order is very weak one calculates that the total width of the rocking curve is just over 2.2°. The width at half maximum would appear to be a little over 1°.

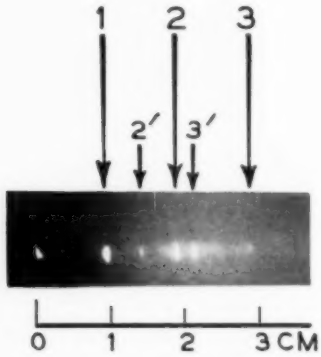

FIG. 3. Bragg reflections of 0.059A electrons from the (110) face of a tungsten crystal. Bragg reflections are also shown from a crystal of unknown composition on the surface of the tungsten. This crystal has crystallographic planes parallel to the surface separated by 3.00A.

In Fig. 3 are shown other reflections designated as 2′ and 3′, which are respectively the second and third order Bragg reflections from another single crystal. By turning the tungsten to about the right glancing angles the first and fourth orders are readily found. These four reflections correspond to crystal planes parallel to the surface separated by 3.00A. This is probably the spacing of some compound of tungsten which has been formed during or immediately after the etch treatment. The relative intensities of the tungsten reflections and these additional reflections have varied greatly after different treatments of the crystal. The latter were, however, never entirely absent.

In x-ray examinations of the iron and tungsten crystals I failed to find any evidence of imperfection. The method was crude and I could have detected, with certainty, only imperfections large enough to produce rocking curves having widths at half maximum of about a fifth of a degree (12′). More recently Mr. F. E. Haworth of these laboratories has obtained x-ray rocking curves for the three crystals used in these experiments. He has obtained 14′ as the width at half maximum for the iron crystal, 24′ for the nickel crystal, and 6′ for the tungsten crystal. In these measurements the $K\alpha$ radiation from molybdenum was used (0.71A).

More extensive measurements have since been made for the purpose of reconciling Mr. Haworth's value of 14′ for the iron crystal with the earlier conclusion that the width at half maximum was definitely less than 12′. These measurements have shown that the width of the x-ray rocking curve is determined, in part at least, by the condition of the surface of the crystal. The iron and nickel crystals were etched a number of times, and after each etch the width of the rocking curve was determined. The widths at half maximum varied considerably, and in some cases they were as large as 0.7°. All of these tests, however, show lesser degrees of imperfection than are found by the electron method. One concludes that the surfaces of the metal crystals used in these experiments are less perfectly aligned than the bodies of the crystals. Furthermore, x-rays of wave-length 0.71A are not sufficiently penetrating to yield a rocking curve which is certainly characteristic of the bulk of a metal crystal.

A possible explanation of the extremely imperfect surfaces suggests itself when one considers the fact that none of the Bragg reflections obtained with electrons shows displacement due to refraction. If the electrons which form the diffraction spots pass in and out of the metal through the same plane surface we would expect to observe considerable displacements due to this cause. For example a potential difference of any value greater than 12 volts between the outside and inside of the metal would result, in the upper photograph of Fig. 1, in a reflected beam which would not emerge above the mean plane of the surface and could not register on the photographic plate. (This calculation is based on the assumption that the gross plane of the surface is made up entirely of etch planes of the various mosaic crystals of which the block is made.) The absence of any observed displacement of the Bragg beams leads to the interpretation that the reflected beams are made up of electrons which have passed entirely through projecting metal,[3]

[3] See G. P. Thomson, Phil. Mag. **6**, 939 (1928); Thomson, Proc. Roy. Soc. **A128**, 658 (1930).

left exposed presumably as a result of the etching process. Thus one is led to conclude that the considerable misalignment of constituent parts of the crystals, found by electron diffraction, may be limited to this projecting metal. The forces on the atoms in such projections must be unsymmetrical. Possibly such unsymmetrical forces result in twisting small mosaic crystals, which project from the surface, by as much as the observed amount, one or two degrees. In this connection it should be pointed out that the surface metal, which is found to be imperfect, lay before etching far below the crystal surface. From the x-ray observations we know that, before etching, this metal was much more perfectly aligned.

* * * * * * * * * * * * * * * * *

In experiments similar to the above G. P. Thomson[4] and others have found diffraction patterns from the etched surfaces of metallic single crystals which are essentially like the cross grating *N* patterns first obtained by Kikuchi in the transmission of electrons through mica. It seems to me probable that the failure to observe complete cross grating patterns in the present experiments is due simply to the fact that a crystal was never adjusted in azimuth to put the primary electron beam along an important zone axis.

Recently Kikuchi and Nakagawa[5] have interpreted the Thomson patterns of the Kikuchi cross grating type as due to misalignment of crystals in the projecting crystallites through which the electrons pass. An essentially similar interpretation of the cross grating mica transmission patterns had already been given by W. L. Bragg.[6] Kikuchi and Kakagawa also attribute the occurrence of the surface grating patterns from natural or cleaved crystal surfaces found by Kirchner and Raether[7] to a similar slight variation in the direction of the crystal axes from one point to another on the surface. Kikuchi and Nakagawa estimate the degree of misalignment from the extent of the Thomson cross grating patterns, and from the vertical lengths of the spots in the patterns due to surface gratings. A value of about 1.5° is obtained in each case.

* * * * * * * * * * * * * * * * *

The tungsten crystal used in these experiments was cut from an ingot which was given to Dr. C. J. Davisson by Dr. Irving Langmuir of the General Electric Company. The iron crystal was produced in this laboratory by Mr. P. P. Cioffi. I am also indebted to Dr. R. M. Bozorth and Mr. F. E. Haworth for advice and assistance in the x-ray measurements, and especially to Dr. Davisson for his supervision and constant interest and assistance.

[4] Thomson, Proc. Roy. Soc. **A133**, 1 (1931).

[5] Kikuchi and Nakagawa, Sci. Papers, Inst. Phys. and Chem. Res. **21**, 80 (1933).

[6] Bragg, Nature **124**, 125 (1929).

[7] Kirchner and Raether, Phys. Zeits. **33**, 510 (1932). Raether, Zeits. f. Physik **78**, 527 (1932).

The Effect of Alkali Ions on the Photoelectric Emissivity of Tungsten

A. KEITH BREWER, *Fertilizer Investigations, Bureau of Chemistry and Soils, U. S. Department of Agriculture, Washington, D. C.*

(Received August 24, 1933)

Known quantities of Na^+, K^+, Rb^+ and Cs^+ ions were deposited on tungsten and the changes in the photoelectric current measured. For wave-lengths below 2800A the current increases proportional to the fraction of the surface covered as long as f is small. The emissivity for longer wave-lengths is low at first, and then rises sharply beyond some critical value of f, which increases with the wave-length. The results indicate that the work function is not uniform over these composite surfaces; this makes it impossible to fix a definite threshold for the various values of f. The emissivity increases with temperature to about 500°C, where fatigue becomes appreciable. As the filament fatigues for photoelectric emission the positive ion emissivity increases, reaching a maximum when the threshold returns to that for clean tungsten. The results show that the alkali dissolves so rapidly in the tungsten that the dependence of the work function on f cannot be determined at temperatures above 500°C.

IN a previous article the effect of small measured amounts of potassium on the photoelectric emissivity of iron was described.[1] In the present paper a similar study is made of the effect of small deposits of various alkali ions on the emissivity of tungsten.

Apparatus and Method

The technique employed in depositing a known amount of alkali on the tungsten was to pass a positive ion current for a definite period of time from a catalyst ion source[2] to the tungsten. The fraction of the tungsten surface covered by ions was obtained by dividing the surface area by the cross-sectional area of the ions multiplied by the number passed.[3]

The experimental setup was essentially the same as that used before except that the photocurrent was measured with an FP-54 Pliotron in place of an electrometer.

The tungsten emitting surface was a ribbon 6 cm long, 3 mm wide and 0.01 mm thick placed edgewise to the positive ion source. The sources were iron catalyst impregnated with the oxide of the alkali desired. The catalysts were thoroughly reduced in hydrogen at a temperature just below redness; the tungsten was glowed in hydrogen at approximately 1500°C and subsequently glowed in a vacuum at 1800°C until gassing ceased.

Since the positive ion emitters always gas slightly in operation, it was necessary to keep the pumps running continuously throughout each experiment. The pressure was maintained below the limit of a McLeod gauge, no other precaution being taken for extremely high vacuum.

In operation the tungsten was first glowed until a just detectable emission could be obtained with λ2483. A known positive ion current was next passed from the catalyst to the tungsten for a given time. The photoelectric emissivity for the various mercury lines was then measured. The original threshold of the tungsten was restored by glowing a few minutes at bright redness, after which the process was repeated as desired. Substantially the same results were obtained when the alkali was deposited in successive amounts or at a single time.

The contamination of the surface by the deposition of atoms was measured by the difference in the photocurrents after an accelerating and a retarding potential for positive ions had been placed upon the tungsten for the same catalyst heating current and time. The emission from atoms exceeded that from ions for fresh catalysts but decreased rapidly with time. The results given were taken when the enhancement of the photocurrent due to the deposition of atoms was less than one percent of that due to ions.

[1] A. Keith Brewer, Phys. Rev. **38**, 401 (1931).

[2] C. H. Kunsman, J. Frank. Inst. **204**, 635 (1927).

[3] The radii given by Pauling, J. A. C. S. **49**, 765 (1927), are: Na^+, 1.10A; K^+, 1.30A; Rb^+, 1.5A; Cs^+, 1.75A.

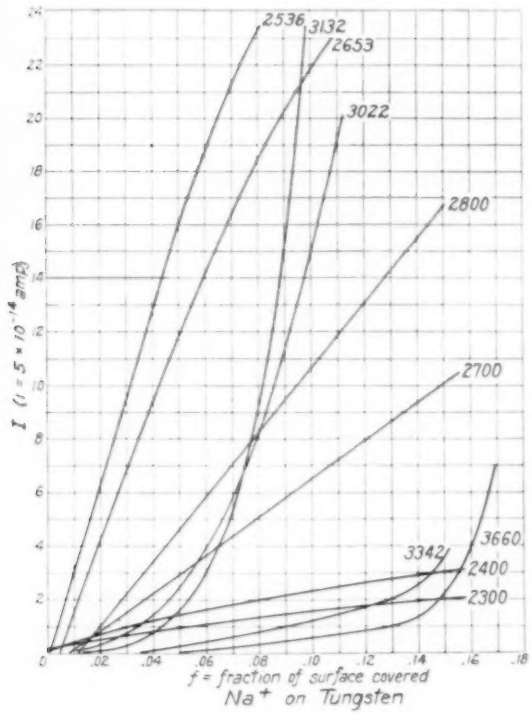

FIG. 1. Effect of fraction of surface covered by sodium ions on the photo-emission of tungsten under excitation by various mercury lines.

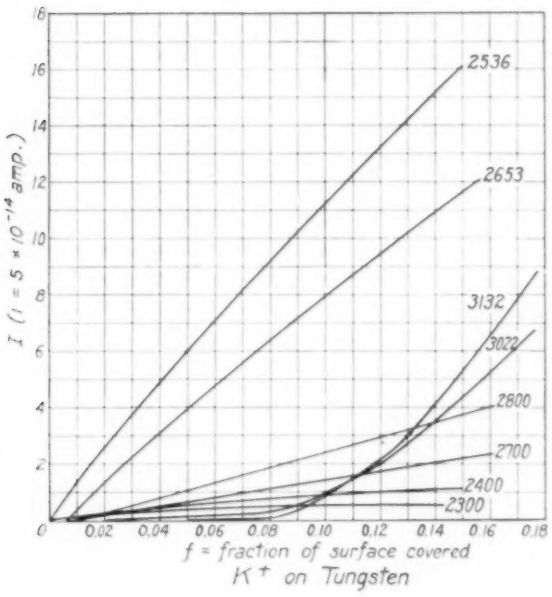

FIG. 2. Effect of fraction of surface covered by potassium ions on the photo-emission of tungsten under excitation by various mercury lines.

RESULTS

The effect of the fraction of the surface covered (f) by the different alkali ions on the emissivity for the various mercury lines is shown in Figs. 1, 2 and 3.

Readings were taken for difference in f of 0.0025 up to $f = 0.02$, and for differences of 0.01 thereafter. The points all fell closely on the curve, the curves in general being drawn through the points. The results obtained with rubidium lie intermediate between those of potassium and caesium. The temperature of the tungsten filament when these results were taken was about 250°C, chosen because it was below where "fatigue" became appreciable and yet was sufficiently high for the emissivity of the surface to become constant within a few minutes after the alkali was deposited.

It will be noted that results are given only for small values of f; above a specific fraction covered

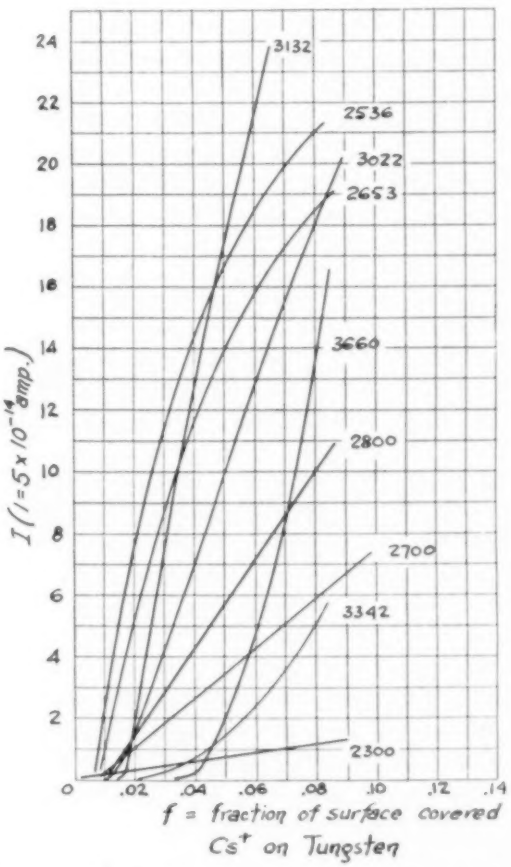

FIG. 3. Effect of fraction of surface covered by caesium ions on the photo-emission of tungsten under excitation by various mercury lines.

for each ion the emissivity no longer increased with the deposition of more ions. This specific value is about $f=0.16$ for Na, $f=0.13$ for K and $f=0.05$ for Rb and Cs. It is possible that the inability to build up larger layers by this method is due both to evaporation and to an increased solution of the alkali in the tungsten at the higher concentrations.

The results show that for λ2700 and λ2800 the photocurrent increases linearly with f. For shorter wave-lengths the curves are only slightly concave downward; for longer wave-lengths they rise sharply above a certain critical value of f.

The effect of the chemical nature of the adsorbed ions on the intensity of the photoelectric current is comparatively small. The relative efficiency is in the order of caesium, rubidium, sodium and potassium. The fact that sodium showed a slightly greater effect than potassium is surprising but several check experiments invariably gave the same results.

The effect of temperature on the photocurrent is similar for the different surfaces. From room temperature to 300°C the current increased by about 50 percent. Above 300°C the current rose more rapidly to about three times the original value at 500°C; at the higher temperatures the filaments fatigued badly. Caesium on tungsten ($f=0.01$) showed only a few percent fatigue in an hour at temperatures below 300°C; at 500°C the photocurrent dropped to a small value in the course of several hours, while at 700°C it dropped to that of pure tungsten in a few minutes. The other filaments behaved similarly.

Since the photocurrents respond only to alkali that is on the surface, the fatigue effect just described must result either from an evaporation of alkali off the surface or from a solution in the tungsten. A test of these two possibilities was made by studying the positive ion emission of the tungsten, before and after the alkali was deposited. In these experiments the tungsten filament was glowed until no positive ion emission could be detected below 950°C to 1000°C. A quantity of alkali was then deposited on the tungsten and the temperature determined where a positive ion current could be detected, after which the photoelectric emissivity for the various frequencies was measured. From time to time the change in the positive ion current as well as the photoelectric current was measured, the filament temperature being kept practically constant.

In Table I are the results obtained from rubidium on tungsten at 560°C. The interval of time between successive readings of the positive ion current varies between twenty and thirty minutes.

TABLE I. *Positive ion and photocurrents from rubidium on tungsten.*

I^+	I_{2536}	I_{2700}
4.0×10^{-12} amp.	18.5×10^{-12} amp.	2.0×10^{-12} amp.
11.0	9.0	.9
12.5	8.2	.8
17.5	6.7	.65
27.0	6.2	.5
34.0	5.2	.3
41.0	2.3	0.0

These results, typical of all the alkali deposits, show clearly that while the photocurrent fatigues with time the positive ion current increases to its greatest value at the point where the photoelectric threshold reaches that for pure tungsten, i.e., where the surface is free of adsorbed alkali. This, in light of the fact that an equivalent positive ion current would not be obtained from the tungsten previous to the deposition of the alkali at a temperature 500°C above that used in these experiments, is a direct indication that the photoelectric fatigue observed at temperatures above 300°C must be due to a solution of the alkali within the tungsten. This conclusion is not surprising since such a solution should be expected from the chemistry involved. The evaporation probably does not contribute materially to the loss of alkali from the surface until much higher temperatures are reached. It seems apparent, therefore, that the effect of adions on the work function cannot be obtained by any method necessitating the heating of the tungsten appreciably above 300°C.

An attempt was made to determine the fraction of the deposited alkali that could be evaporated from the tungsten in the form of positive ions. After the tungsten surface became free of alkali the positive ion current remained nearly constant for an appreciable time, then gradually fatigued to a negligible value. This fatiguing effect made an accurate estimation impossible al-

though it is evident that the quantity of positive ions deposited and emitted is of the same order of magnitude.

The thermionic emission of electrons yielded no direct information regarding the dependence of the work function on the fraction of the surface covered under the conditions of these experiments. In the case of rubidium for $f=0.01$ a thermoelectron emission was detectable at 700°C but it did not increase with temperature in the usual manner below 875°C. These temperatures are well above those at which the photoelectric measurements show that rubidium dissolves rapidly in the tungsten. The difference between these results and those reported by Ives[4] is doubtless due to the thickness in the layer of adsorbed alkali.

A determination of the variation in the photoelectric threshold with f involves considerable uncertainty since the data presented in Figs. 1, 2 and 3 show that the composite surfaces exhibit a varying degree of photosensitivity over a wide range of frequencies. Thus in Fig. 1 the detection of a photocurrent for λ3660, for instance, is more dependent on the sensitivity of the apparatus than on some specific value of f.

In Fig. 4 the emissivity per unit light intensity is plotted against the wave-length. The continuous lines are for caesium and the dotted lines for sodium. The numbers refer to the values of f expressed in hundredths. The intensity of the various lines was measured with a Hilger thermopile.

The curves for $f=0$ and $f=0.01$ show sharp feet and are characteristic of those obtained from clean surfaces. The curves for larger values of f exhibit a marked enhancement in the photoelectric yield for the longer wave-lengths, the point of greatest emissivity shifting towards the red as f increases. This shift is more pronounced for caesium than for sodium.

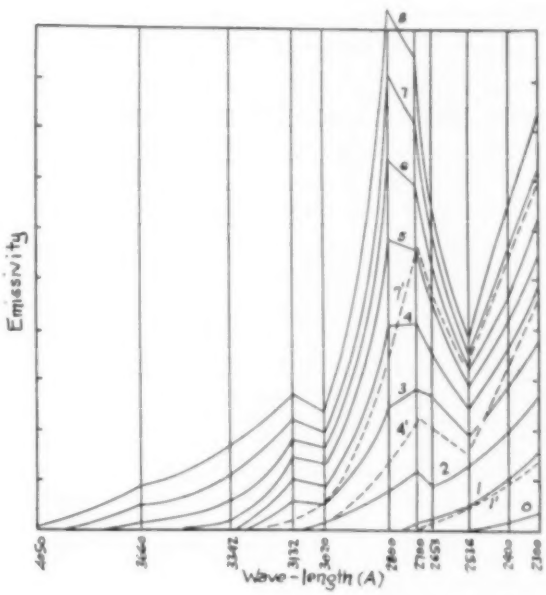

FIG. 4. Emissivity of tungsten to unit light intensity as a function of wave-length.

DISCUSSION OF RESULTS

Results of the type presented in this paper are in general accord with the ion grid theory proposed by Becker.[5] This theory presumes that the work function of a composite emitter is lowest at some point near the ion and increases to that for the clean metal at a distance of order of ten diameters removed.

It is not surprising therefore that emission characteristics for wave-lengths above and below the threshold for the clean metal are distinctly different. For wave-lengths near or below the threshold of tungsten the photocurrent increases in a perfectly definite manner with the concentration of the adions, a change of $f=0.01$ resulting in a change in current equivalent to a shift in threshold of approximately 65A for sodium and potassium and 85A for caesium. This is due to the fact that the entire surface is photoelectrically active for these frequencies.

The emissivity for wave-lengths considerably above the threshold of tungsten is very low for small values of f, indicating, possibly, that only a small region about the ion is photosensitive. As f increases a point is reached, specific for each frequency, where the emissivity undergoes a rapid increase; this suggests that the entire surface has now become photosensitive. The observation that the point of inflection in these curves occurs at higher values of f for the longer wave-lengths is to be expected.

[4] H. E. Ives, Astrophys. J. **64**, 128 (1926).

[5] J. A. Becker, Trans. Am. Electrochem. Soc. **55**, 21 (1929).

Measurement of the Townsend Coefficients for Ionization by Collision

FREDERICK H. SANDERS, *University of California*

(Received September 6, 1933)

The photoelectric current between parallel plates in dry air was measured as a function of plate distance for constant field strength and pressure over plate distances ranging from 1 to 7 cm and at a pressure of 1 mm of mercury. The simple Townsend relation $i=i_0\epsilon^{\alpha d}$ was found to give excellent agreement for values of X/p from 40 to 110. The least squares values of α/p plotted as a function of X/p lie on a smooth curve which does not fit either the equation $\alpha/p=N\epsilon^{-NV_0p/X}$ suggested by Townsend, nor the empirical relation $\alpha/p=A\epsilon^{bX/p}$, found by the writer to hold for values of X/p from 20 to 36.5. Voltages and plate distances were measured to within 1/10 of 1 percent and pressures to 1/2 of 1 percent or better. For X/p's from 120 to 160 the current was found to increase with plate distance more rapidly than the simple exponential relation would indicate, as was observed by Townsend for plate distances less than 1 cm at much greater X/p's. The early appearance of this deviation may be ascribed to the greater sensitivity given by larger plate distances. Both of the relations suggested by Townsend:

$$i=i_0(\alpha-\beta)\epsilon^{(\alpha-\beta)d}/[\alpha-\beta\epsilon^{(\alpha-\beta)d}],$$

which was derived on the assumption that each positive ion produces β new pairs of ions by collision in 1 cm of path, and

$$i=i_0\epsilon^{\alpha d}/[1-\gamma(\epsilon^{\alpha d}-1)],$$

which assumes γ new electrons liberated by each positive ion which strikes the cathode, fit the experimental curves equally well. The values of β/p were observed to increase with X/p as found by Townsend for higher X/p's. The coefficient γ, which is approximately equal to β/α was observed to increase only very slightly over this small range of X/p's.

INTRODUCTION

IN a recent paper[1] the writer describes in detail the results of an investigation on the value of the Townsend coefficient for ionization by collision in air at large plate distances and near atmospheric pressure. In that investigation the value of the Townsend coefficient α was obtained at or near atmospheric pressure for a range of values of X/p (the ratio of the field strength in volts per cm to pressure in mm) from 20, below which point the value of α began to be indistinguishable from the natural unsaturation of the ionization curve, up to $X/p=36.5$ which was within two percent of spark breakdown. The results obtained gave a relation for α/p as a function of X/p of:

$$\alpha/p=2.67\times10^{-8}\epsilon^{0.350X/p}, \qquad (1)$$

which was in disagreement with the equation:

$$\alpha/p=N\epsilon^{-NV_0p/X} \qquad (2)$$

deduced by Townsend[2] and found applicable by him to values of X/p above 300 in air. Paavola[3] concluded that for values of X/p above 40 in air at atmospheric pressure the currents required not only ionization by electrons giving the value of α but also by positive ions when the field was within three percent of sparking. This was not observed in the writer's investigation even within two percent of sparking. The original investigations of Townsend were confined to low pressures and small plate distances (below 1 cm) and did not extend much below $X/p=100$ although one or two points were obtained down to $X/p=40$. In Townsend's measurements[4] the deviation from the law for ionization by electron impacts only was not observed below $X/p=175$. In view of the importance of ionization by positive ions in the mechanism of spark breakdown it seemed of considerable importance to make a complete investigation in the range from $X/p=40$ to $X/p=160$ or thereabouts with the high resolving power and increased accuracy possible with the modern techniques now available in the writer's laboratory.

[1] F. H. Sanders, Phys. Rev. **41**, 667 (1932).

[2] J. S. Townsend, Phil. Mag. **1**, 557 (1902); **1**, 389 (1903); *Electricity in Gases*, Chapter VIII.

[3] M. Paavola, Archiv f. Elektrotechnik **22**, 443 (1929).

[4] J. S. Townsend, Phil. Mag. **2**, 598 (1903); **2**, 738 (1904); *Electricity in Gases*, Chapter IX.

Apparatus and Experimental Procedure

The apparatus was essentially the same as that used in the earlier investigation. For values of X/p from 70 to 160 the measurements were carried on at pressures very near 1 mm so that a bank of B-batteries giving a maximum potential of 900 volts replaced the high-tension set previously used. The positive side of the battery was connected to ground and the negative side to the illuminated plate of the ionization chamber. To set the voltage more closely than the 2 volt intervals between successive cells, five or ten cells were connected across the fixed terminals of a slide-wire rheostat and the sliding contact connected to the ionization chamber.

The potential across the chamber was first set to within one percent or so with a voltmeter after which it could be set to one-tenth of one percent with a ratio box, potentiometer and standard cell. The ratio box and potentiometer resistances and the e.m.f. of the standard cell were accurate to within a few hundredths of one percent. Plate distances were measured with a cathetometer and were of the same order of accuracy.

For the pressure measurements two McLeod gauges were constructed, one reading from 0.5 to 1.5 mm and the other from 3.0 to 40 mm. The capillary tubes of these gauges were accurately calibrated over their complete operating length and it is believed that the pressure readings are accurate to one-half of one percent or better.

The same ionization chamber was used as in the earlier experiments but it was found possible at these lower pressures to operate over a range of plate distances from 1 to 7 cm. A 220-volt quartz mercury-arc lamp was used as before but considerably greater constancy of operation was obtained as follows:

It was found that although the current through the arc was sensibly constant, the potential drop would suddenly increase from time to time even after the arc had reached its equilibrium temperature. By decreasing the current by ten percent or so below its normal operating value for a few minutes the potential drop could be brought back to its equilibrium value after which the current was increased to normal and the arc again operated steadily. As all measurements were taken over periods varying from ten to thirty seconds, this method of obtaining steady photoelectric emission worked very well.

Because of the steadiness of the battery potential the currents were measured by the "rate of deflection" method with a quadrant electrometer of a sensitivity of 500 mm per volt. Capacities varying from 350 to 6970 cm were used in parallel with the electrometer to give a considerable range of sensitivities. By this means, currents ranging from 1×10^{-13} ampere to 6×10^{-9} ampere could be measured.

For values of X/p of 40, 50 and 60, it was found advisable to work at higher pressures than 1 mm. As the approximate values of α/p were known from early data taken at 1 mm, pressures were chosen in each case which would give α a value of about 0.5 as this had proved to give a rate of current increase which could be measured with the greatest accuracy. At these pressures it was necessary to use voltages greater than could be obtained with the batteries and hence the high tension set was used. In this case the potential was measured with a 50-meghom Taylor high voltage resistor unit, accurate to one-half of one percent. The grounded end of the resistor was tapped at 25,000 ohms and connected to the same potentiometer used with the batteries. The current was measured with the same electrometer used at the lower pressures but the rate of deflection method was replaced by the one used in the earlier high pressure investigations where a relatively large capacity was allowed to charge for a known time and its potential measured with the electrometer. This procedure necessitated a correction of one percent or less to the potential because of the fact that the measuring condenser and the ionization chamber formed a set of capacities in series, but was advisable as a protection to the electrometer in case of sparkover.

It was found impossible at these higher pressures to go to the large plate distances used at 1 mm because of the geometrical design of the chamber. For instance at $X/p=40$ and $p=25$ mm, the greatest distance obtainable was 3.5 cm. At 4.0 cm sparkover to the walls of the chamber took place. The spark was observed to jump from the mercury contact in the split insulator to the grounded chamber and as this portion of the chamber was electrically screened from the

working section by a grounded metal plate of diameter almost that of the chamber, there was no possibility of distortion of the field just previous to the spark.

The air was dried and admitted to the chamber as before. A slightly oxidized cathode gave much greater constancy of photoelectric emission than a polished plate. The pressure was read in each case before and after a run but in no case was a variation of more than one-tenth of one percent observed. The field was adjusted to give the desired value of X/p for each run and the observations taken by varying the plate distance and voltage to give constant field strength. As in the earlier experiments, the plate distances were chosen at random so that a consistent variation in i_0 would not introduce a consistent error in the value of α.

Experimental Results

The curves giving current as a function of plate distance are shown in Fig. 1. For purposes of assembling the data it was found convenient to plot $(1/p)$ log (i/i_0) against plate distance in cm. Hence the slopes of the curves give α/p directly. The values of α and i_0 were determined by the method of least squares from the actual observations, the reduced values being used for purposes of plotting only. For X/p's of 120 and higher, where the curves depart from the linear form, the values of α and i_0 were computed from the lower portions of the curves where they are sensibly linear. It will be noted that for X/p's of 40, 50 and 60, the curves are shown on an enlarged scale. This was done to avoid crowding and to indicate their linear form. Up to $X/p=110$ the curves are strictly linear indicating that within the limits of accuracy of these measurements, the ionization by collision is overwhelmingly due to electron impacts and hence proving the validity of the simple Townsend relation:

$$i=i_0\epsilon^{\alpha d} \tag{3}$$

for these lower X/p's. At $X/p=120$ definite evidence for the existence of ionization either by positive ions or by some mechanism other than pure electron impact begins to appear. An

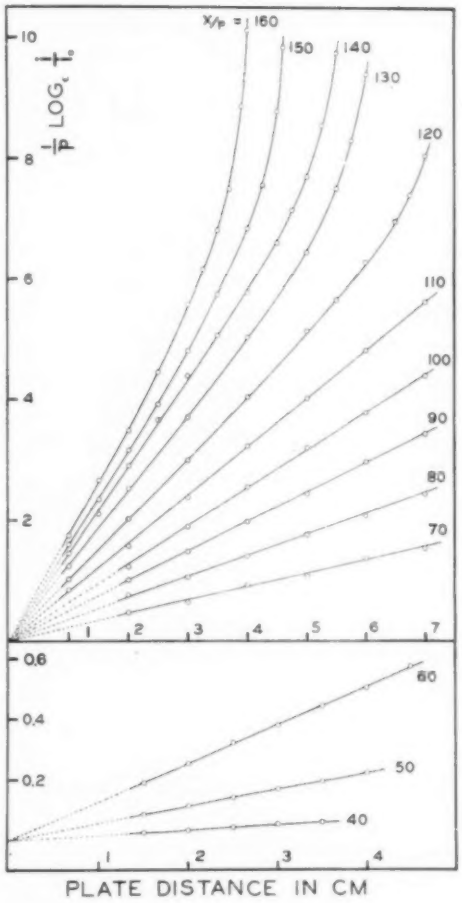

Fig. 1. Current as a function of plate distance.

analysis of the curves using either the classical Townsend relation:

$$i=i_0(\alpha-\beta)\epsilon^{(\alpha-\beta)d}/[\alpha-\beta\epsilon^{(\alpha-\beta)d}], \tag{4}$$

in which β is the number of ion pairs produced by one positive ion in 1 cm of path, or the Townsend equation:

$$i=i_0\epsilon^{\alpha d}/[1-\gamma(\epsilon^{\alpha d}-1)], \tag{5}$$

in which γ is the number of electrons liberated by one positive ion on impact with the cathode, showed that both the equations fit the experimental data equally well. The reason for this is quite apparent. By means of a simple substitution Eq. (5) may be reduced to the form:

$$i=i_0(\alpha-\beta')\epsilon^{\alpha d}/[\alpha-\beta'\epsilon^{\alpha d}]. \tag{6}$$

Now at $X/p=160$ the value of β obtained from Eq. (4) is 0.00165 while the corresponding value of α is 1.759. The difference between α and $\alpha-\beta$

is hence only one part in one thousand, which is considerably less than the probable error in α, so that Eqs. (4) and (5) become absolutely identical for these lower X/p's. In fact it can be shown that all the equations relating current to plate distance which have been suggested, by using various mechanisms of secondary ionization or combinations of these mechanisms, lead to an equation which can be reduced to one of the above forms. Hence these curves give no clue as to the nature of the secondary increase.

The values of α/p are shown as a function of X/p in Fig. 2. The experimental data lie on a very smooth curve, but it is obviously not a simple exponential relation either of the Townsend form nor of that found by the writer to fit below $X/p=36.5$. In Fig. 3 these same data are shown plotted on a logarithmic scale, as are also the data obtained earlier at high pressure. It is seen that from $X/p=20.0$ to 36.5 the observations lie on a very good straight line but that for $X/p=40$ and higher the curve falls off rapidly. Several attempts were made to fit this curve by the use of combinations of exponentials, but apparently no simple combination will fit the data

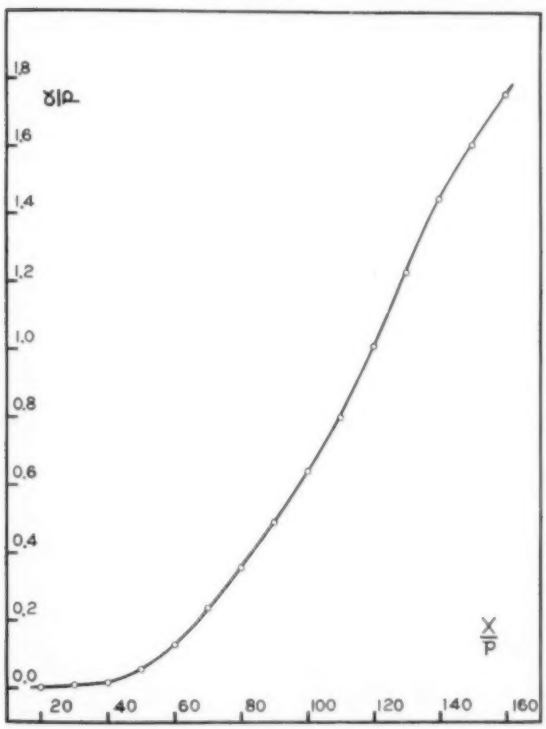

FIG. 2. Values of α/p as functions of X/p.

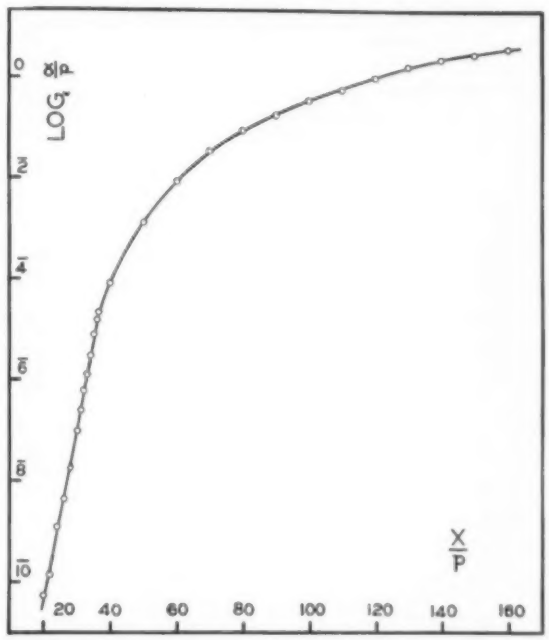

FIG. 3. Logarithm of α/p as a function of X/p.

at all well. The Townsend form of equation which gives a rectangular hyperbola when plotted on such a logarithmic scale fits very approximately, but the deviations are well outside of the maximum allowable error of the observations. When the Townsend values of the constants are used: $N=14.6$ and $V_0=25$, the deviation is exceedingly great. The values of X/p, p and the corresponding α/p with its probable error are given in Table I. In the same table are shown the experimental results of K. Masch,[5] who has recently investigated the same region at small plate distances, ranging from 1 to 6 mm. The agreement is excellent in the region where the two sets of data overlap. Masch, with his small plate distances, was apparently unable to carry his investigations below $X/p=31$, while the writer's work was discontinued at $X/p=160$ as there appeared no point to carrying the investigations into the region of higher X/p's which has been thoroughly investigated by Townsend. It was impossible to compare the writer's data accurately with those of Townsend, as the latter are obtainable only by interpolation from Townsend's curves, but the agreement with these interpolated values is very good.

[5] K. Masch, Archiv f. Elektrotechnik **26**, 589 (1932).

TABLE I. *Values of X/p, p and α/p.*

X/p (v/cm/mm)	p (mm)	α/p (writer)	Probable error	α/p (Masch)
20.0	380.0	0.000034	±0.000004	
22.0	380.0	0.000052	0.000011	
24.0	380.0	0.000134	0.000001	
26.0	380.0	0.000234	0.000028	
28.0	380.0	0.000430	0.000015	
30.0	380.0	0.000910	0.000019	
31.0	380.0	0.00136	0.00002	0.00152
32.0	380.0	0.00201	0.00002	0.00204
33.0	380.0	0.00305	0.00003	0.00309
34.0	380.0	0.00459	0.00005	0.0044
35.0	380.0	0.00605	0.00008	0.0059
36.0	380.0	0.00820	0.00005	0.0076
40.0	25.00	0.0167	0.0001	0.0168
50.0	9.95	0.0554	0.0006	0.057
60.0	4.90	0.127	0.001	0.130
70.0	1.000	0.224	0.005	0.235
80.0	0.980	0.340	0.003	0.365
90.0	0.970	0.491	0.003	0.51
100.0	0.960	0.637	0.006	0.68
110.0	0.975	0.806	0.004	0.85
120.0	0.975	1.007	0.006	1.05
130.0	0.973	1.236	0.019	1.23
140.0	0.950	1.477	0.019	1.40
150.0	0.990	1.602	0.017	1.60
160.0	1.000	1.758	0.038	1.83

TABLE II. *Values of γ, β and β/p.*

X/p	p	γ	β	β/p
120	0.975	0.00058	0.00057	0.00059
130	0.973	0.00062	0.00075	0.00077
140	0.950	0.00040	0.00056	0.00059
150	0.990	0.00063	0.00099	0.0010
160	1.000	0.00094	0.0016	0.0016

The values of γ, β and β/p are shown in Table II. Both coefficients increase with X/p but not in any very consistent fashion. As these data were obtained under the most favorable conditions, i.e., large plate distances which give high resolving power and the very steady source of potential given by batteries, it is extremely doubtful if this increase can be accurately examined at higher pressures and lower X/p's. In this region it would be necessary to use a kenotron-rectifier high-tension set-up from which it is practically impossible to eliminate fluctuations of one-fifth of one percent or so. Since the coefficient α is increasing exponentially with the field strength and the current is itself an exponential function of α, the variation in current for even a one-fifth percent change in field strength becomes exceedingly great for electron ionization alone. If the secondary mechanism now comes into play, the variation of the current becomes enormous and sparkover is likely to occur. As mentioned earlier, Paavola, working at atmospheric pressure, small plate distances and X/p's near 40, apparently observed this secondary increase, but his values of β were found to decrease with increasing X/p. In view of the difficulties just mentioned, this is by no means surprising.

CONCLUSION

Thus it is seen that these two investigations of the writer, having a resolving power which is probably as high as can conveniently be obtained with this method of attack, thanks to the modern developments in technique, have yielded a continuous and, it is hoped, useful set of values of α/p for values of X/p where ionization by collision can just be detected up to values at which the excellent measurements of Townsend have given us reliable data. These data should be of considerable value to all theoretical investigators of the mechanism of spark breakdown, in view of the continuous and accurate set of values covering all ranges of X/p involved in a study of the breakdown mechanism in air. In conformity with Townsend's earlier investigations, they have shown that current studies of this nature are incapable directly of differentiating between the various theories of the mechanism of electron production by positive ions and it appears from an analysis of the results obtained in this and earlier investigations that there is little hope of obtaining the solution to this problem by ionization current measurements.

In conclusion the writer wishes to acknowledge his indebtedness to Dr. L. B. Loeb at whose suggestion the original problem was continued and under whose direction it was carried out. The writer also desires to express his thanks to Miss Florence Ehrenkranz and Mr. W. E. Bowls for their assistance in setting up the apparatus and taking readings. This investigation was made possible through the use of the apparatus, the cost of which was in part defrayed by a grant in aid from the National Research Council.

Hoffmann Stösse and the Origin of Cosmic-Ray Ionization

W. F. G. SWANN, *Bartol Research Foundation of The Franklin Institute*

(Received October 30, 1933)

IT is generally recognized that whatever may be the nature of the primary cosmic radiation, the actual rays which play the rôle in our experiments are charged particles. We are familiar with the existence of groups of charged particles in cosmic-ray phenomena. These groups seem to divide themselves into two more or less distinct categories, that involving a few rays and larger bursts of rays known as Hoffmann Stösse, in which hundreds and even thousands of charged particles may be emitted. The number of these Hoffmann Stösse emitted per unit *volume* per unit time from solids seems to depend little upon the atomic number (see reference 2). In other words it is the *number* of the atoms in a given volume rather than their weight which is significant. It is the purpose of this article to point out that an appreciable part, and possibly nearly the whole of the observed cosmic-ray intensity, may be attributed to bursts of the Hoffmann Stoss type in the atmosphere. Only in the case of a burst originating very near the apparatus will more than a single ray enter the apparatus, so that the observed characteristics of such rays will be those of single rays occurring at random.

Let q be the number of Stösse emitted per second per atom. If q is proportional to the intensity I of some radiation, a photon component of the cosmic radiation, for example, and if subscript s refers to the earth's surface, $q=q_sI/I_s$.

It may readily be proved that the atmosphere may be replaced by its homogeneous water equivalent in all matters except that the number of Stösse emitted per cc of the equivalent water atmosphere must be taken as Nq_s, where N is the number of atoms of air in one gram of air.

Consider the contribution of the Stoss particles which are emitted downwards in a solid angle $1-\cos\theta_0$, determined by a polar angle θ_0 measured from the vertical. As a first approximation, let the particles be emitted uniformly in this solid angle and let n be their number. The number reaching the ground within the solid angle and coming from the element of volume of unit horizontal area and thickness dh at the altitude h in the homogeneous atmosphere is $nNIq_s/I_s$ if $R>h\cos\theta_0$; $nNIq_s(1-\cos\theta)/I_s(1-\cos\theta_0)$ if $R<h/\cos\theta_0<R/\cos\theta_0$; and zero if $h>R$, R being the range of the particle in water and θ being given by $\cos\theta=h/R$ for $\theta<\theta_0$.

The total number of Stoss particles reaching each square centimeter of the earth per second from solid angles determined by θ_0 is, on the average, equal to the total number of this class contributed to the whole earth's surface per second by a vertical column of unit cross-sectional area extending to the top of the atmosphere and this is $J(\theta_0)$, where

$$J(\theta_0)=nNq_s\int_0^{R\cos\theta_0}\frac{I}{I_s}dh+\frac{nNq_s}{1-\cos\theta_0}\int_{R\cos\theta_0}^{R}\frac{I}{I_s}\left(1-\frac{h}{R}\right)dh. \tag{1}$$

It will suffice,[1] as a first approximation, to assume $I/I_s=e^{\mu h}$, where μ is an apparent coefficient of absorption related to the true coefficient of absorption appearing in Gold's formula and calculable from it for limited ranges of h. With this understanding and with H written for $R\cos\theta_0$

$$J(\theta_0)=\frac{nNHq_s}{\mu H}\left[\frac{e^{\mu R}-e^{\mu H}}{R\mu(1-\cos\theta_0)}-1\right]. \tag{2}$$

[1] Strictly speaking one should consider each initial direction of the radiation separately in its capacity of producing a shower within an angle θ_0 about it as axis. The correction involved is small, however, particularly in a calculation which concerns itself only with orders of magnitude.

N has the value $N=4.1\times10^{22}$. For q_s, we have such data as those obtained by Steinke and Schindler and by Montgomery and the writer. According to the latter data, there is a production of about 1×10^{-8} Stoss per cc per second in iron at the surface of the earth. This gives $q_s=1.16\times10^{-31}$. Since $e^{\mu R}$ and $e^{\mu H}$ really represent, respectively, the ratios of the production of Stösse per atom at altitudes R and H to that at the surface of the earth; and since R and H are the logs of these corresponding ratios, formula (2) really gives $J(\theta_0)$ in terms of *experimental* measurements of the variation of rate of production of the large Stösse with altitude, without even any implication as to their origin from photons. Only the exponential law is involved. Unfortunately, there are no data on variation of the large Stösse with altitude sufficiently complete for the purposes of direct calculation. Pending the accumulation of such data, we are driven to make some hypotheses as to the production of the Stösse founded upon their relation to cosmic-ray intensity. It has been suggested by Steinke[2] that the softer photon components of the cosmic radiation are mainly responsible for the production of the large Stösse. At first sight such a view is at variance with the idea that the Stösse arise from the transformation of the energy of the photon into positive and negative particles. For a Stoss giving even 100 rays of energy 10^9 volts would require a photon of energy 10^{11} volts to produce it. The older theories which attributed cosmic-ray photon absorption to the extranuclear electrons would have prohibited the association of a 10^{11} volt photon with the softer components of the cosmic-ray photons; and, while absorption theories have had to suffer changes in the light of the now known importance of the nucleus in such phenomena, one hesitates to take advantage of the slackening of the control of those theories to make assumptions which might well be vetoed by their successors. If, however, we assume that the energy of the Stoss comes from a single atom, we are again in difficulty; for, the complete annihilation of the mass of an iron atom, for example, would provide only about 5×10^{10} electron-volts energy; and, for lighter atoms, the amount would be proportionally smaller. Then, as pointed out by Montgomery and the writer,[3] the number of particles emitted in a large Stoss is larger than that contained in any single atom. A way out of some of these difficulties is suggested by some recent experiments of G. L. Locher made in this laboratory. As a result of observations on cloud photographs of Stoss particles, Locher has been lead to conclude that many atoms may participate in the production of a shower through the intermediary agency of neutrons. If we add to this conclusion the supposition that the Stoss particles and their energy come from the atoms, we are able to invoke the energy of many atoms to account for the Stoss; and such a view enhances the probability that the initiation of the act of production of the Stoss may come about through the agency of a soft photon. We shall investigate the consequences of assuming for the true coefficient of absorption of the radiation concerned the value 0.0055 per cm of water quoted by Millikan[4] as the coefficient for the radiation which is responsible for 90 percent of the cosmic-ray ionization in the atmosphere. The μ in our formula is obtainable from this as an approximation and comes out as $\mu=0.012$ between sea level and an altitude of 250 cm in the homogeneous water atmosphere. We shall consider, tentatively, a range of 250 cm for R.

According to some unpublished measurements of C. G. Montgomery, at least 100 particles are emitted within a cone of vertical angle $\pi/4$, i.e., $\theta_0=\pi/8$. Inserting these values and the values of N and q_s already given, we find, for this case, which we shall call Case (1),

$$J(\theta_0)>6.8\times10^{-4}. \qquad \text{Case (1)}$$

If we should assume that the particles are emitted in the whole angle $\pi/2$ with the same solid angular density as that with which they are

[2] E. G. Steinke, A. Gastell and H. Nie, Naturwiss. **21**, 560 (1933).

[3] W. F. G. Swann and C. G. Montgomery, Phys. Rev. **44**, 52 (1933).

[4] I. S. Bowen, R. A. Millikan and H. V. Neher, Phys. Rev. **44**, 246 (1933). It is realized that to the extent that the photon radiation originates outside the atmosphere, very little of this soft radiation could penetrate to the earth; and the value is used merely by way of illustration. As will be seen later, a value one-fifth this amount, or even a value zero still leaves the Stoss particles a potent agency in contributing to the cosmic-ray intensity.

emitted in the $\pi/8$ angle, we should have[5] $n=100/(1-\cos\pi/8)=1300$. Under these conditions, we find

$$J(\theta_0)>0.32\times10^{-2}. \qquad \text{Case (2)}$$

From measurements of Johnson and Street, the number of cosmic-ray particles given by Geiger-counters as passing through one square centimeter of the earth's surface per second is 1.2×10^{-2}. It will be seen that the value of $J(\theta_0)$ for Case (2), amounts to one-quarter of this value. A total emission of 5000 Stösse particles would be sufficient to make $J(\theta_0)$ equal to the cosmic-ray intensity.

Perhaps one of the weakest points in the foregoing development lies in the assumption of such a large value for μ. However, if, retaining the other hypothesis of Case (2), we take $\mu=0.003$ which represents a true absorption coefficient of 0.0011 and corresponds to the experimental data for the total radiation for the lowest two meters of water equivalent of the atmosphere, we still find $J(\theta_0)>0.10\times10^{-2}$ which corresponds to ten percent of the measured cosmic-ray intensity at the earth's surface. Even the assumption $\mu=0$, which amounts to assuming no increase of Stösse emission with altitude, gives $J>0.08\times10^{-2}$. An increase in the value of R would enhance still further the value of $J(\theta_0)$. We are limited here, however, by the fact that the range of the particles must not be assumed so great that appreciable fractions of them come from altitudes comparable with the total height of the atmosphere as such an assumption would result in a variation of cosmic-ray intensity with altitude which was inconsistent with the facts.

The main purpose of this note is not to insist on any specific values of the quantities taken for illustration in the calculation, but merely to call attention to the order of magnitude of the effect of the Stoss particles in contributing in appreciable amount to the observed cosmic-ray intensity as obtained by Geiger-counters.

[5] Stösse containing as many as 4000 rays have been reported by Steinke (reference 2) and Montgomery has observed Stösse with 5000 rays in this laboratory.

LETTERS TO THE EDITOR

Prompt publication of brief reports of important discoveries in physics may be secured by addressing them to this department. Closing dates for this department are, for the first issue of the month, the twentieth of the preceding month; for the second issue, the fifth of the month. The Board of Editors does not hold itself responsible for the opinions expressed by the correspondents.

The Magnetic Moment of the Proton

O. Stern[1] by his method of molecular rays obtained the surprising result that a proton has a magnetic moment of about $2\frac{1}{2}$ nuclear magnetons with a possible error of 10 percent. It seems now that the same result of an extraordinarily large magnetic moment of the proton can be derived from the magnetic properties of higher nuclei, although instead of Stern's value $2\frac{1}{2}$, the value 2 seems to account best for the observations.

There are four types of nuclei belonging to even and odd charge-number Z and mass number M, namely: (1) Z even, M even; (2) Z even, M odd; (3) Z odd, M even; (4) Z odd, M odd. In type 1 the nucleus consists of α-particles and an even number of neutrons. It is known from experiments that nuclei of this type have no mechanical moment j and no magnetic moment $g \cdot j$. The even arrangements of neutrons and the α-particles seem to form closed shells. They give us no information about the magnetic properties of their elements. Type 4 differs from type 1 only by one additional proton. Hence we suppose that, as a rule, the mechanical and magnetic moment of such a nucleus is due only to the orbit and spin of this one additional proton. Nuclei belonging to type 2 (α-particles and an odd number of neutrons) give us no information about the proton. Type 3 (one additional proton besides α-particles and an odd number of neutrons) does not exist, as a rule, due to an instability that was explained, together with some exceptions of this rule, in a previous paper.[2] So we are left only with type 4 (Z odd and M odd) where the quantum number j (total angular moment) and the magnetic moment $g \cdot j$ is due to the orbit and the spin of one proton only. Since the mechanical spin of the proton is $s=\frac{1}{2}$, its orbital quantum number l is combined with the spin to give one of the two values $j=l\pm\frac{1}{2}$ forming doublet-terms. Their g-values can be calculated according to the general formula of Goudsmit:

$$g=g_l\frac{l(l+1)+j(j+1)-s(s+1)}{2j(j+1)}+g_s\frac{s(s+1)+j(j+1)-l(l+1)}{2j(j+1)},$$

where $s=\frac{1}{2}$, $g_l=1$ and where g_s is the magnetic factor of the proton. According to Stern we should take $g_s\sim 5$. It turns out however that $g_s=4$ agrees better with the observed nuclear data of j and g than any other choice. Table I gives the g-values for various j and l, putting $g_s=4$ according to the above formula. Next we reproduce a table of Goudsmit[3] (Table II) containing the observed values of j and g for various nuclei of type 4. Although the values of j can be said to be observed, the values of g are obtained by rather indirect conclusions and extrapolations. Goudsmit himself classified his results under grades A, B, and C of reliability. Even the accuracy of the g-values graded B may not be considered more than qualitative. The last column gives the theoretical values of g taken from our Table I and selected as close as possible to the observed g. This choice is made in every case between two possibilities only, since j is observed and only l may be either $j+1$ or $j-1$. Thus there is almost no arbitrariness. The case of Ga is omitted from the comparison; apparently it cannot be

TABLE I. $s=\frac{1}{2}$, $g_s=4$.

l	$j=\frac{1}{2}$	$1\frac{1}{2}$	$2\frac{1}{2}$	$3\frac{1}{2}$	$4\frac{1}{2}$
0	4				
1	0	2			
2		2/5	8/5		
3			4/7	10/7	
4				2/3	4/3
5					8/11

TABLE II.

Nuclei	j (obs.)	g (obs.)	g (theor.)
Li^{7} (3)	$1\frac{1}{2}$	2.19 (A)	2 ($l=1$)
Al^{27} (13)	$\frac{1}{2}$	4.2 (B)	4 ($l=0$)
$Cu^{63,\ 65}$ (29)	$1\frac{1}{2}$	1.7 (B)	2 ($l=1$)
$Ga^{69,\ 71}$ (31)	$1\frac{1}{2}$	1.34 (A)	?
		1.70 (A)	
As^{75} (33)	$1\frac{1}{2}$	0.6 (C)	0.4 ($l=2$)
$Rb^{85,\ 87}$ (37)	$2\frac{1}{2}$	0.5 (C)	0.57 ($l=3$)
	$1\frac{1}{2}$	1.8 (C)	2.0 ($l=1$)
In^{115} (49)	$4\frac{1}{2}$	1.2 (B)	1.33 ($l=4$)
$Sb^{121,\ 123}$ (51)	$2\frac{1}{2}$	1.1 (B)	1.6 ($l=2$)
	$3\frac{1}{2}$	0.6 (B)	0.57 ($l=3$)
$Tl^{203,\ 205}$ (81)	$\frac{1}{2}$	3.6 (A)	4 ($l=0$)
Bi^{209} (83)	$4\frac{1}{2}$	0.89 (A)	0.73 ($l=5$)

[1] O. Stern, Helv. Phys. Acta **6**, 426 (1933).
[2] A. Landé, Phys. Rev. **43**, 620 (1933).
[3] S. Goudsmit, Phys. Rev. **43**, 636 (1933).

subordinated to our simple model, since the two isotopes $M=69$ and 71 of Ga with equal j differ only by 2 neutrons. Thus they should not, but do, differ in their values of g. Of course we do not pretend to give here an exact theory of the magnetic properties of nuclei. But we think that at least in first approximation the one proton is responsible for the mechanical and magnetic moment of the whole nucleus of type 4. From this simplified model we infer that *the magnetic moment of a proton is about 2 magnetons* differing from Stern's value by 20 percent. It is quite interesting that the values of the orbital quantum number l assigned to the proton in Table II indicate: *The proton circles around inside or on the surface of the neutron shells only*, and never far outside them. Indeed $l=2$ appears in Table II first with $Z=33$, $l=3$ first with $Z=37$, $l=4$ with $Z=49$, and $l=5$ with $Z=83$, in accordance with a scheme of neutron shells suggested in a previous paper.[2]

ALFRED LANDÉ

Ohio State University,
November 9, 1933 at Zurich.

The Electronic Atomic Weight and e/m Ratio

The atomic weight of the electron, determined from measurements of the interval between corresponding components of the $H^1\alpha$ and $H^2\alpha$ lines, has been found to be $(5.491\pm0.002)\times10^{-4}$. Combining this value with that of the Faraday a value of $(1.757\pm0.001)\times10^7$ e.m.u/gram has been obtained as the e/m ratio for the electron.

The desired radiation was secured by passing an electrical discharge through a modified Wood's tube immersed in liquid air and filled with water vapor that contained both isotopes of hydrogen in about the same order of abundance. This "heavy" water was generously supplied by Professor G. N. Lewis.

Interference patterns of the "doublets" of both the $H^1\alpha$ and $H^2\alpha$ lines, formed by a prism spectrometer and an etalon, were photographed on very fine-grained plates. With a 3 mm etalon spacing the $H^2\alpha$ fringes were displaced about two and one-half interference orders from the corresponding fringes of $H^1\alpha$. The exact displacement in orders was computed from measurements of the positions of maxima on large-scale microphotometer curves of these fringes. The isotopic interval in cm^{-1} between the low frequency members of the doublets was then determined from the etalon equation, not neglecting the cosine factor, for each of the thus computed displacements (22 in all, taken from three different plates). This yielded an average interval, when reduced to vacuo, of 4.148 ± 0.0015 cm^{-1}. The measurements were confined to this member of the doublet in order to eliminate any possible discrepancy that might result, if the separation of the microphotometer peak from the component chiefly responsible for the peak were not the same for the two isotopes. In the first place analyses had shown that this separation was the smaller for the low frequency peak, being of the order of 0.002 cm^{-1} for both isotopes. Furthermore, neither of the two components which are measurably responsible for the position of this peak involves levels that are likely to be affected by any departure from a coulomb field such as probably exists very close to the H^2 nucleus or deuton. The measured isotopic interval may thus be safely considered equal to that between the components in the two isotopes arising from the transition $3d\,^2D_{5/2}\rightarrow 2p\,^2P_{3/2}$.

The ratio of the wave numbers for such a transition for the two isotopes is the same as the ratio of the corresponding Rydberg numbers, since, for the component selected, all quantities involving quantum numbers are the same for both isotopes and accordingly cancel out. This cancellation would occur even if these quantities were in error (evidence for which is accumulating), since any correction would in all probability be the same for both isotopes.

Thus:

$$\frac{\nu(H^1\alpha)}{\nu(H^2\alpha)}=\frac{R_{H^1}}{R_{H^2}}=\frac{M^+{}_{H^1}/(m+M^+{}_{H^1})}{M^+{}_{H^2}/(m+M^+{}_{H^2})},$$

where $M^+{}_{H^1}$, $M^+{}_{H^2}$ and m may be taken to represent the atomic weight of the proton, deuton and electron, respectively.

The atomic weights of H^1 and H^2 reported by Bainbridge[1] were obtained by adding an electronic atomic weight of 0.00055 to his experimentally determined results for ionized atoms. Hence a subtraction of this amount from his published results[2] for neutral atoms yields the values of $M^+{}_{H^1}$ and $M^+{}_{H^2}$. Using these, Houston's[3] value for $\nu(H^1\alpha)$, and the measured isotopic interval, the atomic weight of the electron was found to be $(5.491\pm0.002)\times10^{-4}$. Since the other quantities involved have been measured to a higher percent accuracy than the isotopic interval the uncertainty in this result is due chiefly to the uncertainty in the value of the interval.

Dividing the value of the Faraday, as given by Birge,[4] by this value of the electronic atomic weight, we obtain $(1.757\pm0.001)\times10^7$ e.m.u./gram for the ratio of e/m for the electron. This ratio is in excellent agreement with those obtained by magnetic deflection methods as recently reported by Dunnington[5] and by Kretschmar.[6]

R. C. GIBBS
R. C. WILLIAMS

Department of Physics,
Cornell University,
November 21, 1933.

---

[1] Bainbridge, Phys. Rev. **41**, 115 (1932).
[2] Bainbridge, Phys. Rev. **43**, 103 (1933); **44**, 57 (1933).
[3] Houston, Phys. Rev. **30**, 608 (1927).
[4] Birge, Phys. Rev. Sup. **1**, 1 (1929).
[5] Dunnington, Phys. Rev. **43**, 404 (1933).
[6] Kretschmar, Phys. Rev. **43**, 417 (1933).

The Emission of Electricity from Columbium

Columbium was found when heated to the point where vaporization becomes appreciable to yield positive ions of the metal itself. A determination of the electron and positive ion work functions has been carried out with carefully outgassed specimens. The values found are for the electron, 3.96 volts, with a value of A of 57 amp./cm²/degree². The value for the positive ion work function has been determined as 5.52 volts from the relation $i = BTe^{-\varphi/kT}$ as developed by Fowler. A detailed account of this work will be published later. The work is being extended to rhodium.

H. B. WAHLIN
L. O. SORDAHL

University of Wisconsin,
Madison, Wisconsin,
November 23, 1933.

Influence of Nitrogen and Carbon Dioxide upon the Absorption Spectrum of Mercury Vapor

The widening of the 2536 mercury absorption line on the short wave-length side by an admixture with air or other chemically inert gas was described by one of us in 1907,[1] a photograph being reproduced on Plate 6, Fig. 2, page 432 of Wood's *Physical Optics*. The series of photographs beginning at the bottom represents the absorption of the light of a cadmium spark by a 100 cc quartz flask containing a small amount of mercury, and gradually heated until the mercury is boiling vigorously and condensing on the neck of the flask, having expelled all of the air. It is at once clear that the absorption line is wider on the left-hand side (short λ) in the middle spectrum taken with a mixture of mercury and air than in the top one taken with pure mercury vapor at atmospheric pressure. The total pressure was the same in all cases as the neck of the flask was open. This effect of an inert gas remained unexplained until the subject was reopened by the experiments of Oldenberg[2] and Kuhn and Oldenberg,[3] who found that mixtures of mercury vapor and rare gases showed in some cases, instead of an expected continuous band on both sides of the resonance line, a band spectrum on the long wave side and two diffuse maxima on the short wave side. The band spectrum was explained by nuclear vibrations of a molecule consisting of an excited Hg-atom and a normal rare gas atom. The short wave maxima were ascribed to the sharp rise of the potential energy at short distances between the colliding atoms; the total angular momentum of the excited Hg-atom may point either in the direction of, or at right angles to the line connecting the two nuclei, causing the existence of two separate potential curves and, therefore, two separate maxima.

Similar observations were made by Krefft and Rompe[4] with the spectra of electric discharges in mixtures of other metal vapors and rare gases.

Theoretical considerations become more difficult if one has to deal with collisions between Hg-atoms and polyatomic molecules. Because of the asymmetry of the molecule, the orientation of the excited Hg-atom will no longer be restricted to two well-defined positions. Moreover, the potential energy may depend also upon the orientation of the molecule during the collision and upon its vibrational and rotational state.

The absorption spectra of mercury vapor with added molecular gases have been investigated by the writers. The gas to be investigated was enclosed over a mercury column in a quartz bulb which could be heated electrically, the temperature was varied from 170 to 370°C. Continuous ultraviolet light from a hydrogen discharge tube with a quartz window passed through the bulb. The absorption spectrum was photographed by means of a large quartz spectrograph.

A structure consisting of a broad absorption band on the short wave side of the resonance line appeared when the bulb was filled with a certain amount of nitrogen or carbon dioxide. In the case of nitrogen the band appeared when the width of the pressure-broadened Hg-line was less than 10A, its distance from the line was about 8A,[5] the excess energy being 0.014 volt. The most favorable experimental conditions for the appearance of the band were a temperature of 285°C and a partial pressure of nitrogen of 60 mm. With carbon dioxide in the bulb the data were: Maximum width of pressure-broadened line 16A, distance of the band from the Hg-line 14A, excess energy 0.026 volt, temperature 200°C, partial pressure of carbon dioxide 490 mm.

This structure of the absorption band can be explained by the same mechanism as in Kuhn and Oldenberg's fluorescence experiments: If an absorption process takes place during a collision with a foreign gas molecule, the absorbed energy corresponds to the difference of potential of the normal and of the excited state at short distances between the collision partners. If there is some probability for this effect, an amount of energy higher than that of the resonance line may be absorbed, resulting in a minimum on the short wave side.

R. W. WOOD
H. W. STRAUB

Johns Hopkins University,
November 25, 1933.

---

[1] R. W. Wood, *Modification in the Appearance and Position of an Adsorption Band Resulting from the Presence of a Foreign Gas*, Astrophys. J. **26**, 41 (1907).

[2] Oldenberg, Zeits. f. Physik **47**, 184 (1928); **51**, 605 (1928); **55**, 1 (1929).

[3] Oldenberg and Kuhn, Phys. Rev. **41**, 72 (1932).

[4] H. Krefft and R. Rompe, Zeits. f. Physik **73**, 681 (1932).

[5] This checks fairly well with results obtained by Moore. Science **66**, 543 (1927).

Spectrum of $O^{16}H^2$

Intermittently, for some months, we have been working on the analysis of the spectrum of OH produced in water vapor containing 35 percent of the hydrogen as H^2, from which we have obtained good photographs.[1]

We have been successful in identifying and assigning nearly 500 new lines, in the OH^2 spectrum, which are distributed through eight bands, including the (3,1) and (3,2) bands. Assignments extend beyond $K=30$ in the (0,0) band.

In order to calculate isotope *shifts* between corresponding lines of $O^{16}H^1$ and $O^{16}H^2$ we find that it is necessary to introduce corrections for isotope effects in spin coupling[1] and in Λ-doubling in the ground $^2\Pi$ level and to include γ_e terms in the expansion of the rotational constant B_v in both the upper and the lower levels. The latter is easily accomplished from the rotational constants now in the literature[2] which give:

$$B_e'=17.375 \qquad \alpha_e'=0.838 \qquad \gamma_e'=-0.0075$$
$$B_e''=19.009 \qquad \alpha_e''=0.686 \qquad \gamma_e''=-0.0125$$

The results of the empirical analysis will be published in the near future.

We wish to acknowledge our indebtedness to Professor G. N. Lewis, who generously placed the sample of "heavy water" at our disposal.

HERRICK L. JOHNSTON[3]
DAVID H. DAWSON[4]

The Ohio State University,
Columbus, Ohio,
November 29, 1933.

[1] Cf. Johnston and Dawson, Naturwiss. **21**, 495 (1933).

[2] Johnston, Dawson and Walker, Phys. Rev. **43**, 473 (1933).

[3] Fellow of the John Simon Guggenheim Memorial Foundation while this work was carried out.

[4] DuPont Fellow in Chemistry 1932–3.

On the Breakdown of the Coulomb Law for the Hydrogen Atom

The well-known measurements of the doublet separations in the Balmer series by Kent, Taylor and Pearson,[1] and by W. V. Houston[2] indicate that Hβ is about three percent narrower than predicted by the relativistic fine structure theory, whereas the separations for Hα and Hγ agree with the theory within the limits of experimental error. The more recent observations of Spedding, Shane and Grace[3] indicate, if we interpret their preliminary report correctly, that the $H^1\alpha$ and $H^2\alpha$ doublets are both somewhat less than one percent narrower than expected from the theory. Finally, the new interferometer measurements of Houston and Hsieh[4] increase the discrepancy to about three percent for all the doublets of light hydrogen (H^1). These last experiments were conducted under such conditions that the intensity ratios of the components were those expected theoretically, and the discrepancy is accordingly attributed to a deficiency in the theory. A simple computation shows that this discrepancy can be accounted for by a deviation from the Coulomb law at small distances from the nucleus. Such a deviation is known to occur for heavier nuclei and there exists evidence pointing to the same conclusion for hydrogen.[5] It might be due in the present case to the finite size of the electron and proton suggested by Born,[6] or to an eventual composite structure of the proton (neutron plus positron).

We suppose that the field is Coulomb down to a radius a where a change occurs into some other type of law. A potential attractive as $1/r^n$, where n is greater than or equal to 2, must be rejected on the basis of mathematical considerations.[7] Since the exact shape of the potential curve is not important for such very small distances, we have represented the case where the potential approaches a finite limit by the constant potential e^2/a and the case where the potential becomes positively infinite by a law repulsive as e^2/r. As both types were found to give approximately the same result, we shall discuss only the first, which, according to Born's new theory,[6] should be more nearly correct than an exact Coulomb field. A first order perturbation method, by using the Dirac wave functions, was applied to the $n=l$ level and yielded appreciably the same results as the ordinary Schrödinger functions. The latter were then used to compute the displacements of the energy levels as functions of a. It was readily seen that the s levels were raised by an amount $2a^2e^2/3n^3r_0^3$ equivalent to the introduction of a quantum defect $n-n^*=a^2e^2/3Rhr_0^3$. Here R is the Rydberg constant and r_0 is the radius of the innermost Bohr orbit. This results in a narrowing of the doublets in agreement with experiment. The converse effect of a broadening of the doublets would be difficult to account for, but fortunately does not occur. Combining the relative shifts of the fine structure components of Hα in accordance with the Sommerfeld-Unsöld intensity ratios, new centers of gravity were obtained for the doublet humps. One remains almost fixed and the other moves in by about 40 percent of the computed displacement of the $2s$ energy level, or about $a^2e^2/30r_0^3$. All the doublets are narrowed by approximately this amount in agreement with the results

[1] Kent, Taylor and Pearson, Phys. Rev. **30**, 266 (1927).

[2] W. V. Houston, Astrophys. J. **64**, 81 (1926).

[3] Spedding, Shane and Grace, Phys. Rev. **44**, 58 (1933).

[4] Houston and Hsieh, Bull. Am. Phys. Soc. **8**, No. 6, p. 5, Nov. 24, 1933.

[5] Cf., e.g., Ruark and Urey, *Atoms, Molecules, and Quanta*, p. 49; H. Jensen, Zeits. f. Physik **82**, 794 (1933).

[6] M. Born, Nature **132**, 282 (1933).

[7] G. H. Shortley, Phys. Rev. **38**, 120 (1931).

of Houston and Hsieh. The value of a determined by this method using the estimate of 3 percent for the displacements to be accounted for, is about 5×10^{-12} cm. The hypothesis of a positively infinite potential decreases a to about 4×10^{-12} cm.

The values of a are surprisingly large but could not be reduced to the classical electron radius of 2×10^{-13} cm by any modification of the experimental results which did not affect the order of magnitude of the recently discovered discrepancies.

E. C. KEMBLE
R. D. PRESENT

Harvard University,
December 2, 1933.

The Infrared Spectrum of Heavy Ammonia—ND_3

The writers have made an investigation of the infrared absorption spectrum of ND_3, using a rocksalt prism spectrometer. The sample used was very kindly supplied to us by Professor H. S. Taylor, and was prepared from heavy water estimated to be 99 percent pure. The ammonia sample was estimated to be more than 90 percent ND_3, and the absorption spectrum gave no bands characteristic of ordinary ammonia. By following the procedure of Dennison[1, 2] it is possible to calculate the positions of the fundamental vibrations of this molecule, assuming that the force fields are similar, and that the interatomic distances are the same for the two isotopes. The agreement between observed and calculated values is about as good for the ND_3 as for the values calculated and observed in the literature for the NH_3.[3] These are given in Table I. The spectrum should consist of four bands (of the six possible modes of vibration, two are doubly degenerate), in two of which the change in moment should be perpendicular to the symmetry axis. In the NH_3, the bands at 950 cm^{-1} and 3336 cm^{-1} have been assigned to the parallel vibrations, and the bands at 1631 cm^{-1} and 4417 cm^{-1} are the two fundamental perpendicular vibrations. Of the four bands observed for ND_3, the similarity in the structure of the envelopes of the bands to the corresponding frequencies of NH_3 holds extremely well, and in each case indicates the predicted type of vibration.

TABLE I.

Light ammonia NH_3				Heavy ammonia ND_3			
ν	Calc.	Obs.	Type	ν'	Calc.	Obs.	Type
ν_3	938	950	∥	$\nu_3'=0.762$	$\nu_3=$ 715	770	∥
ν_2	1679	1631	⊥	$\nu_2'=0.708$	$\nu_2=1189$	1158	⊥
ν_1	3336	3336	∥	$\nu_1'=0.715$	$\nu_1=2385$	2421	∥
ν_4	4466	4417	⊥	$\nu_4'=0.742$	$\nu_4=3334$	3287	⊥

The writers are continuing this investigation with a grating spectrometer of higher resolution and further details concerning the rotational structure of the bands will be presented in the future.

The writers are much indebted to Professor H. S. Taylor and Dr. H. Eyring and their co-workers at Princeton University for their kindness in supplying the compound.

S. SILVERMAN
J. A. SANDERSON

Physical Laboratory,
The Johns Hopkins University,
December 2, 1933.

[1] Dennison, Phil. Mag. **1**, 195 (1926).
[2] Dennison, Rev. Mod. Phys. **3**, 280 (1931).
[3] Schaefer and Matossi, *Dasultrarote Spektrum*, p. 251.

AUTHOR INDEX TO VOLUME 44

References with (A) are to abstracts of papers presented at meetings of the Physical Society. References with (L) are to Letters to Editor.

Abbott, R. B. (see Jenkins Ruth O.)—321(A)
——— (see Stevens, T. H.)—321(A)
Adams, Norman I., Jr. Application of probabilities to the counting of α-particles—651
Adel, Arthur. Raman spectrum of gaseous carbon dioxide —691(L)
——— (see Barker, E. F.)—185
——— (see Dennison, D. M.)—131(A)
——— **and D. M. Dennison.** Infrared Spectrum of carbon dioxide, Part II—99
Ahearn, A. J. Effect of temperature on the emission of electron field currents from tungsten and molybdenum —277
Akeley, Edward L. Canonical coordinate system in Riemannian geometry—318(A)
Allen, Robert I. and F. W. Constant. Absolute saturation of cubic cobalt—228
Allis, W. P. (see Morse, P. M.)—269
Allison, Fred (see Bishop, Edna R.)—419(L)
Allison, Samuel K. Natural widths of the $K\alpha$ x-ray doublet from 26Fe to 47Ag—63
Almy, G. M. and F. M. Sparks. Absorption spectrum of diatomic bismuth—365
Ambrose, H. A. and A. G. Loomis. Fluidities of thixotropic gels: Bentonite suspensions—320(A)
Anderson, Carl D. Cosmic-ray positive and negative electrons—406
Anderson, O. E. (see White, H. E.)—128(A)
Arvin, M. J. (see Loomis, F. W.)—126(L)
Ashley, Muriel F. Nuclear spin of phosphorus from band spectrum analysis—919
Asling, Walter Louis and R. T. Dufford. Efficiency of chemiluminescence accompanying the Wedekind reaction—315(A)
Aughey, W. H. and W. D. Lansing. New monochromatic filter—326(A)

Babcock, C. L. (see Lark-Horovitz, K.)—321(A)
——— **and J. V. Hoffacker.** New visco-conductimeter—320(A)
Babcock, Harold D. Remarks on the "lines" of diffraction gratings—129(A)
Bainbridge, Kenneth T. Comparison of the masses of H^2 and helium—57(L)
——— Equivalence of mass and energy—123(L)
——— Masses of the lithium isotopes—56(L)
Baker, R. F. (see DeVore, L. T.)—324(A)
——— (see Morgan, H. E.)—324(A)
Ballard, Stanley S. (see Grace, N. S.)—128(A)
Barker, E. F. (see Plyler, E. K.)—984
——— **and Arthur Adel.** Resolution of the two difference bands of CO_2 near 10μ—185
Barnes, A. H. Structure of the x-ray K absorption limits of the elements manganese to zinc—141
Barnes, R. Bowling. Plasticity of rocksalt and its dependence upon water—898
Barnes, S. W. (see Richtmyer, F. K.)—311(L)
Bartlett, B. W. Errata—Variation of the principal magnetic susceptibilities of certain paramagnetic crystals with temperature—687
Bartlett, J. H., Jr. (see Brown, F. W.)—296
——— **and J. J. Gibbons, Jr.** Isotope shift in neon—325(A); 538
Bayley, P. L. Raman spectra of three amines—510(L)
Bayliss, Noel S. (see Gibson, G. E.)—188; 193
Beams, J. W. Field electron emission from liquid mercury —803
——— **and L. B. Snoddy.** Production of high velocity ions and electrons—784(L)
Bear, Richard S. (see Spedding, F. H.)—287
Beeck, Otto. Production of neutral rays of several hundred ion-volt-equivalent, the absolute measurement of their intensity and the ionizing function of argon rays in argon—317(A)
Bennett, Willard H. Discrepancy between theory and experiment in cold emission—859(L)
——— Self-focussing electron streams—322(A)
Bishop, Edna R. and Fred Allison. Isotopes of chlorine—419(L)
Blair, Julian M. (see Jones, Merton W.)—131(A)
——— **and Malcolm C. Hylan.** Intermittency effect in photographic exposure—131(A)
Bleakney, Walker (see Harnwell, G. P.)—785(L)
——— **and Austin J. Gould.** Relative abundance of hydrogen isotopes—265
Bonner, T. W. Dependence of the absorption of neutrons on their velocity—235(L)
Bowen, I. S., R. A. Millikan and H. V. Neher. New, high-altitude, study of cosmic-ray bands and a new determination of their total energy content—246
Bowie, Robert M. (see Fox, Gerald W.)—345
Bradbury, Norris E. Electron attachment and negative ion formation in oxygen and oxygen mixtures—883; 952(A)
Bramley, Arthur. Band spectra measurement of mass—309(L)
Brasefield, Charles J. Production of secondary electrons by argon positive ions and by argon atoms—1002
Breit, G. Isotope shift of Tl—418(L)
——— (see Johnson, M. H., Jr)—77
——— (see Wheeler, John A.)—948(L)

Breit, G. and Lawrence A. Wills. Hyperfine structure in intermediate coupling—470
Brewer, A. Keith. Effect of alkali ions on the photoelectric emissivity of tungsten—1016
Brode, Robert B. and Edward B. Jordan. Reflection of electrons from liquid mercury—872
Brown, F. W. Charge distributions in fluorine and neon—214
——— **J. H. Bartlett, Jr. and C. G. Dunn.** Charge distribution for the normal atoms from boron to neon—296
Brownscombe, E. R. (see Fricke, H.)—240(L)
Broxom, James W., George T. Meredith and Louis Strait. Relations among fluctuations of the cosmic-ray ionization, of the terrestrial magnetic field, of the atmospheric potential gradient, and of the absolute humidity—253
Bruce, C. W. Electro-optical Kerr effect in gases—682

Cady, W. G. Survey of piezoelectricity—954(A)
Cady, Willoughby M. High terms in the spectra N^v and O^v—128(A)
——— New terms in the spectra of N III, N IV, N V, O III, O IV and O V—821
Carlson, J. F. (see Furry, W. H.)—237(L)
Cassen, Benedict. On the nature of cosmic-ray showers—513(L)
Caswell, A. E. Hooke's law and crystal structure—320(A)
Chamberlain, Katherine and Harold B. Cutter. New bands in the electronic band spectrum of neutral OH—927
Chow, Tung-Ching. Spectrum of sulphur dioxide—638
Cleeton, C. E. and N. H. Williams. Magnetostatic oscillator for the generation of 1 to 3 cm waves—421(L)
Cleveland, Forrest F. Magnetic force and the law of action and reaction—318(A)
Clewell, D. H. and J. Wulff. Reflecting power of aluminum and its alloys in different regions—952(A)
Coates, Wesley M. and E. O. Lawrence. X-rays produced by fast mercury ions—327(A)
Cohn, Willi M. X-ray investigations at high pressures—326(A)
Compton, K. T. and E. S. Lamar. Test of the classical "momentum transfer" theory of accommodation coefficients of ions at cathodes—338
Condon, E. U. and C. W. Ufford. Relative multiplet transition probabilities from spectroscopic stability—740
Constant, F. W. (see Allen, R. I.)—228
Coolidge, A. S. (see James, H. M.)—953(A)
Cooper, F. S. (see Kruger, P. G.)—418(L); 826
——— **and P. Gerald Kruger.** Standard wave-lengths in the copper sepctrum in the region 80A to 650A—324(A)
Cork, J. M. (see Purdon, E. G.)—328(A); 974
Crane, H. R. and C. C. Lauritsen. On the production of neutrons from lithium—783(L)
——— **C. C. Lauritsen and A. Soltan.** Artificial production of neutrons—514(L)
——— **C. C. Lauritsen and A. Soltan.** Production of neutrons by high speed deutons—692(L)
Crawford, F. H. and C. F. Ffolliott. Band spectra of the halides of aluminum—953(A)
Crawford, M. F. (see McLay, A. B.)—986
Cunningham, W. P. and William W. Watson. Zeeman effect and uncoupling phenomena in the CaH bands—815
Cutter, Harold B. (see Chamberlain, Katherine)—927

Darrow, K. K. Elementary particles—954(A)
Dawson, David H. (see Johnston, Herrick L.)—1031(L)
Davey, W. P. (see Singer W. E.)—319(A)
Déjardin, G. and R. Schwégler. Photoelectric properties of magnesium layers—316(A)
Deming, W. Edwards. Probable errors of the parameters in an empirical formula—317(A)
Dennison, D. M. (see Adel, A.)—99
——— **and A. Adel.** Molecular spectra in the photographic infrared—131(A)
Dersham, Elmer. Laws of absorption for soft x-rays—328(A)
DeVore, L. T. Emissivity of a non-black body—324(A)
——— Photographic recording photoelectric densitometer—329(A)
——— (see Morgan, H. E.)—324(A)
——— **and R. F. Baker.** Tungsten filament lamp as a standard source for radiation measurements—324(A)
Dickinson, Beryl H. Specific isotope effect in the lead spectrum—329(A)
Douglas, A. V. (see Foster, J. S.)—325(A)
DuBridge, Lee A. (see Roehr, W. W.)—316(A)
——— **and R. C. Hergenrother.** Effect of temperature on the energy distribution of photoelectrons. I. Normal energies—861
Duffendack, O. S. (see Emeleus, K. G.)—322(A); 945(L)
Dufford, R. T. New observations on the photovoltaic effect—315(A)
——— (see Asling, Walter Louis)—315(A)
——— (see Thomas Clarence Delmar)—315(A)
Dunham, Theodore, Jr. Photoelectric measurement of the shapes of solar absorption lines—329(A)
——— Spectra of Mars, Venus and Jupiter under high dispersion—131(A)
Dunn, C. G. (see Brown, F. W.)—296
Dunning, J. R. and G. B. Pegram. On neutrons from a beryllium-radon source—317(A)
Duveneck, F. B. (see Webster, D. L.)—258

Eaton, V. E. New experiments and apparatus for the elementary physics laboratory—954(A)
Eckart, Carl. Comparison of the nuclear theories of Heisenberg and Wigner. I—109
——— General derivation of the formula for the diffraction by a perfect grating—12
Edlén, Bengt. Ionization potential of Be III—778(L)
Eliason, A. Y. (see White, H. E.)—753
Ellett, A. (see Heydenburg, N. P.)—326(A)
Ellis, Joseph W. and Hans O. Kneser. Combination relation in the absorption spectrum of liquid oxygen—420(L)
Emeleus, K. G. (see Sloane, R. H.)—322(A); 333
——— **and O. S. Duffendack.** Faraday dark space—322(A)
——— **and O. S. Duffendack.** Inert gas molecules—945(L)
Evans, Robley D. Radioactivity and the age of meteorites—131(A)

Evans, Robley D. Uranium and thorium content of rocks determined from their surface radiation—129(A)
——— **and M. C. Henderson.** Failure to detect radioactivity in beryllium—131(A)
——— **and M. C. Henderson.** Failure to detect radioactivity in beryllium with the linear amplifier—59(L)
Evjen, H. M. Contribution to the theory of heteropolar crystals—501
——— New analysis of Slater's compressibility data—491

Fankuchen, I. Crystal structure of potassium uranyl acetate—327(A)
Farnsworth, H. E. Concerning W. T. Sproull's article on "Diffraction of low speed electrons by a tungsten single crystal"—417(L)
Fermi, Enrico and George E. Uhlenbeck. On the recombination of electrons and positrons—510(L)
Ffolliott, C. F. (see Crawford, F. H.)—953(A)
Fisher, Russell A. Analysis of Zeeman patterns—724
Foster, J. S. and A. V. Douglas. Stellar stark line He λ4470—325(A)
Fox, Gerald W. and Robert M. Bowie. New method for determining the thermionic work functions of metals and its application to nickel—345
Frederickson, W. R. and C. R. Stannard. Magnetic rotation spectrum of the red bands of sodium—632
Fricke, Hugo and E. R. Brownscombe. Inability of x-rays to decompose water—240(L)
Furry, W. H. and J. F. Carlson. On the production of positive electrons by electrons—237(L)

Gagge, A. Pharo. Magnetic deflection method for angular distribution of electrons scattered by gas molecules—808
Galli-Shohat, N. Reflection of a spherical light-wave from a moving plane mirror—319(A)
Gans, David M. (see Harkins, William D.)—236(L); 529; 945(L)
——— **William D. Harkins and Henry W. Newson.** Failure to detect the radioactivity of beryllium with the Wilson cloud chamber—310(L)
Genard, J. Fluorescence of diatomic molecules of antimony—468
Germer, L. H. Electron diffraction and the imperfection of crystal surfaces—1012
Giauque, W. F. and D. P. MacDougall. Heat capacity of gadolinium sulfate octahydrate below 1° absolute—235(L)
Gibbons, J. J., Jr. (see Bartlett, J. H., Jr)—325(A); 538
Gibbs, R. C. (see Williams, R. C.)—325(A)
——— **and R. C. Williams.** Electronic atomic weight and e/m ratio—1029(L)
Gibson, G. E. and Noel S. Bayliss. Variation with temperature of the continuous absorption spectrum of diatomic molecules: Part I. Experimental, the absorption spectrum of chlorine—188
——— **O. K. Rice and N. S. Bayliss.** Variation with temperature of the continuous absorption spectrum of diatomic molecules: Part II. Theoretical—193
Gleason, Paul R. Electrical characteristics of barrier-layer photo-cells—315(A)
——— Variation in sensitivity of the photronic cell with x-ray wave-lengths—330(A)
Gould, A. J. (see Bleakney, Walker)—265
Grace, Norman S. Hyperfine structure of the rare earths—603(L)
——— Nuclear moments, and their dependence upon atomic number and mass number—361
——— Suggested dependence of nuclear moments on atomic number—58(L)
——— (see McMillan, Edwin)—949(L)
——— (see Spedding, F. H.)—58(L)
——— **and Stanley S. Ballard.** Hyperfine structure and nuclear moment of columbium—128(A)
——— **and Edwin McMillan.** Hyperfine structure and nuclear spin of tantalum—325(A)
——— **and Kenneth R. More.** Hyperfine structure of molybdenum—128(A)
Granath, L. P. (see Van Atta, C. M.)—60(L)
——— **and C. M. Van Atta.** Nuclear spin and magnetic moment of sodium from hyperfine structure—935
Gray, Newton M. Nuclear spin of Li^7 from hyperfine structure data—570
Green, J. B. and R. A. Loring. Second order Zeeman effect in the arc spectrum of mercury—325(A)

Hafstad, L. R. Application of the FP-54 Pliotron to atomic disintegration-studies—201
Halpern, O. Scattering processes produced by electrons in negative energy states—855(L)
Hansen, W. W. Emission and absorption of radiation—954(A)
——— (see Webster, D. L.)—258
Hanson, Alvin W. Elastic constants of zinc—320(A)
Harkins, William D. (see Gans, D. M.)—310(L)
——— **David M. Gans and Henry W. Newson.** Disintegration of fluorine nuclei by neutrons and the probable formation of a new isotope of nitrogen (N^{16})—945(L)
——— **David M. Gans and Henry W. Newson.** Disintegrations of neon nuclei by fast neutrons—236(L)
——— **David M. Gans and Henry W. Newson.** Disintegration of the nuclei of nitrogen and other light atoms by neutrons. I—529
Harnwell, G. P., W. Bleakney, S. N. VanVoorhis, and J. B. H. Kuper. Faraday effect at high frequencies—785(L)
Harris, Louis (see Johnson, E. A.)—944(L)
Harvey, G. G. Diffuse scattering of x-rays from sylvine. IV. Scattering at high temperatures—133
Hazel, Herbert and R. R. Ramsey. Beat note-combinational tone controversy—321(A)
Henderson, Malcolm C. (see Livingston, M. Stanley)—316(A); 781(L); 782(L)
——— (see Evans, Robley D.)—59(L); 131(A)
Hendricks, S. B. (see Jones, E. J.)—322(A)
Henshaw, C. L. (see Waterman, A. T.)—59(L)
Hergenrother, R. C. (see DuBridge, Lee A.)—861
Herzfeld, K. F. and R. H. Lee. Theory of forced double refraction—625
Heydenburg, N. P. and A. Ellett. Nuclear moment of Na, and polarization of resonance radiation—326(A)

Hirsh, F. R., Jr., and F. K. Richtmyer. Relative intensities of certain *L*-series x-ray satellites in cathode-ray and in fluorescence excitation—955
Hoffacker, J. V. (see Babcock, C. L.)—320(A)
Hollister, S. C. and G. J. Schoessow. Stress concentration at a circular hole in a plate in monaxial tension—330(A)
Hopfield, John J. Study of a new water jet with stroboscope and camera—321(A)
Houston, William V. (see Lewis, Charlton M.)—903
Howell, Lynn G. (see Mott-Smith, Lewis M.)—4
Hughes, A. L. and J. H. McMillen. Electron scattering in methane, acetylene and ethylene—876
——— **and J. H. McMillen.** Inelastic electron scattering by helium atoms—20
Hui, Ching-Young. Crystal structure of sodium thioantimonate—327(A)
Hull, G. F. Cosmic-ray counters and cosmic-ray counts—952(A)
Hunt, Frederick V. Vacuum-tube voltmeter with logarithmic response—952(A)
Hutchisson, E. and A. L. Robinson. Single electrode potentials and the e.m.f. of a cell—323(A)
Hylan, Malcolm C. (see Blair Julian M.)—131(A)

Ingersoll, L. R. and Wesley R. Winch. Dispersion of the Kerr electro-optic effect in the short infrared spectrum—399

James, H. M. and A. S. Coolidge. New treatment of the H_2 molecule—953(A)
Jarvis, C. W. and E. N. Shawhan. Attempt to discover radiation at low critical potentials in mercury vapor—943(L)
Jauncey, G. E. M. (see Pennell, Ford)—328(A)
——— **and Ford Pennell.** Scattering of x-rays from powdered crystals at low temperatures—138
——— **and H. W. Richardson.** Sensitiveness of photographic films to x-rays at low temperatures—328(A)
——— **and P. S. Williams.** Diffuse scattering of x-rays from sodium fluoride. II. Scattering at the temperature of liquid air—794
Jenkins, F. A. and Andrew McKellar. Redetermination of the mass ratio of the lithium isotopes from the band spectrum—325(A)
Jenkins, Ruth O. and R. B. Abbott. Some frequencies of multiple resonators—321(A)
Jeppesen, C. Rulon. Emission spectrum of molecular hydrogen in the extreme ultraviolet—165
Johnson, E. A. and Louis Harris. Thermoelectric force of thin films—944(L)
Johnson, M. H., Jr. and G. Breit. Magnetic interaction of a valence electron with inner shells—77
Johnson, Thomas H. Preliminary report of the results of angular distribution measurements of the cosmic radiation in equatorial latitudes—856(L)
——— **and E. C. Stevenson.** Asymmetry of the cosmic radiation at Swarthmore—125
Johnston, Herrick L. and David H. Dawson. Spectrum of $O^{16}H^2$—1031(L)
Jones, Ernest J. Positive ion excitation of mercury vapor—707
——— **and S. B. Hendricks.** Sources of positive ions: thermionic properties of the system Li_2O, Al_2O_3, SiO_2—322(A)
Jones, Merton W. and Julian M. Blair. Analysis of the action of hydrogen peroxide on photographic emulsions 131(A)
Jordan, Edward B. (see Brode, R. B.)—872

Kabakjian, D. H. Decay of luminescence and light absorption in phosphorescent materials—618
Kaplan, Joseph. New band system in nitrogen—947(L)
——— Unusual nitrogen tube—783(L)
Kaufman, Sidney (see Richtmyer, F. K.)—605
Keck, Paul and Leonard B. Loeb. Study of a powerful source of positive alkali ions—130(A)
Kemble, E. C. Characterization of physically admissible wave functions—954(A)
——— **and R. D. Present.** On the breakdown of the Coulomb law for the hydrogen atom.—1031(L)
Kenty, Carl. Photoelectric yields in the extreme ultraviolet—891
Kirkpatrick, Paul (see Webster, D. L.)—130(A)
Kirkwood, John G. Quantum statistics of almost classical assemblies—31
Kneser, Hans O. (see Ellis, J. W.)—420(L)
Ko, Cheng Chuan. Heat of dissociation of Bi_2 determined by the method of molecular beams—129(A)
Koehler, James F. Quenching of iodine fluorescence by iodine and argon—761
Koenig, Harold D. Calculation of characteristic values for periodic potentials—657
Korff, S. A. Azimuthal investigation of cosmic radiation—130(A); 515(L)
——— Density of energy in the universe—300
Kruger, P. Gerald (see Cooper, F. S.)—324(A)
——— **and F. S. Cooper.** Be III $1snp\ ^1P_1 - 1s^2\ ^1S_0$ series—418(L)
——— **and F. S. Cooper.** Standard copper wave-lengths in the region 100A to 450A—826
——— **and W. E. Shoupp.** Multiplets of O III, O IV, and O V in the region 100A to 650A—324(A)
——— **and W. E. Shoupp.** Multiplets in the spectra of O III, O IV, O V and C III—105

Ku, Z. W. Absorption spectrum of chlorine dioxide—376
——— Intensity distribution in a band system of symmetrical triatomic molecules—383
Kunz, Jakob. Application of a vibrating velocity selector for the determination of the magnetic moment of hydrogen—323(A)
Kuper, J. B. H. (see Harnwell, G. P.)—785(L)
Kurie, Franz N. D. Collisions of neutrons with protons—463

Lamar, E. S. (see Compton, K. T.)—338
——— **and Overton Luhr.** Convenient proton source—947(L)
Lanczos, Cornelius. Fundamental connection between Hamiltonian dynamics and wave mechanics—318(A)
Landé, A. Magnetic moment of the proton—1028(L)
——— Possibility of electric charge—689(L)

Lane, C. T. Variation of the magnetic properties of barium with temperature—43
Lang, R. J. Spectrum of Cb IV—325(A)
Langmuir, Irving (see Taylor, John Bradshaw)—423
Langseth, A. and J. R. Nielsen. Raman spectra of some linear triatomic molecules—326(A)
Lansing, W. D. (see Aughey, W. H.)—326(A)
Lark-Horovitz, K. and C. L. Babcock. Viscosity and conductivity of molten glasses—321(A)
——— **and S. E. Madigan.** Crystallization of polymorphous substances—320(A)
Latimer, Wendell M. and Herbert A. Young. Isotopes of calcium by the magneto-optic method—61(L)
——— **and Herbert A. Young.** Isotopes of hydrogen by the magneto-optic method. The existence of H^3—690(L)
Lauritsen, C. C. (see Crane, H. R.)—514(L); 692(L); 783(L)
Lawrence, Ernest O. (see Coates, W. M.)—327(A)
——— (see Livingston, M. Stanley)—316(A); 781(L); 782(L)
——— (see Lewis, Gilbert N.)—55(L); 317(A)
——— **and M. S. Livingston.** Three types of nuclear disintegration of calcium fluoride by bombarding protons of very great energy—316(A)
——— **M. S. Livingston and G. N. Lewis.** Emission of protons from various targets bombarded by deutons of high speed—56(L)
Lee, R. H. (see Herzfeld, K. F.)—625
Lewis, Charlton M. and William V. Houston. Raman effect in ammonia and some other gases—903
Lewis, Gilbert N. (see Lawrence, Ernest O.)—56(L)
——— **M. Stanley Livingston and Ernest O. Lawrence.** Emission of alpha-particles from various targets bombarded by deutons of high speed—55(L)
——— **M. Stanley Livingston and Ernest O. Lawrence.** Disintegration of nuclei by swiftly moving ions of the heavy isotope of hydrogen—317(A)
Libby, W. F. Stability of beryllium—512(L)
Liben, I. and H. M. O'Bryan. Absorption and reflection of gold between 380A and 1400A—952(A)
Livingston, M. Stanley (see Lawrence, E. O.)—56(L); 316(A)
——— (see Lewis, G. N.)—55(L); 317(A)
——— **Malcolm C. Henderson and Ernest O. Lawrence.** Disintegration of the elements by swiftly moving protons—316(A)
——— **Malcolm C. Henderson and Ernest O. Lawrence.** Neutrons from deutons and the mass of the neutron—781(L)
——— **Malcolm C. Henderson and Ernest O. Lawrence.** Neutrons from beryllium bombarded by deutons—782(L)
Locher, Gordon L. Neutrons from cosmic-ray Stösse—779(L)
Loeb, Leonard N. (see Keck, P.)—130(A)
Long, J. D. (see Singer, W. E.)—319(A)
Loomis, A. G. (see Ambrose, H. A.)—320(A)
Loomis, F. W. and M. J. Arvin. Band spectrum of NaK—126(L)
Lorenz, Egon. Investigation on mitogenetic radiation by means of a photoelectric counter tube—329(A)
Loring, R. A. (see Green, J. B.)—325(A)
Lowan, Arnold N. On the cooling of a radioactive sphere—769
Lozier, W. Wallace. Heats of dissociation of hydrogen and nitrogen—575
Luhr, Overton. Nature of gas ions—459
——— (see Lamar, E. S.)—947 (L)

MacDougall, D. P. (see Giauque, W. F.)—235(L)
Madigan, S. E. (see Lark-Horovitz, K.)—320(A)
Manning, K. V. (see Richtmyer, F. K.)—311(L)
Manning, Millard F. and Nathan Rosen. Potential function for vibrations of diatomic molecules—953(A)
Margenau, Henry. Asymmetries of pressure broadened spectral lines—931; 954(A)
——— (see Watson, William W.)—748
——— **and William W. Watson.** Pressure effects of foreign gases on the sodium *D*-lines—92
Marvin, H. H. Limitations of the theory of complex spectra—818
Matheson, L. A. Atomic polarization of CO—604(L)
Maxwell, Louis R. Electron diffraction by liquids—73
McKeehan, L. W. Magnetic dipole fields in unsaturated cubic crystals—582
——— Magnetic quadruple field and energy in cubic and hexagonal crystals—38
McKellar, Andrew. Mass ratio of the lithium from the spectrum of Li_2—155
——— (see Jenkins, F. A.)—325(A)
McLay, A. B. and M. F. Crawford. Multiplet and hyperfine structure analyses of Bi IV. Discussion of perturbation effects—986
McMillen, Edwin. Isotopic constitution of lithium in the sun—240(L)
——— (see Grace, N. S.)—325(A)
——— **and Norman S. Grace.** Hyperfine structure in the tantalum arc spectrum—949(L)
McMillen, J. H. (see Hughes, A. L.)—20; 876
McPherson, Anna I. Doppler effect in spectra of positive rays of uniform velocity in argon, neon, helium—711
Meredith, George T. (see Broxon, J. W.)—253
Michels, Walter C. Note on the accommodation coefficient for helium—604(L)
Millikan, R. A. (see Bowen, I. S.)—246
Montgomery, C. G. (see Swann, W. F. G.)—52(L)
——— **and D. D. Montgomery.** Distribution of cosmic-ray nuclear disintegration in time—779(L)
Montgomery, D. D. (see Montgomery, C. G.)—779(L)
Mooney, R. C. L. and W. H. Zachariasen. Crystal lattice of ammonium persulphate, $(NH_4)_2S_2O_8$, and the structure of the persulphate group—327(A)
More, Kenneth R. (see Grace, N. S.)—128(A)
Morey, D. R. (see Webb, J. S.)—589
Morgan, H. E., L. T. DeVore and R. F. Baker. New method for amplifying and recording small e.m.f.'s—324(A)
Morse, Philip M. and W. P. Allis. Effect of exchange on the scattering of slow electrons from atoms—269

Morton, G. A. Directional effects in electron diffraction from single crystals—952(A)
Mott-Smith, Lewis M. and Lynn G. Howell. Airplane cosmic-ray intensity measurements—4
Mouzon, J. Carlisle. Ionization of the Noble gases by positive alkali ions. A correction—688(L)
Müller, Hans. Properties of Rochelle salt—854(L)
Mulliken, R. S. and D. S. Stevens. New O_2^+ bands. Dissociation energy of O_2^+ and ionization potential of O_2—720
Muskat, Morris. Reflection of plane wave pulses from plane parallel plates—319(A)

Nedelsky, Leo and J. R. Oppenheimer. Production of positives by nuclear gamma-rays—948(L)
Neher, H. V. (see Bowen, I. S.)—246
Nelson, H. R. Electron diffraction by hydrocarbons—717
Newson, Henry W. (see Harkins, William D.)—236(L); 529, 945(L)
——— (see Gans, David M.)—310(L)
Nielson, J. Rud. Rotational structure of the Raman band (0000)→(020±2) in linear symmetrical molecules YX_2—326(A); 911
——— (see Langseth, A.)—326(A)
Niewodniczanski, Henryk. Forbidden lines in the arc spectrum of lead—854(L)
Norris, Lawrence and A. G. Worthing. Rate of vaporization of molybdenum in vacuo—323(A)
Norton, Gardner A. Velocity of high frequency sound in tubes—951(A)
Nottingham, Wayne B. Measurements on the effect of light on spurious contact potentials and "trapped" electrons—311(L)

O'Bryan, H. M. (see Liben, I.)—952(A)
——— **and H. W. B. Skinner.** Experimental determination of the distribution of conduction electrons in metals—602(L)
Oppenheimer, J. R. (see Nedelsky, Leo)—948(L)
——— **and M. S. Plesset.** On the production of the positive electron—53(L)
Osgood, T. H. L x-ray spectrum of solid aluminum—517
Otis, H. N. Magnetic analysis of nickel films deposited by evaporation—843

Page, Leigh. Magnetized spheroid immersed in a permeable medium—112
Parker, Allan E. Further analysis of the N_2^+ bands—914
——— Rotational analysis of the perturbed (13, 15) 2Σ–$2\Sigma N_2^+$ band—90
——— Zeeman effect for perturbed N_2^+ terms—84
Parratt, Lyman G. Experimental study of the rocking curves of the Mn $K\alpha$ lines from pure Mn and from several Mn alloys—328(A)
——— Experimental study of the widths and shapes of the $K\alpha$ x-ray doublet from Ca (20) to Ni (28)—695
Patten, C. G. Magnitude of the L absorption discontinuities of thallium—328(A)
Pegram, G. B. (see Dunning, J. R.)—317(A)
Pekeris, C. L. Rotation-vibration coupling in diatomic molecules—953(A)
Pennell, Ford (see Jauncey, G. E. M.)—138
——— **and G. E. M. Jauncey.** Scattering of x-rays from powdered crystals at low temperatures—328(A)
Phillips, Melba. On the inversion of doublets in alkali-like spectra—644
Plesset, M. S. (see Oppenheimer, J. R.)—53(L)
Plyler, E. K. and E. F. Barker. Infrared bands and molecular constants of HBr—984
Pockman, L. T. (see Webster, D. L.)—130(A)
Pollard, W. G. Energy distribution in cosmic rays—703
Polvani, G. General form of the equation of state for a monoatomic ideal gas—123(L)
Pool, M. L. and S. J. Simmons. Hyperfine structure absorption in optically excited mercury vapor—997
——— **and S. J. Simmons.** Hyperfine structure intensities of the $2^3S_1 - P_{0,1,2}$ triplet in optically excited mercury vapor—744
Present, R. D. (see Kemble, E. C.)—1031(L)
Purdom, E. G. and J. M. Cork. Measurement of x-ray emission wave-lengths in the M series by means of the ruled grating—974
——— **and J. M. Cork.** Wave-lengths of certain M series lines by the ruled grating—328(A)

Ramsey, R. R. (see Hazel, Herbert)—321(A)
Randall, H. M. (see Wright, Norman)—391
Rao, S. Ramachandra. Ferromagnetism of nickel colloids—850
Rashevsky, N. On the calculation of the permeability of the cell surface to oxygen—322(A)
Revans, R. W. Transmission of waves through an ionized gas—798
Rice, O. K. Binding forces in the alkali metals according to the free electron theory—318(A)
——— (see Gibson, G. E.)—193
Richards, L. A. Use of triode vacuum tube rectifiers to supply constant voltage—324(A)
Richardson, H. W. (see Jauncey, G. E. M.)—328(A)
Richtmyer, F. K. and Sidney Kaufman. X-ray satellites of high atomic number elements—605
——— (see Hirsh, F. R., Jr.)—955
——— **S. W. Barnes and K. V. Manning.** Effect of grinding and etching on a pair of split calcite crystals—311(L)
Robertson, H. P. On E. A. Milne's theory of world structure—318(A)
Robinson, A. L. (see Hutchisson, E.)—323(A)
Roehr, Walter W. Effect of temperature on the energy distribution of photoelectrons. II. Total energies—866
——— **and L. A. DuBridge.** Effect of temperature on the energy distribution of photoelectrons—316(A)
Rose, Bernhard A. Measurements on contact potential difference between different faces of copper single crystals—585
Rosen, Nathan (see Manning, M. F.)—953(A)
Ross, P. A. K absorption discontinuities of the elements zirconium to iodine—130(A); 977
Ruark, Arthur E. Exponential law of radioactive disintegration—316(A); 654
——— Method to supplement dimensional analysis—329(A)

Ruark, Arthur E. (see Western, Forrest)—675
Ruedy, J. E. Arc spectrum of sulfur in the ultraviolet—757

Samson, E. W. (see Van Atta, L. C.)—316(A)
Sanders, Frederick H. Measurement of the Townsend coefficients for ionization by collision—129(A); 1020
Sanderson, J. A. (see Silverman, S.)—1032(L)
Sänger, Raymund. Some remarks on the frequency dependence of super-conductivity and ferromagnetism—302
Sawyer, J. H. Secondary and tertiary particles produced by cosmic rays—241
Schoessow, O. J. (see Hollister, S. C.)—330(A)
Schwégler, R. (see Déjardin, G.)—316(A)
Shane, C. D. (see Spedding, F. H.)—58(L)
Shaw, A. E. Electron orbits in crossed electric and magnetic fields—1006
Shawhan, E. N. (see Jarvis, C. W.)—943(L)
Shortley, George H. Energy levels of the rare-gas configurations—666
Shoupp, W. E. (see Kruger, P. Gerald)—105; 324(A)
Silverman, S. and J. A. Sanderson. Infrared spectrum of heavy ammonia—ND_3—1032(L)
Simmons, S. J. (see Pool, M. L.)—744; 997
Singer, W. E., J. D. Long and W. P. Davey. Structure of rubber as shown by the time lag of fibering—319(A)
Sixtus, K. J. On irregularities in magnetization—46
Skellett, A. M. (see Stewart, J. Q.)—125(L)
Skinner, H. W. B. (see O'Bryan, H. M.)—602(L)
Slater, J. C. Virial and molecular structure—953(A)
Sloane, R. H. and K. G. Emeleus. Effect of positive space charge in collector analysis of discharges—333
——— **and K. G. Emeleus.** Effect of space-charge in probe analysis of a plasma—322(A)
Smekal, Adolf G. On the theory of real crystals—308(L)
Smith, Albert. Absorption of NaCl, KCl and KI in the far ultraviolet—520
Smith, K. K. On the calculation of the coefficient C in Frank's formula for change of resistance—856(L)
Smyth, H. D. Emission and fluorescence spectra of sulphur dioxide—690(L)
Snoddy, L. B. Allison magneto-optic effect—691(L)
——— (see Beams, J. W.)—784(L)
Soltan, A. (see Crane, H. R.)—514(L); 692(L)
Sordahl, L. O. (see Wahlin, H. B.)—1030(L)
Sparks, F. M. (see Almy, G. M.)—365
Spedding, Frank H. and Richard S. Bear. Absorption spectra of the samarian ion in solids. III. Absorption of $Sm(BrO_3)_3 \cdot 9H_2O$ and a partial energy-level diagram for the Sm^{+++} ion as it exists in crystalline $Sm(BrO_3)_3 \cdot 9H_2O$—287
———**C. D. Shane and Norman S. Grace.** Fine structure of H^2 alpha—58(L)
Stannard, Carl R. (see Frederickson, W. R.)—632
Stephenson, Seymour Town. Fine structure in the K x-ray absorption spectrum of bromine—349
Sterne, T. E. Relative abundances of elements of even and odd mass number and atomic number—238(L)
Stevens, D. S. (see Mulliken, R. S.)—720
Stevens, T. H. and R. B. Abbott. Tone analysis and physical characteristics of violins—321(A)
Stevenson, E. C. Azimuthal asymmetry of the cosmic radiation in Colorado—855(L)
——— (see Johnson, T. H.)—125(L)
Stewart, J. Q. and A. M. Skellett. Study of images of small areas formed with feeble light—125(L)
Strait, Louis (see Broxon, J. W.)—253
Straub, H. W. (see Wood, R. W.)—1030(L)
Stueckelberg, E. C. G. Theory of continuous absorption of oxygen at 1450A. Erratum—234
Swann, W. F. G. Application of Liouville's theorem to electron orbits in the earth's magnetic field—224
——— Hoffmann Stösse and the origin of cosmic-ray ionization—1025
——— Measurement of the ionization per centimeter of path by individual secondary cosmic rays—961
——— Representation of radiation reaction in wave mechanics—943(L)
——— Space density of cosmic-ray particles—124(L)
——— **and C. G. Montgomery.** Cosmic-ray molecular disintegrations—52(L)

Taylor, John Bradshaw and Irving Langmuir. Evaporation of atoms, ions and electrons from caesium films on tungsten—423
Thomas, Clarence Delmar and R. T. Dufford. Efficiency of chemiluminescence accompanying oxidation of Grignard compounds—315(A)
Thompson, G. P. Comments on W. T. Sproull's article "Diffraction of low speed electrons by a tungsten single crystal"—417(L)
Thompson, Louis. Resistance function for dense fluids—320(A)
Todd, F. C. Changes in the x-ray diffraction pattern of nitrobenzene produced by an electric field, changes in temperature, and circulation—787
Tykociner, J. Tykocinski. Vibrating velocity selectors for atomic rays—322(A)
Tyler, Rayen Welch. Magnetic susceptibility of MnO as a function of the temperature—776

Ufford, C. W. Configuration interaction in complex spectra—732
——— (see Condon, E. U.)—740
Uhlenbeck, George E. (see Fermi, Enrico)—510(L)

Vallarta, M. S. Interpretation of the azimuthal effect of cosmic radiation—1
Van Atta, C. M. (see Granath, L. P.)—935
——— **and L. P. Granath.** Nuclear spin and magnetic moment of sodium from hyperfine structure—60(L)
Van Atta, L. C., E. W. Samson and R. J. Van de Graaff. Progress report on the electrostatic high voltage generator at Round Hill—316(A)
Van de Graaff, R. J. (see Van Atta, L. C.)—316(A)
Van Velzer, H. L. Thermionic constants for platinum—831
Van Vleck, J. H. and N. G. Whitelaw. Quantum defect of nonpenetrating orbits with special application to Al II—551

Van Voorhis, S. N. (see Harnwell, G. P.)—785(L)
Verwiebe, F. L. Radiation from canal ray impact—15
Vinti, J. P. Continuous absorption spectrum of helium—524

Wahlin, H. B. and L. O. Sordahl. Emission of electricity from columbium—1030(L)
Warburton, F. W. Electric waves, derived from Weber's energy equation—319(A)
Warren, B. E. X-ray diffraction in long chain liquids—952(A); 969
Waterman, A. T. and C. L. Henshaw. Extension of Fowler's theory of photoelectric sensitivity as a function of temperature—59(L)
Watson, William W. (see Cunningham, W. P.)—815
——— (see Margenau, H.)—92
———**and Henry Margenau.** Pressure effects of nitrogen on potassium absorption lines—748
Webb, J. S. and D. R. Morey. On the existence of time lags in the Faraday effect—589
Weber, Ernst. Distribution of conduction electrons in d.c. currents—318(A)
Webster, D. L., W. W. Hansen and F. B. Duveneck X-ray line intensities and cathode-ray retardation in thick targets of silver—258
——— **L. T. Pockman and Paul Kirkpatrick.** Probabilities of *L* ionizations of Au by cathode rays—130(A)
Western, Forrest and Arthur Ruark. Half-life of actino-uranium and the problem of geologic time—675
Wetzel, W. W. Quantum mechanical cross section for ionization of helium by electron impact—25
Wheeler, John A. and G. Breit. Li^+ fine structure and wave functions near the nucleus—948(L)
White, H. E. and O. E. Anderson. Hyperfine structure and nuclear spin of lanthanum—128(A)
——— **and A. Y. Eliason.** Relative intensity tables for spectrum lines—753
Whitelaw, N. G. Multiplet separations and perturbed terms—544
——— (see Van Vleck, J. H.)—551
Williams, John H. Relative intensities and transition probabilities of the *K*-series lines of the elements 24 to 52 by the ionization chamber method—146
Williams, Morgan L. Soft x-rays from (100) and (111) faces of copper single crystals—610
Williams, N. H. (see Cleeton, C. E.)—421(L)
Williams, P. S. (see Jauncey, G. E. M.)—794
Williams, R. C. and R. C. Gibbs. Fine structure of H_α—325(A)
——— (see Gibbs, R. C.—1029(L)
Wills, Lawrence A. (see Breit, G.)—470
Wilson, H. A. Alpha particles from radium C′—858(L)
——— Disintegration energies of radioactive nuclei—858(L)
Winch, Wesley R. (see Ingersoll, L. R.)—399
Wood, R. W. Remarkable optical properties of the alkali metals—353
——— **and H. W. Straub.** Influence of nitrogen and carbon dioxide upon the absorption spectrum of mercury vapor—1030(L)
Workman, E. J. Charging devices for portable ionization electroscopes—130(A)
Worthing, A. G. (see Norris, L.)—323(A)
Wright, Norman and H. M. Randall. Far infrared absorption spectra of ammonia and phosphine gases under high resolving power—391
Wright, W. H. Photographic studies of the planets in light of different wave-lengths—131(A)
Wu, Ta-You. Characteristic values of the two minima problem, and quantum defects of *f* states of heavy atoms—727
Wulff, John. Hyperfine structure and nuclear moment of gold—512(L)
——— (see Clewell, D. H.)—952(A)

Yamins, H. G. and W. A. Zisman. New method of studying the electrical properties of monomolecular films on liquids—323(A)
Yoe, John H. Lead isotopes by the magneto-optic method—420(L)
Young, Herbert A. (see Latimer, Wendell M.)—61(L); 690(L)

Zabel, R. M. Scattering of molecular rays in gases—53(L)
Zacharias, Jerrold. Temperature dependence of Young's modulus for nickel—116
Zachariasen, W. H. Crystal structure of boric acid—327(A)
——— (see Mooney, R. C. L.)—327(A)
Zeleny, John. Variation with temperature of the electrification produced in air by the disruption of water drops and its bearing on the prevalence of lightning—837
Zisman, W. A. (see Yamins, H. G.)—323(A)

ANALYTIC SUBJECT INDEX TO VOLUME 44

Absorption and reflection of light (see also **Spectra, absorption**)
Of Al and alloys, D. H. Clewell, J. Wulff—952(A)
By Au between 380A and 1400A, I. Liben, H. M. O'Bryan—952(A)

Accommodation coefficient
Classical "momentum transfer" theory, K. T. Compton, E. S. Lamar—338
For He, W. C. Michels—604(L)

Acoustics
Beat note-combinational tone controversy, H. Hazel, R. R. Ramsey—321(A)
Frequencies of multiple resonators; studies on the violin, R. O. Jenkins, R. B. Abbott—321(A)
Sound from a water jet, J. J. Hopfield—321(A)
Tone analysis and physical characteristics of violins, T. H. Stevens, R. B. Abbott—321(A)
Velocity of high frequency sound in tubes, G. A. Norton—951(A)

Alpha-particles (see **Radioactivity**)

Arcs (see also **Discharge of electricity in gases**)
Field electron emission and Hg arc, J. W. Beams—803

Astrophysics
Abundances of elements, T. E. Sterne—238(L)
Density of energy in universe, S. A. Korff—300
Hubble's constant and atomic constants, O. Halpern—855(L)
Li isotope in the sun, E. McMillan—240(L)
Milne's theory of world structure and relative cosmology, H. P. Robertson—318(A)
Shapes of solar absorption lines, T. Dunham, Jr.—329(A)

Atmospheric electricity (see **Meteorology**)

Atomic form factors
At low temperatures, G. E. M. Jauncey, F. Pennell—138; 328(A)

Atomic mass
Of electrons from components of $H^1\alpha$ and $H^2\alpha$, R. C. Gibbs, R. C. Williams—1029(L)
Of H^2 and He, K. T. Bainbridge—57(L)
Of Li isotope, K. T. Bainbridge—56(L)
And nuclear moments, N. S. Grace—58(L), 603(L), 361
Ratio of Li isotopes from spectrum, F. A. Jenkins, A. McKellar—325(A)

Atomic and molecular beams
Atomic rays of several hundred ion-volt-equivalent, O. Beeck—317(A)
Heat of dissociation of Bi_2 by method of molecular beams, C. C. Ko—129(A)
Scattering of molecular rays in gases, R. M. Zabel—53(L)
Vibrating velocity selectors, J. T. Tykociner—322(A)

Atomic and molecular radii (see **Scattering of electrons and ions**)

Atomic structure (see also **Energy states of atoms; Spectra, atomic**)
Breakdown of the Coulomb law for the H_2 atom, E. C. Kemble, R. D. Present—1031(L)

Barrier-layer photo-cells
Electrical characteristics, P. R. Gleason—315(A)
Sensitivity of the photronic cell to x-rays, P. R. Gleason—330(A)

Biophysics
Decomposition of H_2O by x-rays, H. Fricke, E. R. Brownscombe—240(L)
Mitogenetic radiation; search for, E. Lorenz—329(A)
Permeability of the cell surface to O_2, N. Rashevsky—322(A)

Canal rays
Radiation from canal ray impact, F. L. Verwiebe—15

Chemiluminescence
Efficiency; oxidation of Grignard compounds, C. D. Thomas, R. T. Dufford—315(A)
Efficiency; Wedekind reaction, W. L. Asling, R. T. Dufford—315(A)

Cold emission (see **Field currents**)

Collision diameter (see also **Scattering of electrons and ions**)
Quantum mechanical cross section for ionization of He, W. W. Wetzel—25

Collision phenomena (see **Scattering of electrons and ions**)

Colloids
Ferromagnetism of Ni colloids, S. R. Rao—850

Contact Potentials
Between faces of Cu single crystals, B. A. Rose—585
Effect of light, W. B. Nottingham—311(L)

Cosmic radiation
Airplane intensity measurements, L. M. Mott-Smith, L. G. Howell—4
Angular distribution in equatorial latitudes, T. H. Johnson—856(L)

Cosmic radiation (Continued)
Asymmetry at Swarthmore, T. H. Johnson, E. C. Stevenson—125(L)
Asymmetry, east and west counts, S. A. Korff—130(A); 515(L)
Azimuthal asymmetry in Colorado, E. C. Stevenson—855(L)
Density of energy, S. A. Korff—300
Distribution of nuclear disintegrations in time, C. G. Montgomery, D. D. Montgomery—779(L)
Energy distribution, W. G. Pollard—703
Factors that may produce fluctuations, J. W. Broxon, G. T. Meredith, L. Strait—253
High-altitude study; total energy content, I. S. Bowen, R. A. Millikan, H. V. Neher—246
Hoffmann Stösse and origin of ionization, W. F. G. Swann—1025
Interpretation of azimuthal effect, M. S. Vallarta—1
Ionization per cm of path by individual secondary rays, W. F. G. Swann—961
Liouville's theorem and electron orbits, W. F. G. Swann—224
Nature of showers, B. Cassen—513(L)
Neutrons from Stösse, G. L. Locher—779(L)
Nuclear disintegrations, W. F. G. Swann, C. G. Montgomery—52(L)
Positive and negative electrons, C. D. Anderson—406
Production of the positive electron, J. R. Oppenheimer, M. S. Plessett—53(L)
Ray counters and ray counts, G. F. Hull—952(A)
Secondary and tertiary particles, J. H. Sawyer—241
Space density, W. F. G. Swann—124(L)

Critical potentials (see **Potentials, critical**)

Crystal structure
Of ammonium persulphate and the persulphate group, R. C. L. Mooney, W. H. Zachariasen—327(A)
Of boric acid, W. H. Zachariasen—327(A)
Of KBr, S. T. Stephenson—349
Of potassium uranyl acetate, I. Fankuchen—327(A)
Of sodium thio-antimonate, C. Y. Hui—327(A)

Crystalline state
Analysis of Slater's compressibility data, H. M. Evjen—491
Binding forces in the alkali metals, O. K. Rice—318(A)
Conduction electrons in aluminum, T. H. Osgood—517
Contact potential between faces of copper single crystals, B. A. Rose—585
Crystallization of polymorphous substances on various surfaces, K. Lark-Horovitz, S. E. Madigan—320(A)
Elastic constants of Zn, A. W. Hanson—320(A)
Electron diffraction and imperfection of crystal surfaces, L. H. Germer—1012
Electron diffraction by hydrocarbons, H. R. Nelson—717
Electron diffraction from single crystals, G. A. Morton—952(A)
Electron, diffraction from W single crystals, J. H. Farnsworth—417(L); G. P. Thomson—417(L)
Ferromagnetism of Ni colloids, S. R. Rao—850
Forced double refraction, K. F. Herzfeld, R. H. Lee—625
Heteropolar crystals, theory of, H. M. Evjen—501
Hooke's law and crystal structure, A. E. Caswell—320(A)
Irregularities in magnetism, K. J. Sixtus—46
Magnetic dipole fields in cubic crystals, L. W. McKeehan—582
Magnetic field and energy in cubic and hexagonal crystals, L. W. McKeehan—38
Magnetic properties of Ba as function of temperature, C. T. Lane—43
Magnetic properties of Ni films, H. N. Otis—843
Magnetic saturation of cubic Co, R. I. Allen, F. W. Constant—228
Plasticity of rocksalt and its dependence, R. B. Barnes—898
Properties of Rochelle salt, H. Müller—854(L)
Susceptibility of MnO as a function of temperature, R. W. Tyler—776
Temperature dependence of Young's modulus for Ni, J. Zacharias—116
Theory of real crystals; secondary structure, A. G. Smekal—308(L)
X-ray investigations at high pressures, W. M. Cohn—326(A)

Deutons (see **Isotopes, Disintegration of nucleus**)

Diamagnetism (see **Magnetic properties**)

Dielectric constants (see **Dielectrics and dielectric properties**)

Dielectrics and dielectric properties
Atomic polarization of CO, L. A. Matheson—604(L)

Diffraction of electrons (see **Electron diffraction**)

Diffusion
Permeability of living cell to O_2, N. Rashevsky—322(A)

Dimensions and dimensional analysis
Method to supplement dimensional analysis, A. E. Ruark—329(A)

Discharge of electricity in gases (see also **Arcs; Electrons in gases**)
Faraday dark space, K. G. Emeleus, O. S. Duffendack—322(A)
Measurement of the Townsend coefficients, F. H. Sanders—1020; 129(A)
Probe analysis of a plasma, R. H. Sloane, K. G. Emeleus—322(A); 333
Waves in an ionized gas, R. W. Revans—798

Discharge of electricity in high vacua (see also **Thermionic emission; High voltage tubes and machines**)
Self-focussing electron streams, W. H. Bennett—322(A)
Temperature effect on field currents, A. J. Ahearn—277
Theory and experiment in cold emission, W. H. Bennett—859(L)

Disintegration of nucleus

α-particles from targets bombarded by deutons, G. N. Lewis, M. S. Livingston, E. O. Lawrence—55(L)
Application of the FP-54 Pliotron, L. R. Hafstad—201
Of Be by deuton bombardment, M. S. Livingston, M. C. Henderson, E. O. Lawrence—782(L)
Of Be by He ions, H. R. Crane, C. C. Lauritsen, A. Soltan—514(L)
Cosmic-ray disintegrations, W. F. G. Swann, C. G. Montgomery—52(L)
Energies of Ra C′, H. A. Wilson—858(L)
Energies of radioactive nuclei—H. A. Wilson—858(L)
Equivalence of mass and energy, K. T. Bainbridge—123(L)
Of F and formation of N^{16}, W. D. Harkins, D. M. Gans, H. W. Newson—945(L)
Of heavy H_2, M. S. Livingston, M. C. Henderson, E. O. Lawrence—781(L)
By ions of the heavy isotope of H_2, G. N. Lewis, M. S. Livingston, E. O. Lawrence—317(A)
Of N, C and Be by neutrons, W. D. Harkins, D. M. Gans, H. W. Newson—529
Of Li; production of neutrons, H. R. Crane, C. C. Lauritsen—783(L)
Of Li and Be by deutons, H. R. Crane, C. C. Lauritsen, A. Soltan—692(L)
By protons, M. S. Livingston, M. C. Henderson, E. O. Lawrence—316(A)
Protons from targets bombarded by deutons, E. O. Lawrence, M. S. Livingston, G. N. Lewis—56(L)
Three types of disintegration of calcium fluoride, E. O. Lawrence, M. S. Livingston—316(A)

Dissociation

Heat of dissociation of Bi_2, C. C. Ko—129(A)
Heats of H_2 and N_2, W. W. Lozier—575
Of O_2, R. S. Mulliken, D. S. Stevens—720

Doppler effect

In A, Ne and He canal rays, A. I. McPherson—711

Dynamics

Application of Liouville's theorem, W. F. G. Swann—224
Connection between Hamiltonian dynamics and wave mechanics, C. Lanczos—318(A)

Efficiency of ionization

Of Au by cathode rays, D. L. Webster, L. T. Pockman, P. Kirkpatrick—130(A)
Of the Noble gases by positive alkali ions—a correction, J. C. Mouzon—688(L)
Quantum mechanical cross section for ionization of He, W. W. Wetzel—25

Elasticity

Binding forces in the alkali metals, O. K. Rice—318(A)
Elastic constants of Zn, A. W. Hanson—320(A)
Hooke's law and crystal structure, A. E. Caswell—320(A)
Plasticity of rocksalt; dependence, upon water, R. B. Barnes—898
Reflection of plane wave pulses, M. Muskat—319(A)
Stress at a circular hole in a plate, S. C. Hollister, G. J. Schoessow—330(A)
Structure of rubber, W. E. Singer, J. D. Long, W. P. Davey—319(A)
Temperature dependence of Young's modulus for Ni, J. Zacharias—116

Electrical conductivity and resistance

Coefficient C in Frank's formula for change of resistance, K. K. Smith—856(L)
Conduction electrons in Al, T. H. Osgood—517
Frequency dependence of superconductivity, R. Sänger—302

Electrolytic cells

Single electrode potentials, E. Hutchisson, A. L. Robinson—323(A)

Electromagnetic theory

Electric waves, and from Weber's energy equation, F. W. Warburton—319(A)
Liouville's theorem and electron orbits in a magnetic field, W. F. G. Swann—224
Magnetic force and law of action and reaction, F. F. Cleveland—318(A)
Magnetized spheroid in a permeable medium, L. Page—112
Possibility of electric charge, A. Landé—689(L)

Electron diffraction (see also **Scattering of electrons**)

By hydrocarbons, H. R. Nelson—717
And imperfection of crystal surfaces, L. H. Germer—1012
By liquids, L. R. Maxwell—73
Scattering from liquid Hg, R. B. Brode, E. B. Jordan—872
From single crystals, G. A. Morton—952(A)
Sproull's results on W crystals, explanation of, H. E. Farnsworth—417(L); G. P. Thompson—417(L)

Electron tubes

Voltmeter with logarithmic response, F. V. Hunt—952(A)

Electrons in gases

Negative ion formation in O_2 and O_2 mixtures, N. E. Bradbury—883; 952(A)

Electrons in metals

Binding forces in the alkali metals, O. K. Rice—318(A)
Coefficient C in Frank's formula for change of resistance, K. K. Smith—856(L)
Conduction electrons in Al, T. H. Osgood—517
Distribution of electrons in direct currents, E. Weber—318(A)
Distribution from x-ray lines, H. M. O'Bryan, H. W. B. Skinner—602(L)

Electrons, positive (see **Positive electrons**)

Electrons, scattering of (see **Scattering of electrons and ions**)

Electrons, secondary
Produced by A atoms and ions, C. J. Brasefield—1002

Electrons, thermionic (see **Thermionic emission**)

Electro-optical effects (see also **Photoelectric effect and properties**)
Kerr effect in CO_2, N_2 and H_2, C. W. Bruce—682
Kerr effect in the infrared, L. R. Ingersoll, W. R. Winch —399

e/m
From components of $H^1\alpha$ and $H^2\alpha$; R. C. Gibbs, R. C. Williams—1029(L)
Surface charges on electrodes, orbits in crossed fields, A. E. Shaw—1006

Energy states of atoms (see also **Spectra, atomic**)
Charge distribution in F and Ne, F. W. Brown—214; In Be to Ne, F. W. Brown, J. H. Bartlett, Jr., C. G. Dunn—296
F states of heavy atoms, quantum defects, T-Y. Wu, —727

Equations of state
General form for a monoatomic ideal gas, G. Polvani—123(L)

Errata
Ionization of the noble gases by positive alkali ions, J. C. Mouzon—688(L)
Theory of continuous absorption of O_2 at 1450A, E. C. G. Stueckelberg—234
Variation of the principal magnetic susceptibilities of certain paramagnetic crystals with temperature, B. W. Bartlett—687

Errors of Measurement
Parameters in an empirical formula, W. E. Deming—317(A)

Evaporation
Of atoms, ions and electrons from Cs films on W, J. B. Taylor, I. Langmuir—423
Of Mo in vacuo, L. Norris, A. G. Worthing—323(A)

Excitation of atoms and molecules
Positive ion excitation of Hg vapor, E. J. Jones—707
Radiation at low critical potentials in Hg vapor, C. W. Jarvis, E. N. Shawhan—943(L)

Faraday effect (see **Magneto-optical effects**)

Field currents
Discrepancy between theory and experiment, W. H. Bennett—859(L)
Effect of temperature, A. J. Ahearn—277
From liquid Hg, J. W. Beams—803

Fine structures (see also **Spectra, etc., and Hyperfine structure**)
Of $H^2\alpha$, F. H. Spedding, C. D. Shane, N. S. Grace—58(L); R. C. Williams, R. C. Gibbs—325(A)
Of Li^+, wave function near nucleus, J. A. Wheeler, G. Breit—948(L)
Width of Balmer lines, E. C. Kemble and R. D. Present—1031(L)

Fluorescence (see also **Spectra, etc.**)
L-series x-ray satellites in fluorescence, F. R. Hirsh, Jr., F. K. Richtmyer—955
Of Sb_2, J. Genard—468

Geometry
Canonical coordinate system in Riemannian geometry, E. L. Akeley—318(A)

Geophysics
Cooling of a radioactive sphere, A. N. Lowan—769
Geologic time and half-life of actinouranium, F. Western, A. Ruark—675
Reflection of plane waves, M. Muskat—319(A)
U and Th content of rocks, R. D. Evans—129(A)

Hall effect
And coefficient *C* in Frank's formula for resistance change, K. K. Smith—856(L)

Heat conduction
Cooling of a radioactive sphere, A. N. Lowan—769

Heat of dissociation (see **Dissociation**)

High voltage tubes and machines
Production of high velocity ions and electrons, J. W. Beams, L. B. Snoddy—784(L)
High voltage generator at Round Hill, L. C. Van Atta, E. W. Samson, R. J. Van de Graaff—316(A)

Hydrodynamics
Resistance function for dense fluids, L. Thompson—320(A)
Study of a new water jet with stroboscope and camera, J. L. Hopfield—321(A)

Hyperfine structure (see also **Nuclear moments and spin**)
Absorption in optically excited Hg vapor, M. L. Pool, S. J. Simmons—997
Of Au, J. Wulff—512(L)
Of Bi IV; perturbation effects, A. B. McLay, M. F. Crawford—986
Intensities of triplet in optically excited Hg vapor, M. L. Pool, S. J. Simmons—744
Of Na, C. M. Van Atta, L. P. Granath—60(L)
And nuclear spin of Co, N. S. Grace, S. S. Ballard—128(A)
And nuclear spin of La, H. E. White, O. E. Anderson—128(A)
Of Mo, N. S. Grace, K. R. More—128(A).
Of Ta, N. S. Grace, E. McMillan—325(A)
In Ta I, E. McMillan, N. S. Grace—949(L)
Theory in intermediate coupling; comparison with experiment, G. Breit, L. A. Wills—470

Intensities in spectra (see also **Spectra, etc.**)
Hyperfine structure in Hg triplet, M. L. Pool, S. J. Simmons—744
Relative intensity tables. H. E. White, A. Y. Eliason—753

Ionization by positive ions (see also **Ionization potentials**)
Efficiency of ionization by alkali ions—a correction, J. C. Mouzon—688(L)
Positive ion source, E. J. Jones, S. B. Hendricks—322(A)
Positive ions from Cb, H. B. Wahlin, L. O. Sondahl—1030(L)
Proton source, E. S. Lamar, O. Luhr—947(L)
Source of positive alkali ions, P. Keck, L. B. Loeb—130(A)
Townsend coefficients, F. H. Sanders—1020; 129(A)

Ionization potentials
Of A by A atoms, O. Beeck—317(A)
Of Be III, P. G. Kruger, F. S. Cooper—418(L); B. Edlén—778(L)
Of O_2, R. S. Mulliken, D. S. Stevens—720

Ions in gases (see also **Electrons in gases**)
Analysis by mass-spectrograph, O. Luhr—459
Electron attachment in O_2, N. Bradbury—952(A)

Isotopes
Of Ca by the magneto-optic method, W. M. Latimer, H. A. Young—61(L)
Of Cl by magneto-optic method, E. R. Bishop, F. Allison—419(L)
Detection of H^3 by magneto-optic method, W. M. Latimer, H. A. Young—690(L)
Equivalence of mass and energy, K. T. Bainbridge—123(L)
Formation of N^{16}, W. D. Harkins, D. M. Gans, H. W. Newson—945(L)
H^2, infrared spectrum of $NH_3{}^2$, S. Silverman and J. A. Sanderson—1032(L)
H^2 shifts in spectra of $O^{16}H^2$, H. L. Johnston, D. H. Dawson—1031(L)
Of Li, A. McKellar—155
Of Li in the sun, E. McMillan—240(L)
Masses of H^2 and He, K. T. Bainbridge—57(L)
Masses of Li isotopes, K. T. Bainbridge—56(L); from spectrum, F. A. Jenkins, A. McKellar—325(A)
Measurement of mass by various methods, A.Bramley—309(L)
Of Pb by magneto-optic method, J. H. Yoe—420(L)
Of Pb by magneto-optic method, L. B. Snoddy—691(L)
Relative abundance of H_2 isotopes, W. Bleakney, A. J. Gould—265
Shift in Ne spectrum, J. H. Bartlett, Jr., J. J. Gibbons, Jr.—325(A); 538

Kerr effect (see **Electro-optical effects**)

Kinetic theory of gases
Scattering of molecular rays, R. M. Zabel—53(L)

Liquids
Properties of monomolecular films on liquids, H. G. Yamins, W. A. Zisman—323(A)
X-ray diffraction in long chain liquids, B. E. Warren—969

Low temperature phenomena
Gadolinium sulfate octahydrate below 1° absolute, W. F. Giauque, D. P. MacDougall—235(L)

Luminescence
Decay and light absorption in phosphorescent materials, D. H. Kabakjian—618

Magnetic fields
And energy in cubic and hexagonal crystals, L. W. McKeehan—38
Magnetized spheroid in a permeable medium, L. Page—112

Magnetic properties
Adiabatic demagnetizations of gadolinium sulfate, W. F. Giauque, D. P. MacDougall—235(L)
Of Ba, variation with temperature, C. T. Lane—43
Diamagnetism of crystals, A. E. Caswell—320(A)
Erratum, variation of the principal magnetic susceptibilities of certain paramagnetic crystals with temperature, B. W. Bartlett—687
Ferromagnetism of Ni colloids, S. R. Rao—850
Frequency dependence of ferromagnetism, R. Sänger—302
Irregularities in magnetization, K. J. Sixtus—46
Magnetic dipole fields in cubic crystals, L. W. McKeehan—582
Magnetic energy in cubic and hexagonal crystals L. W. McKeehan—38
Of Ni films deposited by evaporation, H. N. Otis—843
Saturation of cubic Co, R. I. Allen, F. W. Constant—228
Susceptibility of MnO at low temperatures, R. W. Tyler—776

Magneto-optical effects
Existence of time lags in the Faraday effect; test for, J. S. Webb, D. R. Morey—589
Faraday effect at high frequencies, G. P. Harnwell, W. Bleakney, S. N. Van Voorhis, J. B. H. Kuper—785(L)
Study of Allison magneto-optic effect, L. B. Snoddy—691(L)

Mass defects (see also **Isotopes**)
Nuclear theories of Heisenberg and Wigner, C. Eckart—109

Mass-spectrograph (see also **Methods and instruments**)
Analysis of gas ions, O. Luhr—459
Masses of H^2 and He, K. T. Bainbridge—57(L)
Masses of Li isotopes, K. T. Bainbridge—56(L)

Mechanics (see **Dynamics**)

Mechanics, quantum—atomic structure and spectra
Breakdown of Coulomb law for H atom, E. C. Kemble, R. D. Present—1031(L)
Characteristic values of the two minima problem, T-Y. Wu—727
Charge distributions in F and Ne, F. W. Brown—214; In B to Ne, F. W. Brown, J. H. Bartlett, Jr., C. G. Dunn—296
Configuration interaction in complex spectra, C. W. Ufford—732
Continuous absorption spectrum of He, J. P. Vinti—524
Levels of the rare gas configurations, G. H. Shortley—666

Mechanics, quantum—atomic structure and spectra (Continued)
Isotope shift in Ne, J. H. Bartlett, Jr., J. J. Gibbons, Jr. —325(A); 538
Magnetic interaction of a valence electron with inner-shells, M. H. Johnson, Jr., G. Breit—77
Multiplet separations and perturbed terms, N. G. Whitelaw—544
Quantum defect of nonpenetrating orbits, J. H. Van Vleck, N. G. Whitelaw—551
Theory of complex spectra, H. H. Marvin—818
Transition probabilities from spectroscopic stability, E. U. Condon, C. W. Ufford—740

Mechanics, quantum—general
Characteristic values for periodic potentials, H. D. Koenig—657
Connection between Hamiltonian dynamics and wave mechanics, C. Lanczos—318(A)
Cross section for ionization of He by electron impact, W. W. Wetzel—25
Emission and absorption of radiation, W. W. Hansen—954(A)
Physically admissible wave functions, E. C. Kemble —954(A)
Representation of radiation reaction, W. F. G. Swann—943(L)
Scattering by electrons in negative energy states, O. Halpern—855(L)

Mechanics, quantum—molecular structure and spectra
Intensity distribution in bands of triatomic molecules, Z. W. Ku—383
New treatment of the H_2 molecule, H. M. James, A. S. Coolidge—953(A)
Potential function for diatomic molecules, W. F. Manning, N. Rosen—953(A)
Raman effect in ammonia, C. M. Lewis, W. V. Houston —903
Rotation-vibration coupling in molecules, C. L. Pekeris —953(A)
Rotational structure of Raman band, J. R. Nielsen—911

Mechanics, statistical
Quantum statistics of almost classical assemblies, J. G. Kirkwood—31
Relative abundances of elements, T. E. Sterne—238(L)

Metals (see **Crystalline state**)

Meteorology
Electrification produced by the disruption of water drops; prevalence of lightning, J. Zeleny—837

Methods and instruments
Aligning of slits, J. Kunz—323(A)
Amplifying and recording small e.m.f's, H. E. Morgan, L. T. DeVore, R. F. Baker—324(A)
Charging devices for portable electroscopes, E. J. Workman—130(A)
Collector analysis in space charge, R. H. Sloane, K. G. Emeleus—333
Condensed discharge as source of spectrum, W. M. Cady—821
Cosmic-ray counters and ray counts, G. F. Hull—952(A)
Effect of grinding and etching calcite crystals; x-ray reflection, F. K. Richtmyer, S. W. Barnes, K. V. Manning—311(L)
Electrical properties of monomolecular films on liquids, H. G. Yamins, W. A. Zisman—323(A)
Electron collectors, A. E. Shaw—1006
Electron orbits in crossed electric and magnetic fields, A. E. Shaw—1006
Faraday effect at high frequencies, G. P. Harnwell, W. Bleakney, S. N. Van Voorhis, J. B. H. Kuper—785(L)
FP-54 Pliotron, an application, L. R. Hafstad—201
High voltage generator at Round Hill, L. C. Van Atta, E. W. Samson, R. J. Van de Graaff—316(A)
" Lines " of diffraction gratings, H. D. Babcock—129(A)
Magnetic deflection method for angular distribution of scattered electrons, A. P. Gagge—808
Magnetostatic oscillator for 1 cm waves, C. E. Cleeton, N. H. Williams—421(L)
Monochromatic filter for 4358A, W. H. Aughey, W. D. Lansing—326(A)
New method for determining thermionic work functions, G. W. Fox, R. M. Bowie—345
Parameters in an empirical formula and probable error, W. E. Deming—317(A)
Photoelectric photometer, T. Dunham, Jr.—329(A)
Positive ion source, E. J. Jones, S. B. Hendricks—322(A)
Production of high velocity ions and electrons, J. W. Beams, L. B. Snoddy—784(L)
Proton source, E. S. Lamar, O. Luhr—947(L)
Radioactive content of rocks determined from their surface radiation, R. D. Evans—129(A)
Recording photoelectric densitometer, L. T. DeVore—329(A)
Reflecting power of Al, D. H. Clewell, J. Wulff—952(A)
Reflection and absorption of light by Au, I. Liben, H. M. O'Bryan—952(A)
Relative intensities of x-ray lines, J. H. Williams—146
Source of positive alkali ions, P. Keck, L. B. Loeb—130(A)
Standard source for radiation measurements, L. T. DeVore, R. F. Baker—324(A)
Standard wave-lengths in the Cu spectrum, P. G. Kruger, F. S. Cooper—324(A); 826
Triode vacuum tube rectifiers, L. A. Richards—324(A)
Vacuum-tube voltmeter with logarithmic response, F. V. Hunt—952(A)
Velocity selectors for atomic rays, J. T. Tykociner—322(A)
Visco-conductimeter, C. L. Babcock, J. V. Hoffacker—320(A)
Wilson chamber illuminator, W. D. Harkins, D. M. Gans, H. W. Newson—529
Zeeman pattern analysis, R. A. Fisher—724

Molecular beams (see **Atomic and molecular beams**)

Molecular structure and constants (see also **Spectra molecular and Raman spectra**)
Absorption of Cl_2 at various temperatures, G. E. Gibson, O. K. Rice, N. S. Bayliss—193
Of Bi_2, G. M. Almy, F. M. Sparks—365
Of chlorine dioxide, Z. W. Ku—376
Of CO_2, E. F. Barker, A. Adel—185
Of HBr, E. K. Plyler, E. F. Barker—984
Of the H_2 molecule, H. M. James, A. S. Coolidge—953(A)
Of Li_2, A. McKellar—155
Of linear triatomic molecules, A. Langseth, J. R. Nielson —326(A)
Molecular structure and the virial, J. C. Slater—953(A)
Of NaK, F. W. Loomis, M. J. Arvin—126(L)
Of N_2, A. E. Parker—914
Of N_2^+ from rotational analysis, A. E. Parker—90
Of P_2, M. F. Ashley—919
Of Sb_2, J. Genard—468

Multiplets (see also **Spectra, atomic**)
Separations and perturbed terms, N. G. Whitelaw—544

Neutrons
From Be bombarded by deutons, M. S. Livingston, M. C. Henderson, E. O. Lawrence—782(L)
From Be and Li bombarded by deutons, H. R. Crane, C. C. Lauritsen, A. Soltan—692(L)
Collisions with protons, F. N. D. Kurie—463
Comparison of theories of Heisenberg and Wigner, C. Eckart—109
From cosmic-ray Stösse, G. L. Locher—779(L)
Dependence of absorption on velocity, T. W. Bonner—235(L)
From deutons and the mass of the neutron, M. S. Livingston, M. C. Henderson, E. O. Lawrence—781(L)
Disintegrations of Ne nuclei, W. D. Harkins, D. M. Gans, H. W. Newson—236(L)
From Li bombarded by protons, H. R. Crane, C. C. Lauritsen—783(L)
Nuclear constitution of H^2, E. O. Lawrence, M. S. Livingston, G. N. Lewis—56(L)
Produced by high speed He ions, H. R. Crane, C. C. Lauritsen, A. Soltan—692(L); By deutons 692(L); 783(L)
Produced by million volt He ions, H. R. Crane, C. C. Lauritsen, A. Soltan—514(L)
Scattering, path in magnetic field, J. R. Dunning, G. B. Pegram—317(A)

Nuclear moments and spin (see also **Hyperfine structure**)
And atomic number and mass number, N. S. Grace—58(L); 361; 603(L)
Of Li^7 from hyperfine structure, N. M. Gray—570
Magnetic moment of proton, A. Landé—1028(L)
Of Na, N. P. Heydenburg, A. Ellett—326(A); L. P. Granath, C. M. Van Atta—935
Of P_2 from spectrum, M. F. Ashley—919

Nucleus (see also **Disintegration of nucleus**)
α-particles from targets bombarded by deutons, G. N. Lewis, M. S. Livingston, E. O. Lawrence—55(L); Protons from targets—56(L)
Disintegrations of Ne nuclei, W. D. Harkins, D. M. Gans, H. W. Newson—236(L)
Magnetic moment of H_2, J. Kunz—323(A)

Optical constants and properties
Of the alkali metals in the ultraviolet, R. W. Wood—353
Forced double refraction in cubic crystals, K. F. Herzfeld, R. H. Lee—625

Optical instruments (see also **Methods and instruments**)
Formula for diffraction by grating, C. Eckart—12

Optical theory
Forced double refraction in crystals, K. F. Herzfeld, R. H. Lee—625
Formula for diffraction by grating, C. Eckart—12
Reflection from a moving mirror, N. Galli-Shohat—319(A)
Reflection of plane wave pulses, M. Muskat—319(A)

Oscillators (see also **Electrical circuits**)
Beat-note-combinational tone controversy, H. Hazel, R. R. Ramsey—321(A)
Magnetostatic oscillator producing 1–3 cm waves, C. E. Cleeton, N. H. Williams—421(L)

Phosphorescence
Decay of luminescence, D. H. Kabakjian—618

Photoelectric effect and properties; cells
Alkali ions and emissivity of W, A. K. Brewer—1016
Amplifying and recording small e.m.f.'s by photo-cells, H. E. Morgan, L. T. DeVore, R. F. Baker—324(A)
Current between parallel plates, F. H. Sanders—1020
Extension of Fowler's theory, A. T. Waterman, C. L. Henshaw—59(L)
Properties of Mg layers, G. Déjardin, R. Schwégler —316(A)
Temperature and energy distribution of photoelectrons, W. W. Roehr, L. A. DuBridge—316(A)
Temperature and energy distribution; normal energies, L. A. DuBridge, R. C. Hergenrother—861
Temperature and energy distribution; total energy, W. W. Roehr—866
Yields in extreme ultraviolet from Ni, W, Mg, W-O and Constantan, C. Kenty—891

Photography
Action of hydrogen peroxide, M. W. Jones, J. M. Blair—131(A)
Images formed with feeble light, J. Q. Stewart, A. M. Skellett—125(L)
Intermittency effect, J. M. Blair, M. C. Hylan—131(A)

Photometry
Intermittency effect, J. M. Blair, M. C. Hylan—131(A)
Photoelectric photometer, T. Dunham, Jr.—329(A)
Recording photoelectric densitometer, L. T. DeVore—329(A)

Photons
Images formed with feeble light, J. Q. Stewart, A. M. Skellett—125(L)

Photovoltaic effect
Cells containing Grignard solutions, T. R. Dufford—315(A)

Photronic cells (see **Barrier-layer photo cells**)

Plasmoidal discharges (see **Discharge of electricity in gases**)

Polarization of radiation
Of Na resonance radiation, N. P. Heydenburg, A. Ellett—326(A)

Positive electron
Cosmic-ray positive and negative electrons, C. D. Anderson—406
Produced by nuclear γ-rays, L. Nedelsky, J. R. Oppenheimer—948(L)
Production by electrons, W. H. Furry, J. F. Carlson—237(L)
Recombination of electrons and positrons, E. Fermi, G. E. Uhlenbeck—510(L)
Theory of production, J. R. Oppenheimer, M. S. Plessett—53(L)

Potentials, critical (see also **Ionization potentials**)
Positive ion excitation of Hg vapor, E. J. Jones—707
Radiation at low critical potentials in Hg, C. W. Jarvis, E. N. Shawhan—943(L)
Soft x-ray potentials: Cu single crystals, M. L. Williams—610

Probability of ionization (see **Efficiency of ionization**)

Quantum defect
F states of heavy atoms, T-Y Wu—727
Of nonpenetrating orbits, J. H. Van Vleck, N. G. Whitelaw—551

Quenching of radiation
Of I fluorescence by I and A, J. F. Koehler—761

Radiation (see also **Thermal radiation**)
From canal ray impact, F. L. Verwiebe—15

Radioactivity
α-particles from Ra C′, H. A. Wilson—858(L)
Application of probabilities, N. I. Adams, Jr.—651
Of Be, failure to detect, R. D. Evans, M. C. Henderson—59(L); 131(A); D. M. Gans, W. D. Harkins, H. W. Newson—310(L); W. F. Libby—512(L)
Disintegration energies, H. A. Wilson—858(L)
Exponential law of decay, A. E. Ruark—654
Half-life of actinouranium and geologic time, F. Western, A. Ruark—675
Probability and the exponential law, A. E. Ruark—316(A)
Th content of rocks; radiations from surfaces of solids, R. D. Evans—129(A)
U and Th content of rocks, R. D. Evans—129(A)

Raman spectra
In ammonia and other gases, C. M. Lewis, W. V. Houston—903
Of gaseous CO_2, A. Adel—691(L)
Of linear triatomic molecules, A. Langseth, J. R. Nielsen—326(A)
Structure of band in molecules of type X-Y-X, J. R. Nielsen—911
Structure of the Raman band in linear symmetrical molecules, J. R. Nielsen—326(A)
Of three amines, P. L. Bayley—510(L)

Reflecting power (see **Absorption and reflection of light**)

Relativity
Dirac's theory of the electron, E. Fermi, G. E. Uhlenbeck—510(L)
Milne's theory of world structure and relativistic cosmology, H. P. Robertson—318(A)

Scattering of electrons and ions (see also **Collision diameter; Electrons in gases; Electron diffraction**)
Effect of exchange, P. M. Morse, W. P. Allis—269
Inelastic scattering by He atoms, A. L. Hughes, J. H. McMillen—20
From liquid Hg, R. B. Brode, E. B. Jordan—872
Magnetic deflection method for angular distribution, A. P. Gagge—808
In methane, acetylene and ethylene, A. L. Hughes, J. H. McMillen—876

Scattering of light
Produced by electrons in negative energy states, O. Halpern—855(L)

Secondary electrons (see **Electrons, secondary**)
From liquid Hg, R. B. Brode, E. B. Jordan—872

Solid state (see **Crystalline state**)

Sound (see **Acoustics**)

Specific heat
Of gadolinium sulfate octahydrate below 1° absolute, W. F. Giauque, D. P. MacDougall—235(L)

Spectra, absorption (see also **Absorption of light**)
Of Bi_2; analysis, G. M. Almy, F. M. Sparks—365
Of chlorine dioxide, Z. W. Ku—376
Of Cl_2, G. E. Gibson, N. S. Bayliss—188
Of Cl_2, theory of variation with temperature, G. E. Gibson, O. K. Rice, N. S. Bayliss—193
Of CO_2 near 10μ, E. F. Barker, A. Adel—185
Continuous spectrum of He; calculations, J. P. Vinti—524
Of Hg vapor, influence of N_2 and CO_2, R. W. Wood, H. W. Straub—1030(L)
Infrared of ammonia and phosphine gases, N. Wright, H. M. Randall—391
Of Li_2, A. McKellar—155
Of liquid O_2, J. W. Ellis, H. O. Kneser—420(L)
Of NaCl, KCl, and KI in far ultraviolet, A. Smith—520

Of O_2 at 1450A, erratum, E. C. G. Stueckelberg—234
Pressure effects of gases on the Na *D*-lines, H. Margenau, W. W. Watson—92
Pressure effects of N_2 on *K* lines, W. W. Watson, H. Margenau—748
Of the Sm ion in solids, F. H. Spedding, R. S. Bear—287
Of SO_2, T.-C. Chow—638; H. D. Smyth—690(L)

Spectra, atomic
Of Be III, P. G. Kruger, F. S. Cooper—418(L); B. Edlén—778(L)
Components of $H^1\alpha$ and $H^2\alpha$, R. C. Gibbs, R. C. Williams—1029(L)
Of Cb IV, R. J. Lang—325(A)
Configuration interaction, C. W. Ufford—732
Doppler effect in canal rays, A. I. McPherson—711
Fine structure of $H^2\alpha$, R. C. Williams, R. C. Gibbs—325(A); F. H. Spedding, C. D. Shane, N. S. Grace—58(L)
Forbidden lines in Pb I, H. Niewodniczanski—854(L)
Hfs of Bi IV; perturbation effects, A. B. McLay, M. F. Crawford—986
Inversion of doublets in alkali-like spectra, M. Phillips—644
Isotope effect in Pb, B. H. Dickinson—329(A)
Isotope shift in Ne, J. H. Bartlett, Jr., J. J. Gibbons, Jr.—325(A); 538
Isotope shift of Tl, G. Breit—418(L)
Li^+ fine structure, J. A. Wheeler, G. Breit—948(L)
Magnetic interaction terms, M. H. Johnson, Jr., G. Breit—77
Multiplet separations and perturbed terms, N. G. Whitelaw—544
Multiplet transition probabilities, E. U. Condon, C. W. Ufford—740
Multiplets of O III, O IV, and O V, and C III, P. G. Kruger, W. E. Shoupp—105; 324(A)
New terms in N III, N IV, N V, O III, O IV, and O V, W. M. Cady—821; 128(A)
Quantum defect of nonpenetrating orbits, application to Al II, J. H. Van Vleck, N. G. Whitelaw—551
Rare-gas configurations, energy levels, G. H. Shortley—666
Relative intensity tables, H. E. White, A. Y. Eliason—753
Of S in ultraviolet, J. E. Ruedy—757
Stellar stark line He λ4470, J. S. Foster, A. V. Douglas—325(A)
Theory of complex spectra, H. H. Marvin—818
Width of Balmer lines, E. C. Kemble and R. D. Present—1031(L)

Spectra, general
Asymmetries of pressure broadening, H. Margenau—931; 954(A)
Cu wave-lengths in the region 100A to 450A, P. G. Kruger, F. S. Cooper—826
Hfs absorption in optically excited Hg vapor, M. L. Pool, S. J. Simmons—997
Pressure effects of gases on the Na *D*-lines, H. Margenau, W. W. Watson—92
Quenching of I fluorescence by I_2 and A, J. F. Koehler—761
Radiation at low critical potentials in Hg vapor, C. W. Jarvis, E. N. Shawhan—943(L)

Spectra, molecular (see also **Molecular structure and constants**)
Of Al halides, F. H. Crawford, C. F. Ffolliott—953(A)
Of CO_2, infrared, A. Adel, D. M. Dennison—99
From an unusual N_2 tube, J. Kaplan—783(L)
Of H_2 in ultraviolet, C. R. Jeppesen—165
Inert gas molecules, K. G. Emeleus, O. S. Duffendack—945(L)
Infrared bands of HBr, E. K. Plyler, E. F. Barker—984
Infrared, of heavy ammonia—ND_3, S. Silverman, J. A. Sanderson—945(L)
Intensity distribution in bands of triatomic molecules, Z. W. Ku—383
Magnetic rotation spectrum of Na, W. R. Frederickson, C. R. Stannard—632
Of NaK, F. W. Loomis, M. J. Arvin—126(L)
N_2^+ band analysis, A. E. Parker—914
NH_3^2 isotope shift of vibration bands, S. Silverman and J. A. Sanderson—1032(L)
Of neutral OH; new electron bands, K. Chamberlain, H. B. Cutter—927
New band system in N_2, J. Kaplan—947(L)
New O_2^+ bands, R. S. Mulliken, D. S. Stevens—720
Of $O^{16}H^2$; isotope shifts, H. L. Johnston, D. H. Dawson—1031(L)
Potential function for diatomic molecules, M. F. Manning, N. Rosen—953(A)
Rotation-vibration coupling, C. L. Pekeris—953(A)
Rotational analysis, (13, 15) N_2^+ band, A. E. Parker—90
Of SO_2, T.-C. Chow—638; H. W. Smyth—690(L)
Zeeman effect and uncoupling phenomena in CaH bands, W. P. Cunningham, W. W. Watson—815

Spectroscopy, technique
Standard wave-lengths in the Cu spectrum; 80A to 650A, P. G. Kruger, F. S. Cooper—324(A); 826

Statistical mechanics (see **Mechanics, statistical**)

Superconductivity (see **Electrical conductivity and resistance**)

Surface phenomena
Alkali ions and emissivity of W, K. A. Brewer—1016
Cs on W, J. B. Taylor, I. Langmuir—423

Thermal radiation
Emissivity of a non-black body, L. T. DeVore—324(A)
Standard source for radiation measurements, L. T. DeVore, R. F. Baker—324(A)

Thermionic emission of electrons; emitting surfaces (see also **Electron tubes**)
From Cs films on W, J. B. Taylor, I. Langmuir—423
Spurious contact potentials and "trapped" electrons, W. B. Nottingham—311(L)
Thermionic constants for Pt, H. L. Van Velzer—831

Work function of Co, H. B. Wahlin, L. O. Sordahl—1030(L)
Work functions of Ni by new method, G. W. Fox, R. M. Bowie—345

Thermionic emission of positive ions
From CO, H. B. Wahlin, L. O. Sordahl—1030(L)
From Cs films on W. J. B. Taylor, I. Langmuir—423
From oxides, E. J. Jones, S. B. Hendricks—322(A)

Thermoelectric phenomena
Thermoelectric force of thin films, E. A. Johnson, L. Harris—944(L)

Vacuum tubes (see also **Electron tubes**)
Rectifiers to supply constant voltage, L. A. Richards—324(A)

Viscosity
And conductivity of molten gases, K. Lark-Horovitz, C. L. Babcock—321(A)
Fluidities of thixotropic gels, H. A. Ambrose, A. G. Loomis—320(A)
New visco-conductimeter, C. L. Babcock, J. V. Hoffacker—320(A)

Wave mechanics (see **Mechanics, quantum, etc.**)

Work functions (see **Thermionic emission, etc.**)

X-rays, absorption
Decomposition of H_2O, H. Fricke, E. R. Brownscombe—240(L)
Of the elements Zi to I, P. A. Ross—977
Fine structure in *K* spectrum of Bi, S. T. Stephenson—349
K discontinuities of the elements Zi to I, P. A. Ross—130(A)
K limits of the elements Mn to Zn, A. H. Barnes—141
L discontinuities of Tl, C. G. Patten—328(A)
Laws for soft x-rays, E. Dershem—328(A)

X-rays, diffraction, scattering, reflection, refraction and polarization
Changes in diffraction of nitrobenzene produced by various factors, F. C. Todd—787
Diffraction at high pressures, W. M. Cohn—326(A)
Diffraction in long chain liquids, B. E. Warren—969; 952(A)
Diffuse scattering, variation with temperature and angle, G. E. M. Jauncey, P. S. Williams—794
Effect of high temperature on scattering, G. G. Harvey—133
Formula for diffraction by grating, C. Eckart—12
Scattering from powdered crystals at low temperatures, F. Pennell, G. E. M. Jauncey—138; 328(A)

X-rays, emission (see also **X-rays, spectra and spectroscopy, etc.**)
Form of *L* spectrum of Al, T. H. Osgood—517
Form of lines from light elements, H. M. O'Bryan, H. W. B. Skinner—602(L)
From (100) and (111) faces of Cu single crystals, M. L. Williams—610
Intensities of *L*-series satellites in cathode-ray and in fluorescence excitation, F. R. Hirsh, Jr., F. K. Richtmyer—955
Line intensities and cathode-ray retardation, D. L. Webster, W. W. Hansen, F. B. Duveneck—258
M-series wave-lengths by ruled grating, E. G. Purdom, J. M. Cork—974
Probabilities of ionizations of Au, D. L. Webster, L. P. Pockman, P. Kirkpatrick—130(A)
Radiation produced by fast Hg ions, W. M. Coates, E. O. Lawrence—327(A)
Rocking curves of $K\alpha$ lines from Mn alloys, L. G. Parratt—328(A)
Satellites of high atomic number elements, F. K. Richtmyer, S. Kaufman—605
Widths of the $K\alpha$ doublet from 26Fe to 47Ag, S. K. Allison—63
Widths and shapes of the $K\alpha$ doublet from Ca to Ni, L. G. Parratt—695

X-rays, spectra and spectroscopy, wave-length measurements (see also **X-rays, emission**)
Relative intensities and transition probabilities *K*-series, elements 24 to 52, J. H. Williams—146
Sensitiveness of photographic films at low temperatures, G. E. M. Jauncey, H. W. Richardson—328(A)
Transmission through filters, P. A. Ross—977
Wave-lengths by the ruled grating, E. G. Purdom, J. M. Cork—328(A)

X-rays, tubes, apparatus
Effect of grinding and etching calcite crystals, F. K. Richtmyer, S. W. Barnes, K. V. Manning—311(L)
Formula for diffraction by grating, C. Eckart—12

Zeeman effect
Analysis of patterns, R. A. Fisher—724
And uncoupling phenomena in CaH bands, W. P. Cunningham, W. W. Watson—815
For perturbed N_2^+ terms, A. E. Parker—84
Second order effect in the Hg I, J. B. Green, R. A. Loring—325(A)